Functional evolution of haloalkane dehalogenases for the degradation of persistent environmental pollutants

博士論文

Functional evolution and engineering of haloalkane dehalogenases for the degradation of persistent organic pollutants

(ハロアルカンデハロゲナーゼの難分解性環境汚染物質分解能の機能進化に関する研究)

令和 2 年度

東北大学大学院生命科学研究科

分子化学生物学専攻

陳楠楠

Ph.D. Thesis

Functional evolution and engineering of haloalkane dehalogenases for the degradation of persistent organic pollutants

Laboratory of Microbial Evolution and Function Research,

Graduate School of Life Sciences, Tohoku University

Nannan Chen

Contents

Background

Pesticides, which are effective in pest and disease control management, are important for agriculture and public health purposes, but their excessive use affects food security and concurrent health threats for humans (Macdonald et al., 2000). Most of traditional pesticides are recalcitrant organic compounds which are not easily degraded by natural means and they are referred to as persistence organic pollutants (POPs). POPs are of two types, the organophosphate pesticides and the organochloride pesticides, and are of great environmental and health concerns due to their toxic, persistent and bio-accumulative capacities (Barber et al., 2005). Many of them may form residual compounds which are more toxic in the soil and can be accumulated in living tissue through direct or indirect means, and thus they can get into the food chain of an ecosystem and affect wide range of organisms.

0-1 γ-Hexachlorocyclohexane

γ-Hexachlorocyclohexane (γ-HCH), which is a broad-spectrum organochloride insecticide, was one of the most popular organochloride pesticides that had been used extensively worldwide for the control of agricultural pests and mosquitoes in malaria health programs prior to the 1990's (Li et al., 2003). γ-HCH production by chlorination of benzene under suitable conditions leads to a mixture of isomers, and γ-HCH and its isomers were extensively applied since the 1940s and were added to the list of persistent organic pollutants (POPs) in 2009 (Vijgen et al., 2011). HCH is available in two formulations: technical-grade HCH (60-70 % α-HCH, 5-12 % β-HCH, 10-15 % γ-HCH, 6-10 % δ-HCH, and 3-4 % ε-HCH) and lindane (almost pure γ-HCH) (Abhilash et al., 2008). HCH isomers differ not only in the spatial orientation of the chlorine atoms bound to the aliphatic carbon ring (Fig. 0-1), but also in toxicity, water solubility (and thus mobility and bioavailability) and recalcitrance. Among the HCH isomers, α-HCH and γ-HCH dominate in the atmosphere due to their higher volatility and lower partition coefficient, while β-HCH is the most persistent in nature and less volatile isomer and tends to accumulate in soils (Vijgen et al., 2011). Only γ-isomer exhibited insecticidal activity, and it was widely used since 1953 as a cheap and effective insecticide especially in developing countries (Lal et al., 2010). Lindane is extremely toxic to humans and deleterious for environment. It is rapidly absorbed from the gastrointestinal tract of mice or rats and gets extensively distributed in fat, liver, ovarian tissues and brain. Although it has been banned in many countries because of its toxicity and recalcitrance (Lal et al., 2010), it is still being used in developing countries because of its efficacy and low cost. Thus it has caused seriously environmental problems.

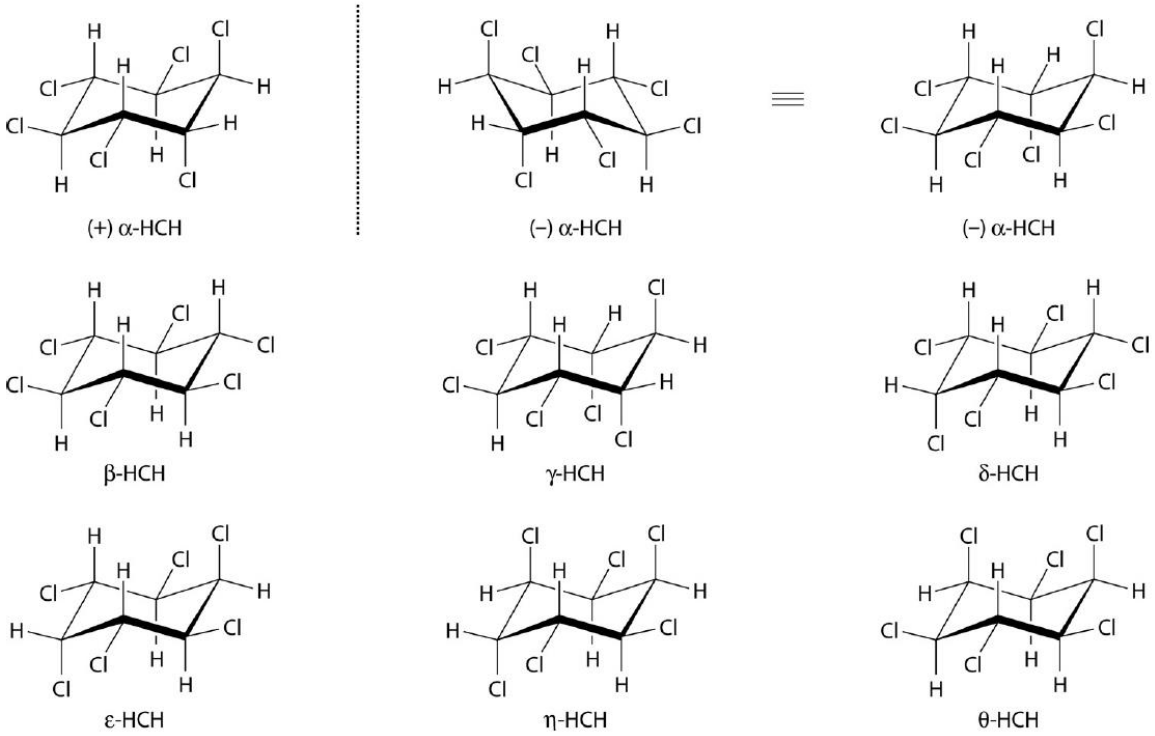

Fig. 0-1 Axial versus equatorial arrangements of chlorine atoms in the five major isomers of HCH. α-HCH exists in two enantiomeric (+and -) forms (Lal et al., 2010).

0-2 Biodegradation of γ-HCH

γ-HCH is usually degraded under both aerobic and anaerobic environments, but it can be mineralized only in aerobic condition (Naqvi et al., 2014). Many bacteria has been reported for γ-HCH degradation (Böltner et al., 2005), and the γ-HCH degradation pathway and genes and enzymes involved in the degradation have been well studied in *Sphingobium japonicum* UT26 which was isolated from γ-HCH-polluted soil (Nagata et al., 2007). γ-HCH degradation and mineralization was also reported by other species of *Sphigobium*, such as *S. indicum* strain B90 (Kumari et al., 2002) and B90A from India (Dogra et al., 2004) and *S. francense* strain Sp+ from France (Cérémonie et al., 2006).

The microbial aerobic degradation pathway of γ-HCH was revealed in *S. japonicum* UT26 (Fig. 0-2) (Nagata et al., 2011). In this pathway, γ-HCH is converted to 2,5-dichlorohydroquinone (2,5-DCHQ) by sequential reactions catalyzed by LinA (γ-HCH dehydrochlorinase), LinB (1,3,4,6-tetrachloro-1,4-cyclohexadiene chlorohydrolase), and LinC (2,5-dichloro-2,5-cyclohexadiene-1,4-diol dehydrogenase). 2,5-DCHQ is then dechlorinated to chlorohydroquinone (CHQ) by LinD (2,5-dichlorohydroquinone dechlorinase), and CHQ is further transformed to β-ketoadipate by LinE (chlorohydroquinone 1,2-dioxygenase) and LinF (maleylacetate reductase). β-Ketoadipate is further degraded by the β-ketoadipate pathway that is generally found in environmental bacteria.

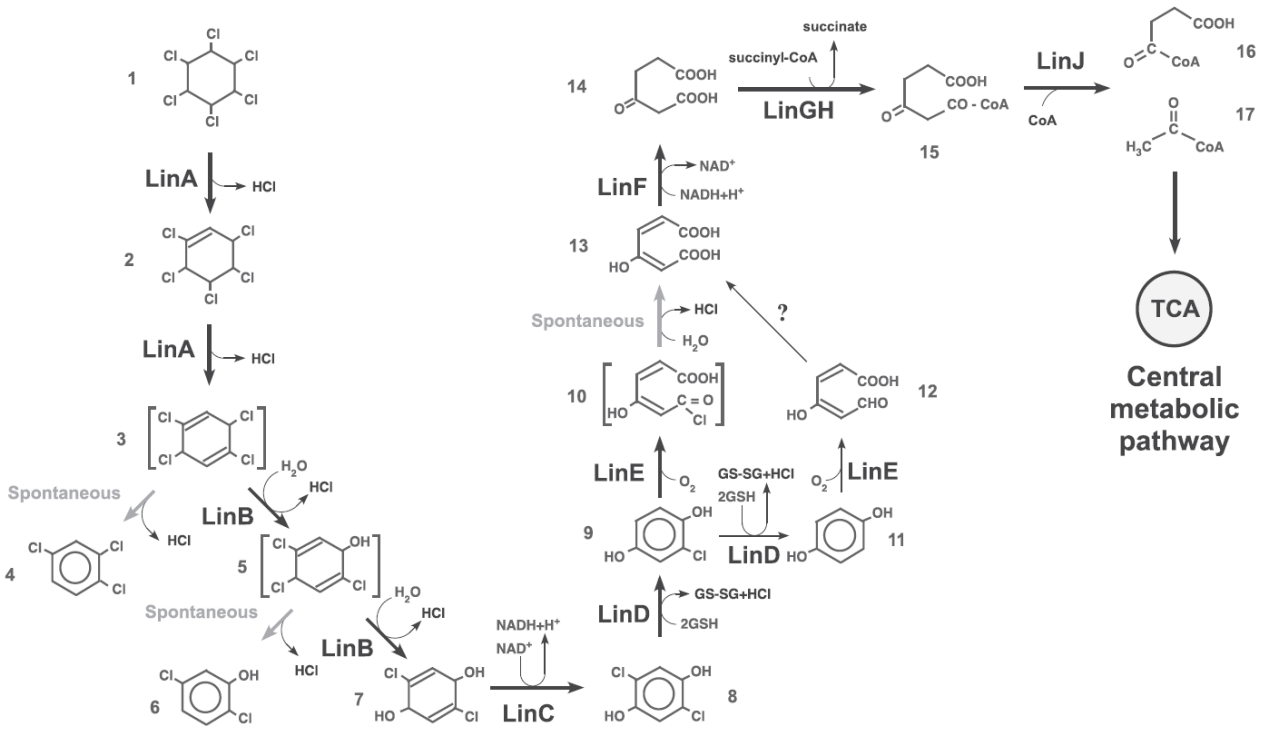

Fig. 0-2 Degradation pathway of γ-HCH in *Sphingobium japonicum* UT26. Compounds: 1, γ-HCH; 2, γ-pentachlorocyclohexene; 3, 1,3,4,6-tetrachloro-1,4-cyclohexadiene; 4, 1,2,4-trichlorobenzene; 5, 2,4,5-trichloro-2,5-cyclohexadiene-1-ol; 6, 2,5-dichlorophenol; 7, 2,5-dichloro-2,5-cyclohexadiene-1,4-diol; 8, 2,5-dichlorohydroquinone; 9, chlorohydroquinone; 10, acylchloride; 11, hydroquinone; 12, c-hydroxymuconic semialdehyde; 13, maleylacetate; 14, b-ketoadipate; 15, 3-oxoadipyl-CoA; 16, succinyl-CoA; 17, acetyl-CoA. TCA, citrate/tricarboxylic acid cycle (Tabata et al., 2016)

0-3 The *lin* genes involved in the γ-HCH degradation

The *linA* to *linF* genes in *S. japonicum* UT26 are dispersed on the three large circular replicons: the *linA*, *linB*, and *linC* genes on the 3.6-Mb chromosome I; the *linF* gene on the 670-kb chromosome II; and the *linDE* operon with its regulatory gene (*linR*) on a 185-kb plasmid, pCHQ1 (Nagata et al., 2006).

Nearly identical *lin* genes have also been identified in other HCH-degrading bacterial strains, such as *S. indicum* B90 (Kumari et al., 2002) and B90A (Dogra et al., 2004) from India and *S. francense* Sp+ from France (Cérémonie et al., 2006); most of the *lin* genes in these strains are closely associated with an insertion sequence (IS), IS*6100* (Lal et al., 2006). pCHQ1 is conjugally transferable from *S. japonicum* UT26 to another *Sphingomonas paucimobilis* strain (Nagata et al., 2006), and another report showed that the *linA* and *linB* genes in other strains are also located on plasmids (Cérémonie et al., 2006). These observations indicate that *lin* genes must be spread by mobile genetic elements (MGEs).

0-4 Haloalkane dehalogenases (HLDs)

0-4-1 Introduction of HLDs

Halogenated compounds are widely used in industry and agriculture, and as components (*i.e.*, solvents) in daily household items (Zulkifly et al., 2010). Haloalkane dehalogenases (HLDs) are key enzymes for the degradation of halogenated aliphatic compounds that occur as soil pollutants (Ballschmiter, 2003). HLDs (EC 3.8.1.5) make up one such important class of enzymes because of their ability to attack polychlorinated

aliphatic hydrocarbons, which are produced in several industrial processes (Ang et al., 2018). Nowadays, various practical applications of HLDs are known, and the number is increasing with the growing knowledge of their properties and structure-function relationships: bioremediation of environmental pollutants, biosensors for toxic chemicals (Ang et al., 2018), industrial biocatalysis (Janssen, 2007), decontamination of warfare agents (Prokop et al., 2006), as well as cell imaging and protein analysis (Los et al., 2008). HLDs belong to the α/β-hydrolase fold superfamily, a very large and diverse group of structurally related hydrolytic enzymes with esterase, lipase or epoxide hydrolase activities (Koudelakova et al., 2011). Phylogenetic study of HLD sequences revealed that HLDs were subdivided into three subfamilies HLD-I, HLD-II, and HLD-III (Chovancová et al., 2007). The composition of amino acid residues that are important for the reaction (see below) is different among the subfamilies: Asp-His-Asp (catalytic triad) and Trp-Trp (halide-stabilizing residues) in HLD-I, Asp-His-Glu and Asn-Trp in HLD-II, and Asp-His-Asp and Asn-Trp in HLD-III. In contrast to HLDs belonging to HLD-I and HLD-II, those belonging HLD-III are poorly characterized experimentally (Chovancová et al., 2007).

0-4-2 Structure and reaction mechanism of HLDs

HLDs have a globular structure and are composed of two domains: a large central catalytic domain with an α/β-hydrolase fold structure and the second domain which lies like a cap on the main domain. The latter domain emerges as a large R-helical excursion between β-strands 6 and 7 of the catalytic core. The interface of the two domains forms the hydrophobic active site. The catalytic triad residues are a nucleophilic aspartate, a base catalyst histidine, and an aspartate or glutamate as the third member. These amino acids form the basis of the dehalogenation reaction and are located in the main domain. Whereas there is significant sequence similarity in the catalytic core, the sequence and structure of the cap domain diverge considerably between different HLDs. The cap domain was proposed to play a prominent role in determining substrate specificity (Koudelakova et al., 2013).

HLDs perform catalysis using an S_N2 (nucleophilic substitution) reaction and subsequent hydrolysis by the addition of water, in which only water is required as a cofactor (Fig. 0-3). This catalytic mechanism involves the catalytic triad of Asp-His-Asp/Glu. The carboxylate oxygen of aspartate initially launches a nucleophilic attack on the partially positive carbon atom of the halogen-bound substrate to produce a halide ion and alkyl-enzyme intermediate with an ester bond. The nearby His-Asp/Glu (acid-base pair) subsequently hydrolyzes a water molecule to produce a nucleophilic hydroxide that will attack the carbon of the ester bond. This generates a tetrahedral intermediate that immediately decomposes to form RCH_2O^- and grabs a proton from the nucleophile to form RCH_2OH (Jong et al., 2003). HLDs possess halide-binding residues, also known as halide-stabilizing residues, which is their unique feature (Chovancová et al., 2007). These residues are critical for the catalytic activity of HLDs as they help to stabilize the halide during formation of the enzyme-substrate complex.

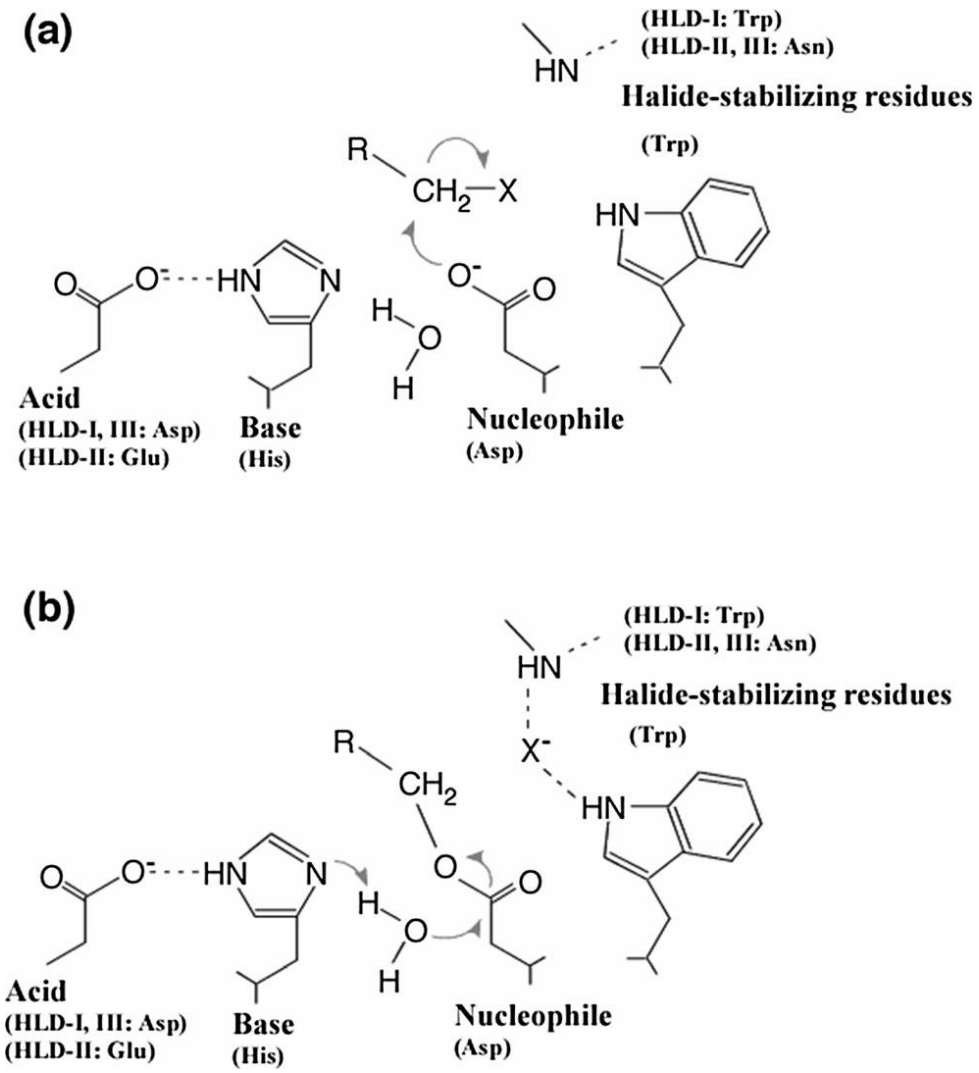

Fig. 0-3 Simplified reaction mechanism of HLDs. a, The ester is formed by S_N2 nucleophilic substitution, and the transition state formed in this step is stabilized by two halide-stabilizing residues. b, A water molecule activated by a histidine-acid pair attacks the ester intermediate to produce an alcohol and halide ion (Nagata et al., 2015)

0-4-3 HLDs and its related proteins used in this study

0-4-3-1 LinA

LinA was initially identified as an enzyme that catalyzes the first step of γ-HCH degradation in *S. japonicum* UT26. LinA catalyzes dehydrochlorination of γ-HCH and γ-PCCH to produce 1,2,4-TCB (Fig. 0-2), and is not a member of HLDs. LinA can also degrade α-HCH and δ- HCH in addition to γ-HCH, but has no activity for β-HCH because β-HCH lacks a 1,2-biaxial HCl pair (Trant ŕek et al., 2001). Degradation assays of various halogenated compounds by purified LinA showed that the substrate specificity of LinA is very narrow. Because no gene significantly homologous to the *linA* gene has been found, its origin is unknown. LinA is thought to be a unique dehydrochlorinase, and its reaction mechanism of dehydrochlorination is of great interest (Trant ŕek et al., 2001). The genetic instability of the *linA* gene described in *S. japonicum* UT26 (Okai et al., 2010) seems to reflect a common feature of xenobiotic degrading pathways (Nagata et al., 2001). The gene loss is often associated with the loss of catabolic transposons or plasmids, or some type of DNA

rearrangements (Peisajovich et al., 2006). It has been shown that two copies of IS*6100* located close to the *linA* gene are involved in its loss in *S. japonicum* UT26 (Nagata et al., 2011).

0-4-3-2 LinB

LinB is one of archetypal HLDs that involved in the γ-HCH degradation pathway and has been well characterized (Marek et al., 2000) (Fig. 0-4a). Site-directed mutagenesis of LinB confirmed that Asp108, His272, and Glu132 comprise the catalytic triad in this enzyme (Oakley et al., 2004).

LinB has a broad substrate specificity, mainly due to a large active site volume, which includes monochloroalkanes (C3-C10), dichloroalkanes, bromoalkanes and chlorinated aliphatic alcohols (Koudelakova et al., 2011). Notably, $LinB_{UT26}$ yields a significantly lower specificity constant for β-HCH (0.02 mM^{-1} s^{-1}) as compared to another relatively well characterized LinB, namely, $LinB_{B90A}$ (identical to $LinB_{MI1205}$, and $LinB_{BHC-A}$ and $LinB_{pLB1}$) from *S. indicum* strain B90A (0.20 mM^{-1} s^{-1}) (Okai et al., 2013). $LinB_{B90A}$ hydrolytically dechlorinates the metabolite 2,3,4,5,6-pentachlorocyclohexanol (PCHL), whereas $LinB_{UT26}$ does not (Ito et al., 2007). A molecular dynamics simulation study suggests that this is mainly due to a difference in the flexibility of the entrance of the substrate access tunnel mediated by six out of the seven amino acid differences between the two enzyme variants (Okai et al., 2013).

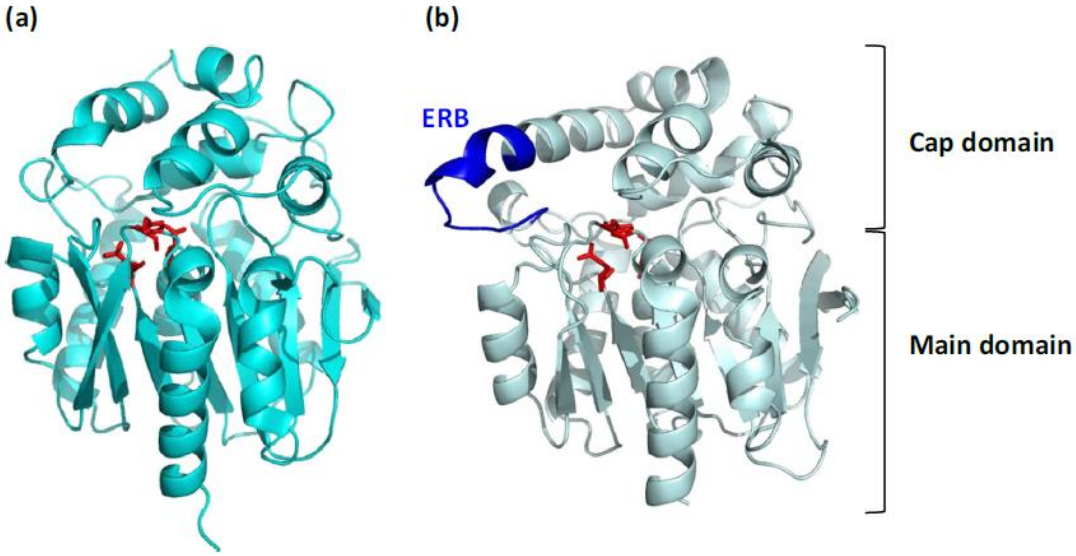

Fig. 0-4 Structures of $LinB_{UT}$ (a) (PDB code, 1CV2) and DbjA (b) (PDB code, 3A2M). Catalytic triads of LinB (Asp108, Glu132, and His272) and DbjA (Asp103, Glu127, and His280) are shown in red. The ERB fragment (^{138}HHTEVAEEQDH^{150}) of DbjA is shown in blue (Nagata et al., 2015)

0-4-3-3 DmmA

DmmA is a HLD with a known tertiary structure that was identified from a marine metagenomic consortium (Gehret et al., 2012). Inspection of its crystal structure revealed that its unusually large active site (Fig. 0-5) can accommodate bulky substrates (Daniel et al., 2015). DmmA belongs to subfamily HLD-II (Gehret et al., 2012). This protein was originally annotated as CurN, and presumed to be the final gene product of the curacin A biosynthetic gene cluster (Chang et al., 2004) from the marine *cyanobacterium Lyngbya majuscula* (now designated *Moorea producta*) (Engene et al., 2012).

DmmA exhibited an exceptionally broad substrate specificity and degraded several halogenated environmental pollutants that are resistant to other members of HLDs. In addition to having this unique substrate specificity, the enzyme was highly tolerant to organic cosolvents such as dimethyl sulfoxide, methanol, and acetone. Its broad substrate specificity, high overexpression yield, good tolerance to organic cosolvents, and a broad pH range make DmmA an attractive biocatalyst for various biotechnological applications (Buryska et al., 2018).

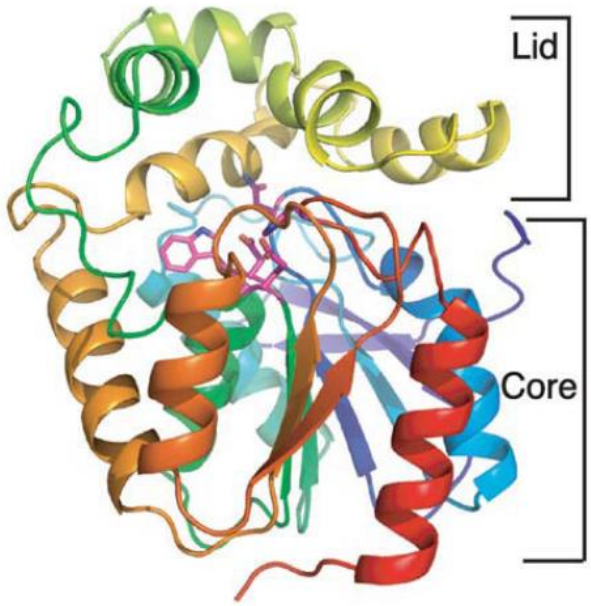

Fig. 0-5 Structures of DmmA. The stereo ribbon diagram is colored as a rainbow from blue at the N terminus to red at the C-terminus with catalytic pentad residues in stick form with magenta C (Gehret et al., 2012).

0-4-3-4 DbjA

DbjA, which was isolated from *Bradyrhizobium japonicum* USDA110 (Sato et al., 2005), possesses new substrate specificity with high catalytic activity towards β-methylated haloalkanes and sufficient enantioselectivity for industrial scale synthesis of optically pure compounds (Zbyněk Prokop et al., 2009). Comparison of the circular dichroism spectra of DbjA and other HLDs strongly suggested that DbjA contains more α-helices than the other HLDs (Sato et al., 2005) (Fig. 0-4b). A sequence comparison between DbjA and other HLDs has suggested that an 11-amino acid insertion between the main and cap domains of DbjA produces a unique active-site structure that results in the unique substrate specificity of DbjA (Sato et al., 2005). Compared with other characterized HLDs, DbjA possesses unique properties. Catalytic activity and structural stability in a broad range of pH conditions combined with high enantioselectivity with selected substrates make DbjA a very versatile biocatalyst (Chaloupkova et al., 2011). Interestingly, DbjA can kinetically discriminate between enantiomers of two distinct groups of substrates, α-bromoesters and β-bromoalkanes; it has enantioselectivity based on distinct molecular interactions, which can be modified separately by engineering of a surface loop; and also it can adopt an inverse temperature dependence of enantioselectivity for β-bromoalkanes, but not α-bromoesters, by mutating this surface loop and a flanking residue (Prokop et al., 2010).

0-4-3-5 Rluc

Luciferase (Luc) from *Renilla reniformis* (Rluc) is not HLD, but is phylogenetically associated with HLD-II. *Renilla* luciferase [*Renilla*-luciferin:oxygen 2-oxidoreductase (decarboxylating), EC 1.13.12.5] catalyzes the oxidative decarboxylation of coelenterazine in the presence of dissolved oxygen to yield oxyluciferin, CO_2, and blue light ($\lambda_{max.}$=480 nm). The molecular weight of Rluc is 36 kDa (Lorenz et al., 1991). Luciferases have become important research tools over the last two decades, due to their ability to emit light and therefore be monitored easily. These bioluminescent proteins are utilized widely as reporter genes in cell culture experiments and more recently in the context of small animal imaging (Contag et al., 1997).

The Rluc mutant (Rluc8) was screened using a consensus sequence-driven strategy, and the results obtained showed that it was 200-fold more resistant to inactivation in murine serum and its light output was 4-fold higher than the wild type. Furthermore, the structure for Rluc8, a luciferase that utilizes coelenterazine as a substrate, was clarified for the first time, demonstrating a typical α/β-hydrolase folding at 1.4 Å resolution (Loening et al., 2006).

0-4-4 Ancestral proteins

The main goal of many protein engineering strategies is to improve enzyme properties for particular industrial or medical applications. One of these strategies is ancestral sequence reconstruction (ASR) (Wijma et al., 2013), in which a hypothetical ancestral sequence of a given set of related present-day sequences is predicted from a phylogenetic tree and reconstructed in a laboratory. This work has been covered in excellent reviews (Harms & Thornton, 2010). ASR has been used to enhance enzyme thermostability (Wijma et al., 2013), solubility (Gonzalez et al., 2014), and activity (Takenaka et al., 2013), and to modify substrate specificity (Smith et al., 2013).

In the last few decades, ASR has been widely used to study the evolution and structure-function relationships of many protein families, such as GFP-like proteins (Ugalde et al., 2004), opsins (Yokoyama, 2002), steroid receptors (Ortlund et al., 2007), G-protein receptors (Babkova et al., 2017), and others (Dean et al., 2007). Using ancestral protein resurrection, two permissive and five restrictive mutations played important roles in the loss of aldosterone sensitivity in the modern glucocorticoid receptors (Ortlund et al., 2007). By introducing five conserved amino acids that were different in red and green vertebrate opsins into the ancestral background, Yokoyama et al. (Yokoyama et al., 2008) successfully recapitulated the shift in the opsin absorbance spectrum from red to green, whereas previous mutagenesis studies using modern proteins had resulted in contradictory results concerning the functional importance of key mutations.

To the best of our knowledge, only a few researches reported ASR for HLDs. Sequences of dehalogenases DbjA (Sato et al., 2007), DbeA (Chaloupkova et al., 2014), DhaA (Newman et al., 1999), DmxA (Tratsiak et al., 2013), and DmmA (Gehret et al., 2012) were predicted by ASR. The present-day enzymes display considerable functional variations even though they are all closely evolutionary related and share similar structural topology, thus providing good models to investigate structural and functional divergence in the HLD-II subfamily. Characterization of the resurrected ancestral enzymes revealed unique functional properties, including enhanced thermostability, improved specific activity, or modified substrate specificity. This study highlights that the ASR method represents a powerful strategy for constructing highly active, stable, and soluble catalysts as robust templates for directed evolution experiments (Babkova et al., 2017).

In order to predict the ancestral sequences of selected experimentally characterized enzymes from the HLD-II subfamily. Predicted ancestral sequences of LinB (*linB-dmbA-anc*) were synthesized and experimentally characterized (Jesensk áet al., 2005). The sequence identity of LinB_dmbA_anc with LinB and

DmbA is 80% and 83%, respectively (Figure 0-6). The differences between the predicted ancestor and both present-day enzymes were mapped on LinB_dmbA_anc homology model (Figure 0-7).

Fig. 0-6 Comparison of LinB_dmbA_anc sequence with LinB and DmbA sequences (red square represents catalytic residue of LinB)

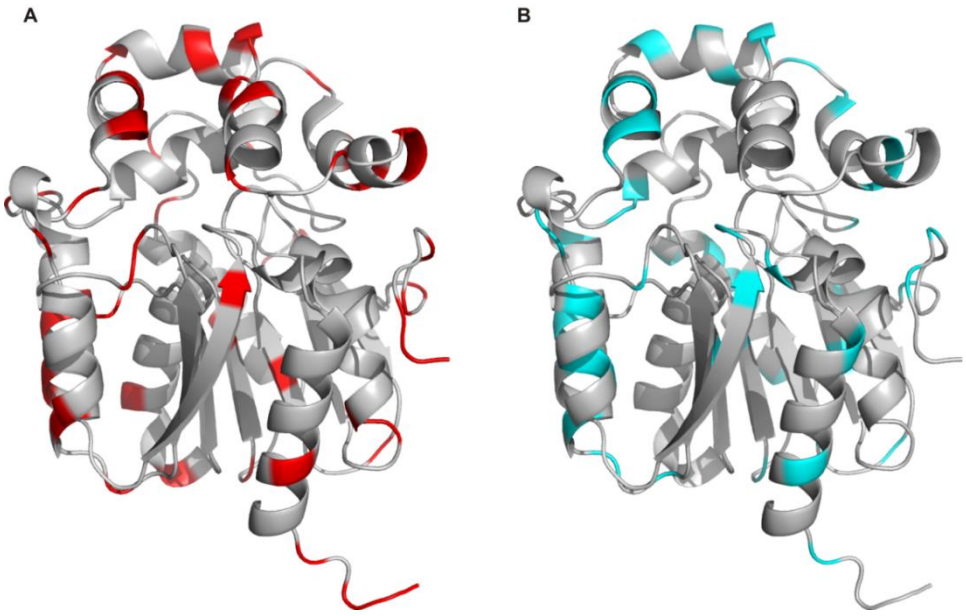

Fig. 0-7 Homology model of ancLinB-DmbA. Amino acid positions occupied by different residues in ancLinB-DmbA and LinB (A) and in ancLinB-DmbA and DmbA (B) are highlighted by red and cyan, respectively.

0-5 Mutagenesis of enzymes

Protein engineering seeks to design or discover proteins with properties useful for technological, scientific, or medical applications. Properties related to a protein's function, such as its expression level and catalytic activity, are determined by its amino acid sequence. Protein engineering inverts this relationship in order to find a sequence that performs a specified function (Yang et al., 2019). One of the goals of protein design and

protein engineering is to construct the enzymes with improved activity and modified specificity. The introduction of mutations into the genes, gene expression and protein purification take considerable effort and it is desirable to extensively characterize constructed mutants to detect even subtle changes in the specificity of the constructs (Marvanová et al., 2001).

0-5-1 Mutagenesis of HLDs

HLDs are attractive targets for protein-engineering studies aimed at improving catalytic efficiency and at broadening the range of substrate specificity for important environmental pollutants. It appears that libraries of structurally and mechanistically related enzymes will play an increasing role in biotransformation reactions, because each biocatalyst has its own characteristic substrate specificity, enantioselectivity, stability, and product inhibition data. Searching of sequenced genomes for putative HLD genes in conjunction with the overexpression and characterization of proteins encoded by these genes is one possible way for meeting the increasing demand for novel HLDs (Chan et al., 2010). Partial improvement in the catalytic properties and modification of the substrate specificities of HLDs by rational design (Chaloupková et al., 2003) and directed evolution approaches (Bosma et al., 2002) have been reported.

A variant of LinB, $LinB_{MI}$ from S*phingobium* sp. MI1205, which is 98%identical (having a difference in only 7 of the 296 amino acid residues) to $LinB_{UT}$ (Fig. 0-8), can catalyze the two-step conversion of β-HCH to 2,3,5,6-tetrachlorocyclohexane-1,4-diol (TCDL) with the first conversion step being an order of magnitude more rapid than that by $LinB_{UT}$ (Ito et al., 2007), while $LinB_{UT}$ cannot convert the PCHL (Nagata et al., 2005). The substitution of the residues forming the catalytic pocket of $LinB_{UT}$ (I134 V/A247H) resulted only a weak effect on β-HCH conversion activity. Furthermore, the reciprocal double mutant of $LinB_{MI}$ (V134I/H247A) retained relatively high $LinB_{MI}$-type activity (Ito et al., 2007). These results indicated that some of the five other residues are also important for the $LinB_{MI}$-type activity. Site-directed mutagenesis and X-ray crystallographic studies (Okai et al., 2013) indicated that all seven residues are important for $LinB_{MI}$-type catalytic activity.

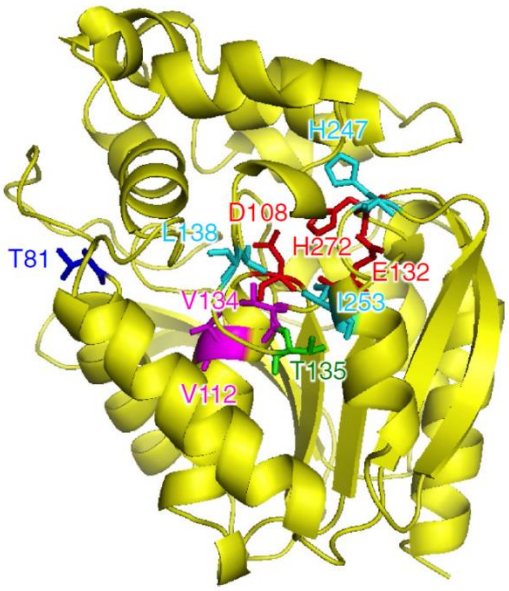

Fig. 0-8 Structure of $LinB_{MI}$ (PDB code 4H77) and location of catalytic triad (D108, E132, and H272; shown in red) and the seven dissimilar amino acid residues between $LinB_{MI}$ and $LinB_{UT}$: V134 and V112 (in magenta), L138, H247, and I253 (in cyan), T135 (in green), and T81 (in blue) (Moriuchi et al., 2014).

0-5-2 Random mutagenesis

"Random mutagenesis" is a technique that allows researchers to develop large libraries of variants of a particular DNA sequence. Once developed, these libraries can then be used for several purposes, including structure-function and directed evolution studies. Random mutagenesis is different from other mutagenesis techniques in that it does not require the researcher to have any prior knowledge about the structural properties of the DNA sequence being targeted, thus allowing for the unbiased discovery of novel or beneficial mutations. For this reason, random mutagenesis is especially useful for protein evolution studies (Forloni et al., 2018).

Error-prone PCR introduces random copying errors by imposing imperfect, and thus mutagenic, or 'sloppy', reaction conditions (e.g. by adding Mn^{2+} or Mg^{2+} to the reaction mixture). This method has proven useful both for generation of random libraries of nucleotide sequences, and also for the introduction of mutations during the expression and screening process in a mutagenesis step (Pritchard et al., 2005). Many researches had obtained excellent mutants with higher activity, thermostability, specific activity by using error-prone PCR combine with site directed mutagenesis (Varriale et al., 2018). Fig. 0-9 showed a model of selecting good evolved protein by using error-prone PCR. The researcher begins with the gene for the parent protein. This parent gene is randomly mutagenized by using error-prone PCR or some similar technique. The library of mutant genes is then used to produce mutant proteins, which are screened or selected for the desired target property (e.g., improved enzymatic activity or increased stability). Mutants that fail to show improvements in the screening/selection are typically discarded, while the genes for the improved mutants are used as the parents for the next round of mutagenesis and screening. This procedure is repeated until the evolved protein exhibits the desired level of the target property.

Compared with site-directed mutagenesis, error-prone PCR offers a more natural way to improve the stabilities or biochemical functions of proteins by repeated rounds of mutation and selection. It could illustrate which one or some mutation sites would be useful during the evolution process. Until now, to our best knowledge, there was no research reported evolved or novel HLDs only by using error-prone PCR.

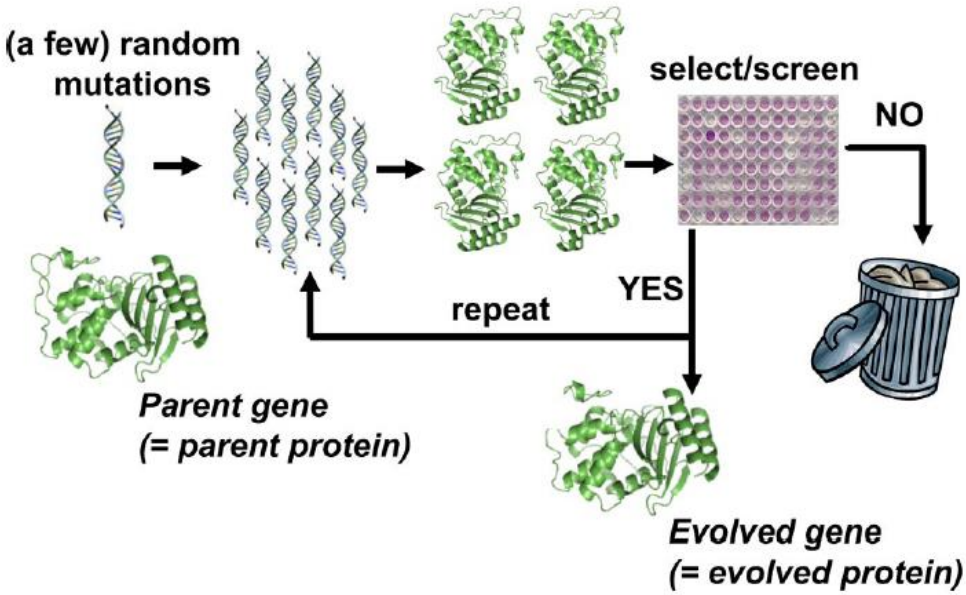

Fig. 0-9 Schematic outline of a typical directed evolution experiment (Bloom et al., 2009).

0-6 Purposes of this study

Various natural HLDs are known, and their activities can be changed dramatically by only small number of mutations, and many fundamental knowledge related to the reaction mechanisms of HLDs has been accumulated. Thus, HLDs are good materials not only for demonstrating the process and mechanism of functional evolution of enzymes but also for engineering of enzymes with novel catalytic activity. It is also suggested that function of HLDs can be evolved rapidly in sphingomonads. LinB is one of prototypical HLDs and was originally identified as an enzyme necessary for utilization of γ-HCH. There are various γ-HCH degraders have been isolated from HCH-isomers-contaminated sites around the world, and they also have identical or almost identical LinBs. Until now, no γ-HCH degrader has been reported that uses other HLDs besides LinB for the γ-HCH utilization. To get some insights into the process and mechanisms of functional evolution of HLDs toward the γ-HCH utilization, the followings are conducted in this study:

1. Construction and characterization of the *linB*-replacement strains.
2. Construction of *in vivo* and *in vitro* evolution system of HLDs toward the γ-HCH utilization.
3. Purification and characterization of the putative evolved HLDs.

Chapter 1 Construction and characterization of the *linB*-replacement strains

1-1 Background

As described in background section, sphingomonads seem to have ideal background for functional evolution of catabolic enzymes for various recalcitrant hydrophobic compounds. In this study, *Sphingobium japonicum* UT26 was used as a host for *in vivo* evolution system, because functional evolution of HLDs is expected to occur rapidly in sphingomonads represented by the case of LinB variants. The *linB* gene has variants whose protein products are different with a small number of amino-acid residues, and $LinB_{UT}$ and $LinB_{MI}$ are 98% identical but their β-HCH degradation activity are remarkably different. The important point is that the sequence variations in such variants are non-synonymous substitutions, which strongly suggests that the *linB* gene are still evolving at high speed under strong selection pressures (Nagata et al., 2015). In addition, although LinB is the only HLD to date involved in the γ-HCH degradation, other HLDs seem to have a chance to evolve toward the γ-HCH degradation by a small number of mutations.

In this chapter, as the first step to get some insights into the evolution process of HLDs toward γ-HCH utilization, *S. japonicum* UT26-derivative strains, in which the $linB_{UT}$ gene was replaced by other HLD or its homologue genes including the putative ancestral genes, were constructed and characterized.

1-2 Materials and methods

1-2-1 Strains, plasmids, medium composition and culture condition

The strains and plasmids used in this chapter were shown in Table 1-1. *E. coli* cells were incubated by using LB medium and *Sphingobium* strains were incubated by using 1/3LB medium. Spot assay for estimating the γ-HCH utilization ability was conducted by using W minimal salt medium containing 750 ppm of γ-HCH at final concentration as a sole carbon source. Compositions of these mediums were shown in Table 1-2. The solid medium was prepared by the addition of 1.5% (w/v) agar. Antibiotics were used at the final concentrations of 25 μg/mL for kanamycin (Km), 100 μg/mL for ampicillin (Ap), 50 μg/mL for streptomycin (Sm), and 10 μg/mL gentamycin (Gm). The incubation temperature of *E. coli* and *Sphingobium* cells was 37℃ and 30℃, respectively. Strains were stocked by addition of 15% glycerol at -80℃.

1-2-2 DNA manipulations

Established methods were employed for DNA manipulations. Plasmids were extracted by using LaboPass™ Plasmid Mini (COSMO Genetech) according to the attached instruction. Ligation of DNA was conducted by using Takara Ligation kit Mighty Mix (Takara). Gibson Assembly kit (New England BioLabs) was also used for assembling of DNA fragments. HIT Competent *E.coli* DH5α 618 cells (RBC Bioscience) were used for transformation of *E. coli*. Hot Start Taq (NEB) and Q5 High-Fidelity DNA Polymerase (NEB) were used for polymerase chain reaction (PCR). When conducting colony PCR, a little cells were picked by toothpicks and mixed with reagents. Primers used in this chapter were shown in Table 1-3. The nucleotide sequences were determined using an ABI PRISM 3130*xl* sequencer and ABI Prism Big Dye Terminator Kit, version 3.1 (Applied Biosystems). The nucleotide and protein sequences were analyzed using the Genetyx program,

version 13 (SDC Inc., Tokyo). The bacterial cells were transformed by electroporation (EP). Cells grown on 1/3LB agar medium for two days were collected by an inoculation loop, washed three times with ice-cold EP buffer (1 mM MOPS and 10% glycerol), diluted appropriately, and mixed with DNA solution. The suspension was transferred to an EP cuvette with a 1 mm gap. EP was conducted under the conditions of 1.8 kV, 200 Ω and 25 μF. After the pulse, 1 mL of ice-cold 1/3LB medium was immediately added, then incubated for 2-10 h and spread onto a 1/3LB agar medium containing appropriate antibiotics.

1-2-3 Construction of the *linB*-deletion and replacement strains

The *linB*-deletion mutant, in which just open reading frame of the *linB* gene has been deleted, was constructed by allelic exchange mutagenesis of *S. japonicum* UT26 using pK18mobsacB (Schäfer et al., 1994), which has the *sacB* gene for counter selection (Schweizer, 1992). The 1.5-kb upstream and downstream regions of the *linB* gene in *S. japonicum* UT26 were cloned into pK18mobsacB, and the resultant plasmid pK18mobsacB::linB_up_down was introduced into UT26 by EP, and the Km^r transformant into which the plasmid had been integrated via single crossover-mediated homologous recombination was selected. The Km^r Suc^S transformant was inoculated on a 1/3LB plate containing sucrose (10%), and the Km^s Suc^r clones were selected. Finally, the *linB*-deletion strain was selected by PCR, and named UTDB2. For introduction of other HLD genes into the *linB* site, allelic exchange mutagenesis of *S. japonicum* UTDB2 was carried out by using pAK405, which has the streptomycin-sensitive *rpsL* allele (*rpsL1*) as a counterselection marker (Kaczmarczyk et al., 2012). Firstly, a plasmid pADB1 (Fig. 1-1) was constructed, which has the 1-kb upstream and downstream regions of the *linB* gene in pAK405. The $linB_{MI}$, *dbjA*, *dmmA*, *rluc*, *rluc_anc*, *rluc_ancM*, and *linB_dmbA_anc* genes were introduced into pADB1, and the resultant plasmids were named pAMM1, pABJ1, pAMM1, pARL1, pALA1, pALA2, and pABA1, respectively. These plasmids were introduced into UTDB2 by EP, and the Km^r Sm^s transformants into which these plasmids had been integrated via single crossover-mediated homologous recombination were selected. The Km^r Sm^s transformants was inoculated on a 1/3LB plate containing Sm, and the Km^s Sm^r clones were selected (Fig. 1-2). Finally, the strains that have the $linB_{MI}$, *dbjA*, *dmmA*, *rluc*, *rluc_anc*, *rluc_ancM*, and *linB_dmbA_anc* genes in the $linB_{UT}$ site were selected by PCR among the Km^s Sm^r clones and designated as UTBM1, UTBJ1, UTMM1, UT2RL1, UTLA1, UTLA2, and UTBA1, respectively. Primers used for amplification and plasmids used as templates of the genes are shown in Table 1-3. The primer sets were designed by NEBuilder (http://nebuilder.neb.com) for assembly with *Eco*RV and *Hin*dIII-digested pADB1 by using a Gibson Assembly system (NEB). UTDB2DAX, in which both the *linB* and *adhX* genes were deleted, was constructed from UTDB2 by the same procedure using pAAXD1, which is a pAK405-based plasmid for deletion of the *adhX* gene (Inaba et al., 2020). DAX series strains, UTBM1DAX, UTBJ1DAX, UTMM1DAX, UTRL1DAX, UTLA1DAX, UTLA2DAX, and UTBA1DAX having the $linB_{MI}$, *dbjA*, *dmmA*, *rluc*, *rluc_anc*, *rluc_ancM* and *linB_dmbA_anc* genes, respectively, in the $linB_{UT}$ site were constructed from UTDB2DAX by the same procedure using pABM1, pABJ1, pAMM1, pARL1, pALA1, pALA2, and pABA1, respectively.

1-2-4 GC analysis for the γ-HCH degradation

Cells were collected and washed, and then dissolved in PBS at final concentration of 5 mg cells /10 μL, and the 10 μL of cell suspension was added into 1 mL reaction mixture (W medium containing 176 mM of γ-HCH) and vortex to start reaction. The reaction mixture was incubated at 30^oC for 60min, and 100 μL of reaction mixture was collected, vortexed with the same volume of ethyl acetate containing 2 ppm of dieldrin as the internal standard, centrifuged, and the upper layer was used to the GC analysis. GC equipped with a ^{63}Ni

electron capture detector (ECD) and Rtx-1 capillary column (30 m×0.25 mm×0.25 μm; Restek) was used, and condition for the analysis is shown in Table 1-4. The concentration of γ-HCH and intermediates were quantified from peak area by using standard chemicals.

1-2-5 Assay for the γ-HCH utilization activity on solid medium (spot assay)

Bacterial cells grown on 1/3LB agar medium were collected by inoculation loop and washed three times with PBS. The bacterial cell suspension was diluted by PBS and adjusted to 100 mg cells/mL. This suspension was diluted 10 (10 mg cells/mL) and 10^2 (1 mg cells/mL) fold, and each 10 μL aliquots of each dilution were spotted on solid W minimal salt medium containing γ-HCH (750 ppm) or glucose (0.2%), or without adding any carbon sources, and incubated for 5 days at 30^{o}C.

Table 1-1 Bacterial strains and plasmids used in this chapter

Strains or plasmid	Relevant characteristics	Source or reference
Sphingomonads		
Sphingobium japonicum UT26S	γ-HCH degrader	(Nagata et al., 2011)
Sphingobium japonicum UTDB2	Δ*linB*	This study
Sphingobium japonicum UTBM1	*linB* -> $linB_{MI}$	(Ito et al., 2007)
Sphingobium japonicum UTBJ1	*linB* -> *dbjA*	(Sato et al., 2005)
Sphingobium japonicum UTMM1	*linB* -> *dmmA*	(Gehret et al., 2012)
Sphingobium japonicum UTLA1	*linB* -> *rluc_ancM*	(Chaloupkova et al., 2019)
Sphingobium japonicum UTLA2	*linB* -> *rluc_anc*	(Chaloupkova et al., 2019)
Sphingobium japonicum UTRL1	*linB* -> *rluc*	(Loening et al., 2006)
Sphingobium japonicum UTBA1	*linB* -> *linB_dmbA_anc*	(Jesensk áet al., 2005)
Sphingobium japonicum UT26DAX	γ-HCH degrader, Δ*adhX*	(Inaba et al., 2020)
Sphingobium japonicum UTDB2DAX	Δ*linB*, Δ*adhX*	This study
Sphingobium japonicum UTBM1DAX	*linB* -> $linB_{MI}$, Δ*adhX*	This study
Sphingobium japonicum UTBJ1DAX	*linB* -> *dbjA*, Δ*adhX*	This study
Sphingobium japonicum UTMM1DAX	*linB* -> *dmmA*, Δ*adhX*	This study
Sphingobium japonicum UTLA1DAX	*linB* -> *rluc_ancM*, Δ*adhX*	This study
Sphingobium japonicum UTLA2DAX	*linB* -> *rluc_anc*, Δ*adhX*	This study
Sphingobium japonicum UTRL1DAX	*linB* -> *rluc*, Δ*adhX*	This study
Sphingobium japonicum UTBA1DAX	*linB* -> *linB_dmbA_anc*, Δ*adhX*	This study
E.coli		
DH5α	*recA1 endA1 gyrA96 thi-1 hsdR17 supE44 relA1 Δ(lacZYA-argF) Φ80lacZΔM15*	(Marietta et al., 1988)
Plasmid		
pK18mobsacB	Suicide plasmid for gene deletion, Km^r	Schgfer et al., 1994
pK18mobsacB_linB_up_down	pK18mobsacB::linB_up_down	This study
pAK405	*ori*pBR322, RP4 *oriT*, *rpsL1*, Km^r	(Kahm et al., 2010)
pADB1	pAK405::linB_up_down_EPH	This study
pBDQ1	pBBR MCS-1 (Cm) -UT26$dnaQ^{exo}$	This study
pABM1	pAK405::linB_up_down_$linB_{MI}$	This study
pABJ1	pAK405::linB_up_down_dbjA	This study
pAMM1	pAK405::linB_up_down_dmmA	This study
pALA1	pAK405::linB_up_down_rluc_ancM	This study
pALA2	pAK405::linB_up_down_rluc_anc	This study
pARL1	pAK405::linB_up_down_rluc	This study
pABA1	pAK405::linB_up_down_linB_dmbA_anc	This study

Table 1-2 Compositions of medium

1/3LB broth	
Per liter.	
Bacto tryptone	3.3g
Bacto yeast extract	1.7g
NaCl	5g
pH 7.0	

LB broth	
Per liter.	
Bacto tryptone	10g
Bacto yeast extract	5g
NaCl	5g
pH 7.0	

W medium	
Per liter	
KH_2PO_4	1.7g
Na_2HPO_4	9.8g
$(NH_4)_2SO_4$	1.0g
$MgSO_4$	48.7mg
$FeSO_4$	0.52mg
MgO	10.75mg
$CaCO_3$	2.0mg
$ZnSO_4$	0.81mg
$CuSO_4$	0.16mg
$CoSO_4$	0.15mg
H_3BO_3	0.06mg

1/10 W was made in which the concentrations of KH_2PO_4, Na_2HPO_4 and $(NH_4)_2SO_4$ were diluted to 1/10 those in the W medium.

Table 1-3 Primers used in this chapter

Primer	Sequence (5'→3')	Purpose
linB_up_FW	CTAGAGTCGACCTGCACCGGGTTTCCCCGCCGACCCCGTC	synthesis of pK18mobsacB::linB_up_down and pK18mobsacB::linB_up_MI_down
linB_up_RV	GTTCCGGACGATATTCTCCTTGAGCGATTTTC	synthesis of pK18mobsacB::linB_up_down and pK18mobsacB::linB_up_MI_down
linB_down_FW	GAATATCGTCCGGAACCGGCTCATTTTCTAAG	synthesis of pK18mobsacB::linB_up_down and pK18mobsacB::linB_up_MI_down
linB_down_RV	GTGCCAAGCTTGCATGTGGCCTTCGGCATTGCCGAGATGC	synthesis of pK18mobsacB::linB_up_down and pK18mobsacB::linB_up_MI_down
pADB1_rluc_F	ctcaaggagaatatcgATGACTTCGAAAGTTTATGATC	Amplification of *rluc*
pADB1_rluc_R	tgagccggttccggaTTATTGTTCATTTTTGAGAACTCG	Amplification of *rluc*
pADB1_rluc_anc_opt_F	ctcaaggagaatatcgATGGTTAGCGCAAGCCAGCG	Amplification of *rluc_anc*
pADB1_rluc_anc_opt_R	tgagccggttccggaTTATTTGGTCAGTTCGTTCAGAAAATCG	Amplification of *rluc_anc*
pADB1_linB_dmbA_anc_F	cgctcaaggagaatatcgATGACCGCACTGGGTGCAG	Amplification of *linB_dmbA_anc*
pADB1_linB_dmbA_anc_R	gaaaatgagccggttccggaTTAAACACCGGCTGCTGCACG	Amplification of *linB_dmbA_anc*
linB_up_1000_CF	GGTATCATGTCAACTGGGGC	Construction of pARL1, pALA2 and pABA1
linB_down_1000_CR	TGGCATGGCACCGAGAAGGC	Construction of pARL1, pALA2 and pABA1
linB_down_1000_CR2	GGCCACGTCGAGCACAAGCTC	Construction of pARL1, pALA2 and pABA1
linB_down_1000_CR3	GATAATAGGCTTCCCGCCCGGAG	Construction of pARL1, pALA2 and pABA1
M4out	GCTGCAAGGCGATTAAG	Construction of pARL1, pALA2 and pABA1
RVout	GGCTCGTATGTTGTGTG	Construction of pARL1, pALA2 and pABA1

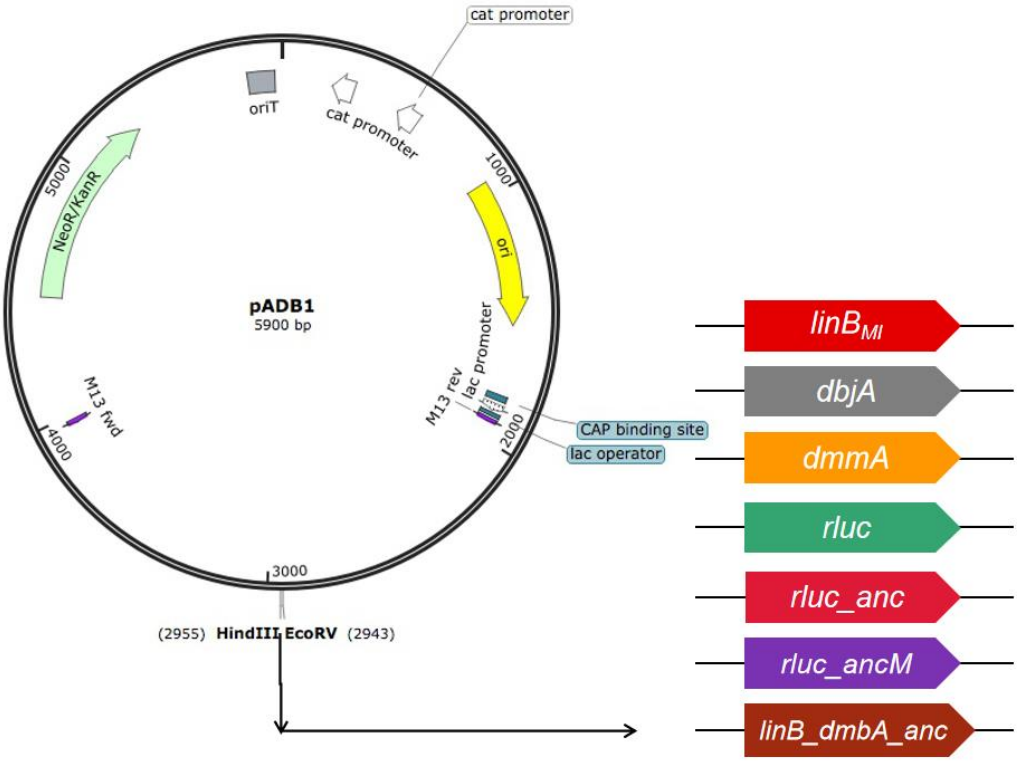

Fig. 1-1 pADB1 and its derivatives with *linB*$_{MI}$, *dbjA*, *dmmA*, *rluc*, *rluc_anc*, *rluc_ancM* and *linB_dmbA_anc*

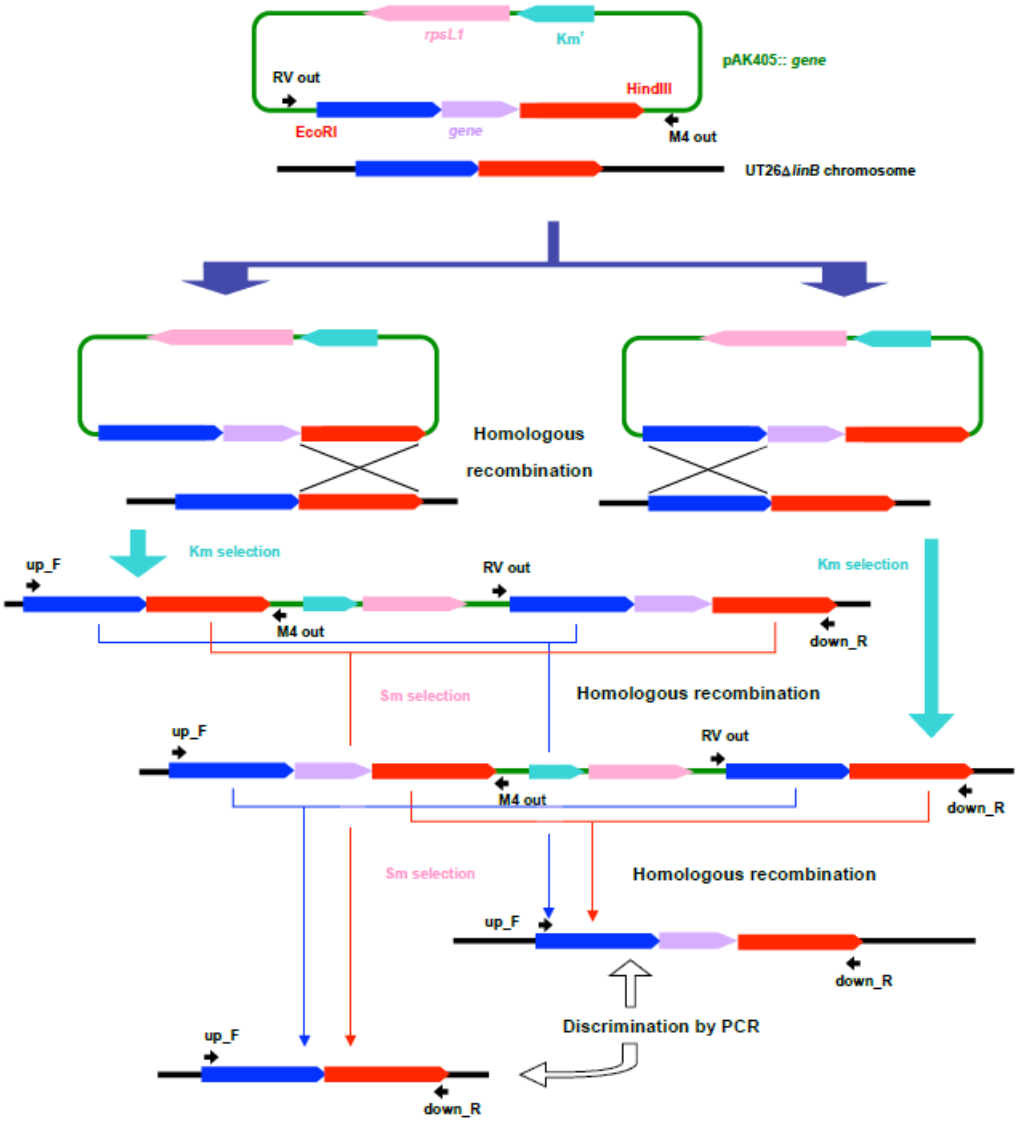

Fig. 1-2 Strategy for construction of the *linB*-replacement strains

Table 1-4 Condition of GC analysis

Column	Rtx-1
Column temperature	160℃-280℃(20℃/min)
Injection temperature	280℃
Gas flow rate	30mL/min

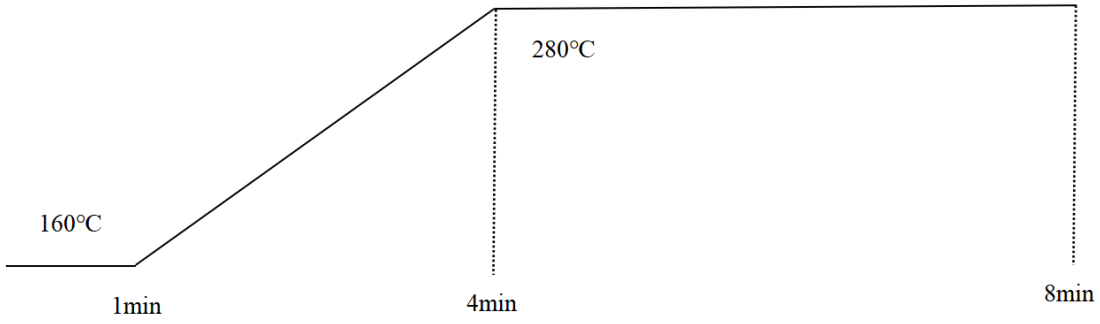

1-3 Results

1-3-1 Construction of the *linB*-replacement strains

Firstly, the *linB*-deletion strain UTDB2 was constructed, in which just open reading frame of the *linB* gene was deleted. This strain can be used as a negative control for the cell having no LinB activity. Indeed, UTDB2 showed neither the LinB activity in the γ-HCH degradation pathway nor the γ-HCH-utilization activity on the γ-HCH plate (see below). Then, pADB1 (Fig. 1-1), which has the 1-kb upstream and downstream regions of *linB*, was constructed by using pAK405 as a base to make it easier to construct plasmids for introduce of various genes into the *linB* site. The resultant plasmids were introduced into UTDB2 and the strains that have the *linB*$_{MI}$, *dbjA*, *dmmA*, *rluc*, *rluc_anc*, *rluc_ancM* and *linB_dmbA_anc* genes (Table 1-5) in the *linB* site were constructed (Fig. 1-2), and named UTBM1, UTBJ1, UTMM1, UT2RL1, UTLA1, UTLA2, and UTBA1, respectively (Fig.1-3).

The phylogenetical relationships of HLDs or HLD homologues used in this study is shown in Fig. 1-4. LinB$_{MI}$ from *Sphingobium* sp. MI1205 is 98% identical (7 amino acid differences among total 296 amino acids) with LinB$_{UT}$ but shows higher activity toward β-HCH than LinB$_{UT}$ (Ito et al., 2007). DbjA is a HLD from *Bradyrhizobium japonicum* USDA110, which prefers bulky substrates (Sato et al., 2005). DmmA is a HLD from a marine metagenome and has an unusually large active site, and thus shows the most versatile substrate specificity among known HLDs (Gehret et al., 2012). Rluc is *Renilla*-luciferin 2-monooxygenase from *Renilla reniformis* (Lorenz et al., 1991), which has luciferase activity toward coelenterazine by monooxygenation mechanism. Rluc is monooxygenase, whose reaction mechanism is completely different from that of HLD, but its amino acid sequence is phylogenetically close to the HLD-II subfamily of HLDs (Fig. 1-6). To date, HLD activity of Rluc toward any HLD substrates has not been detected, but Rluc is considered to be an excellent candidate for investigating the functional evolution of HLDs (Nagata et al., 2015). Rluc_anc is putative ancestral protein of LinB and Rluc (Fig. 1-4) that have been designed *in silico* (Chaloupkova et al., 2019). Rluc_ancM, which was unexpectedly produced on the cloning process, has just one amino acid difference R7P with Rluc_anc (Fig. 1-5). LinB_dmbA_anc is a putative ancestral protein of LinB and DmbA (Fig. 1-4). DmbA is a HLD from *Mycobacterium bovis* 5033/66 and only single amino acid is different with DmtA (K120 is N in DmbA) from *Mycobacterium tuberculosis* (Jesenská et al., 2005).

DAX-series strains, UTBM1DAX, UTBJ1DAX, UTMM1DAX, UTRL1DAX, UTLA1DAX, UTLA2DAX, and UTBA1DAX, were also constructed from the strain UTDB2DAX, in which the *adhX* gene is also deleted in addition to the *linB* gene. If the *adhX* gene is expressed by spontaneous mutation, the strain become to be able to grow on the solid minimal salt medium without adding any carbon sources (Inaba et al., 2020), and thus DAX series strains have a merit to avoid the selection of false positive mutants that grow well on the γ-HCH plate in the next experiments.

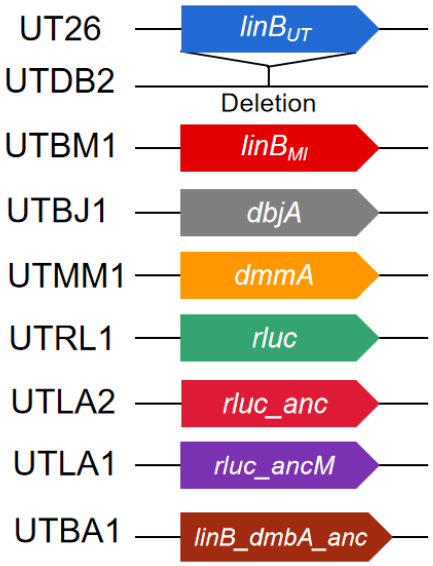

Fig. 1-3 The *linB*-replacement strains construed in this chapter

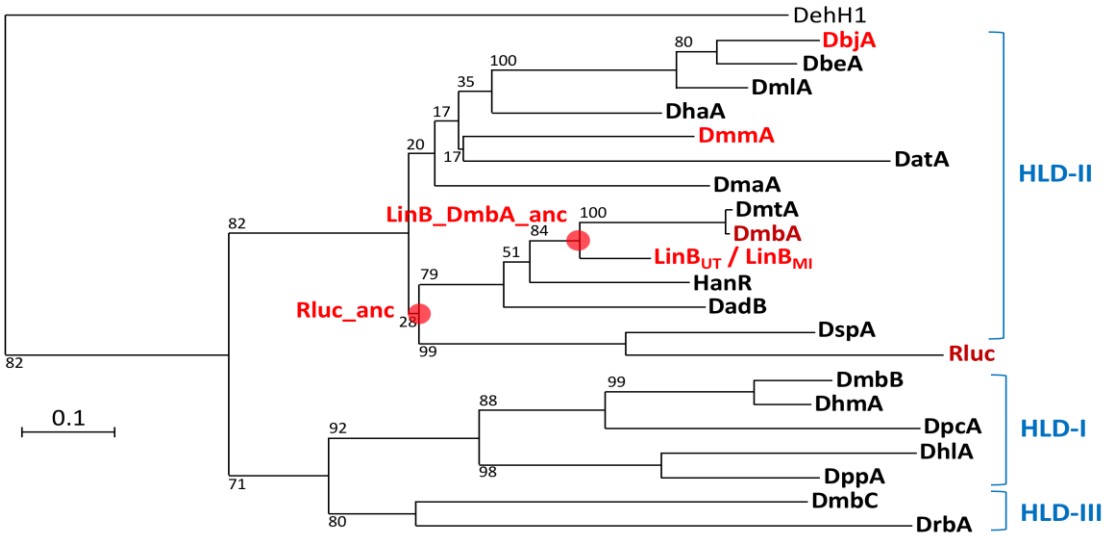

Fig. 1-4 Phylogenetic tree of HLDs and Rluc. HLDs, Rluc, and putative ancestral proteins used in this study are shown in red.

Table 1-5 Specific information of *linB* replacement strains and their corresponding *hlds*

Strain	*hld*	Source of *hld*	Characteristics of HLD	Ref. For *hld*
UT26S	$linB_{UT}$	*Sphingobium japonicum* UT26	γ-HCH degrader	(Nagata et al., 2011)
UTDB2	Δ$linB_{UT}$			(Inaba et al., 2020)
UTBM1	$linB_{MI}$	*Sphingobium sp.* MI1205	Higher activity to β-HCH than $LinB_{UT}$; 7AA differences compared to $LinB_{UT}$	(Ito et al., 2007)
UTBJ1	*dbjA*	*Bradyrhizobium japonicum* USDA110 (forming root nodules on soybeans)	Preference for bulky substrates	(Sato et al., 2005)
UTMM1	*dmmA*	Marine metagenome, synthesized	The most versatile among known HLDs	(Gehret et al., 2012)
UTLA1/LA2	*rluc_anc* */rluc_ancM*	*In silico* design, synthesized	A putative common ancestor of LinB and *Renilla*-luciferin 2-monooxygenase (*Renilla* luciferase) from *Renilla reniformis*; Rluc (monooxygenase) activity	(Chaloupkova et al., 2019)
UTRL1	*rluc*	*Renilla*-luciferin 2-monooxygenase	Luciferase activity toward coelenterazine, is phylogenetically close to the HLD-II subfamily.	(Loening et al., 2006)
UTBA1	*linB_dmbA_anc*	*Mycobacterium bovis* 5033/66	K120 in DmtA is N in DmbA	(Jesenská et al., 2005)

Fig. 1-5 Amino acid sequence alignment of Rluc, Rluc_anc and Rluc_ancM (red squares represent catalytic residues)

1-3-2 γ-HCH degradation activity of the *linB*-replacement strains

S. japonicum UT26 degrades γ-HCH through the pathway shown in Fig. 1-6. γ-HCH is converted by two steps of LinA-catalyzed dehydrochlorination via γ-pentachlorocyclohexene (γ-PCCH) to 1,3,4,6-tetrachloro-1,4-cyclohexadiene (1,4-TCDN), and this compound is productively metabolized by two steps of LinB-catalyzed hydrolytic dehalogenation via 2,4,5-trichloro-2,5-cyclohexadiene-1-ol (2,4,5-DNOL) to 2,5-dichloro-2,5-cyclohexadiene-1,4-diol (2,5-DDOL). 2,5-DDOL is converted to 2,5-dichlorohydroquinone (2,5-DCHQ) by dehydrogenase LinC, and 2,5-DCHQ is further metabolized. In this pathway, two substrates of LinB, 1,4-TCDN and 2,4,5-DNOL, are unstable and have not been directly detected, and their production is predicted by the production of two dead end products, 1,2,4-trichlorobenzene (1,2,4-TCB) and 2,5-dichlorophenol (2,5-DCP), respectively (Nagata et al., 1993). By the GC assay used in this study, we can detect γ-HCH, γ-PCCH, 1,2,4-TCB, 2,5-DCP, 2,5-DDOL, and 2,5-DCHQ, and the important point is that the production of 2,5-DCP, 2,5-DDOL, and 2,5-DCHQ means that the cells have the LinB activity.

The γ-HCH degradation activity of the constructed strains was examined by GC analysis and the concentration of remaining γ-HCH and metabolites produced after the incubation for 60 min are shown in Fig. 1-7. As predicted, 2,5-DCHQ and 2,5-DCP were detected in *S. japonicum* UT26 and UTBM1 that have the *linB* gene, while only γ-PCCH and 1,2,4-TCB were detected as metabolites in UTDB2 lacking the *linB* gene. In UTBJ1, UTRL1, and UTBA1 only γ-PCCH and 1,2,4-TCB were detected, indicating that DbjA, Rluc, and LinB_dmbA_anc have no LinB activity. On the other hand, 2,5-DCHQ and 2,5-DCP were detected in

UTMM1, UTLA1, and UTLA2, indicating that DmmA, Rluc_anc, and Rluc_ancM have the LinB-like activity. The same tendency was obtained in the experiment using the DAX-series strains (Fig. 1-8), supporting the conclusion that DmmA, Rluc_anc, and Rluc_ancM have the LinB-like activity

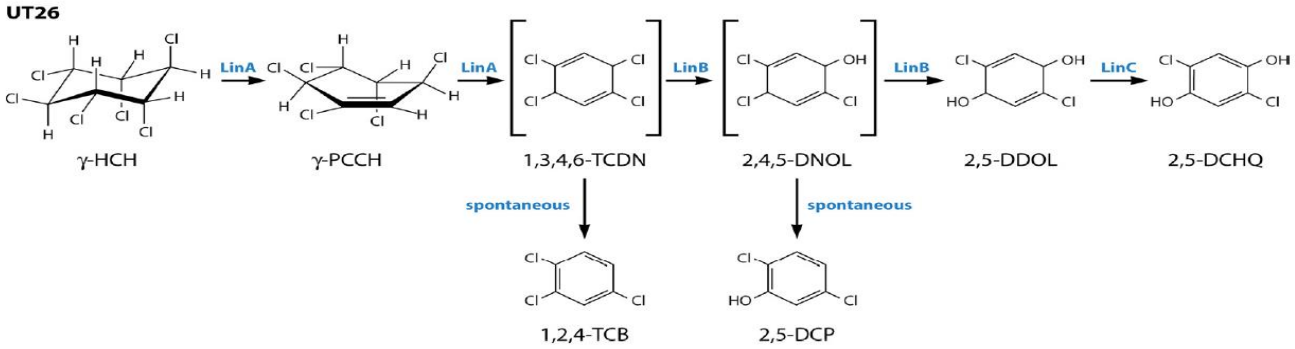

Fig. 1-6 Upstream degradation pathway of γ-HCH in *S. japonicum* UT26

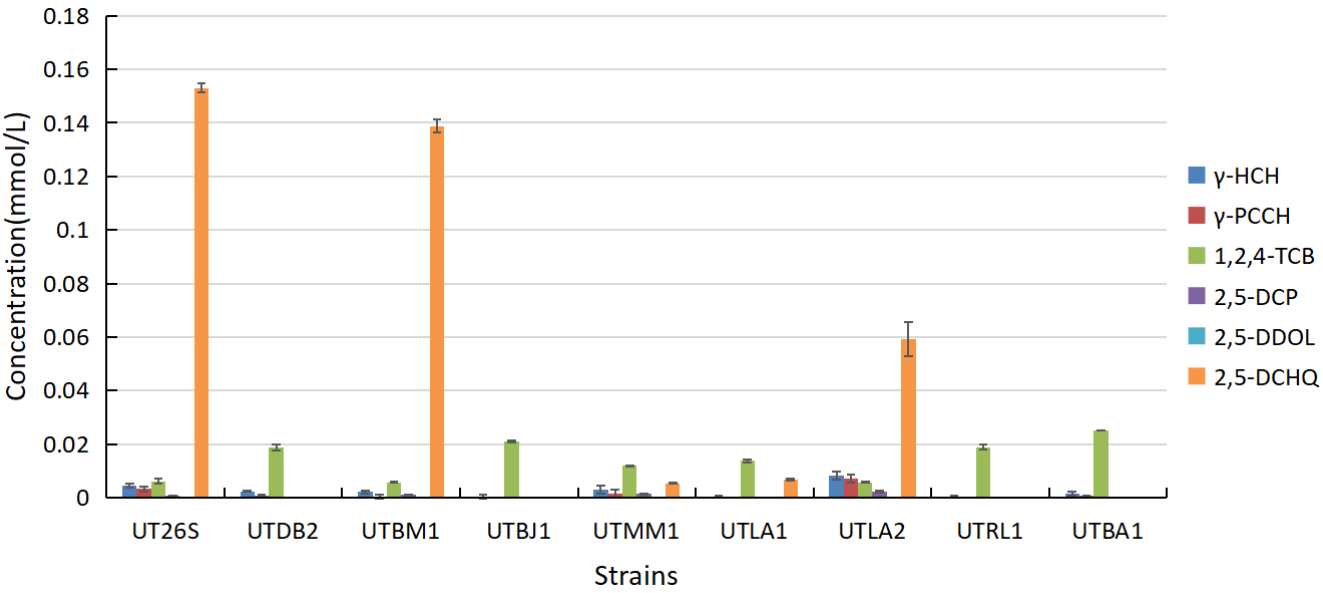

Fig. 1-7 GC analysis of *Sphingobium japonicum* UT series strains

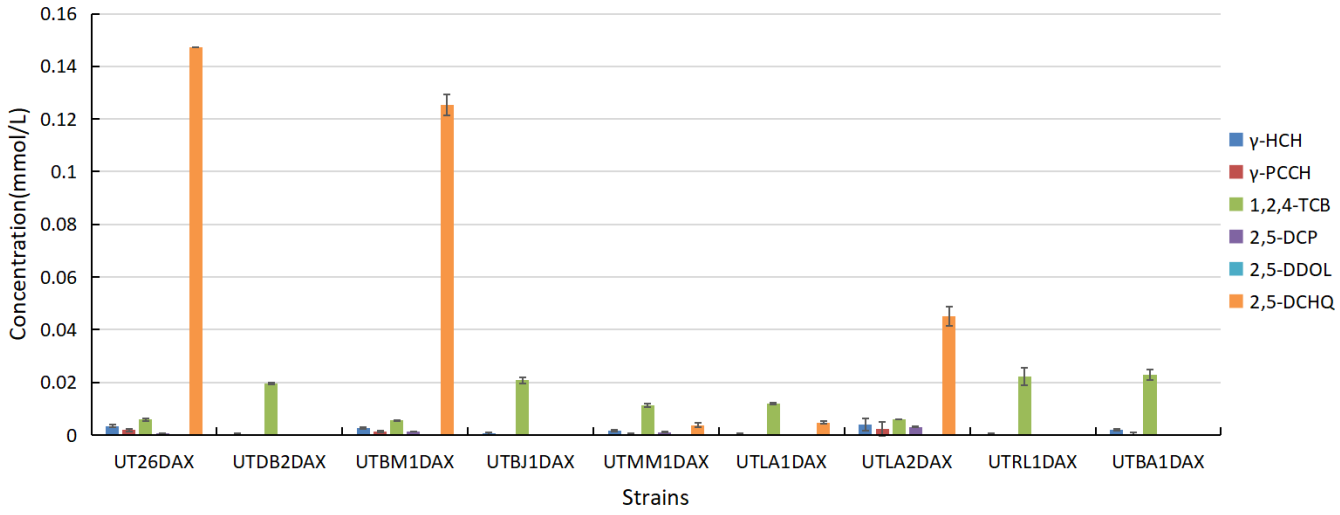

Fig. 1-8 GC analysis of *Sphingobium japonicum* UT-DAX-series strains

1-3-3 γ-HCH utilization activity of the *linB*-replacement strains

γ-HCH utilization activity of the constructed strains was examined to see the growth of cells on the solid W minimal salt medium containing γ-HCH as a sole carbon source (γ-HCH plate). As positive and negative control, cells were also spotted on the solid W minimal salt medium containing glucose (Glucose plate) and adding no carbon source (w/o C plate), respectively. Strains that utilize γ-HCH increase the cell number to the visible state accompanying with clear zone around the spotted area on the γ-HCH plate. Three different concentrations of cells (100, 10 and 1 mg cells/mL) were spotted to distinguish the small difference. As predicted, all the strains grew well on Glucose plate (Fig. 1-10A), but not on w/o C plate (Fig. 1-9A). UT26 and UTBM1 showed obvious γ-HCH utilization activity at the cell concentration of 10 and 1 mg cells/mL, while UTDB2, UTBJ1, and UTRL1 showed no γ-HCH utilization activity (Fig. 1-11A). UTLA2 showed γ-HCH utilization activity at the cell concentration of 10 mg cells/mL, and UTLA1 and UTMM1 formed larger clear zone around the spotted area than UTDB2 at the cell concentration of 100 mg cells/mL (Fig. 1-11A). The same tendency was observed in the experiment using the DAX-series strains (Fig. 1-11B). These results indicate that Rluc_anc, Rluc_ancM, and DmmA have weak LinB-like activity for the γ-HCH utilization.

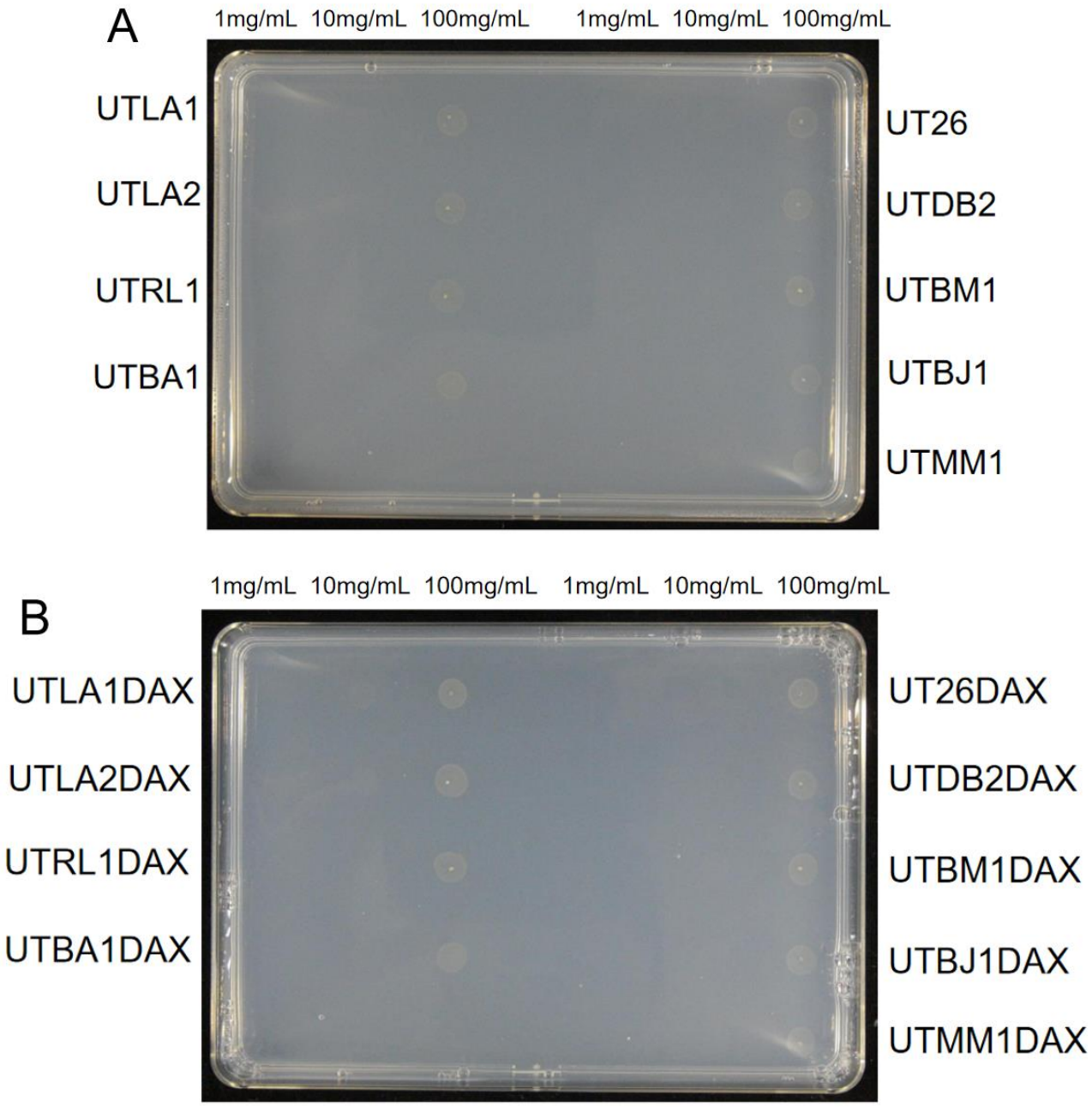

Fig.1-9 Spot assay of *Sphingobium japonicum linB* replacement strains on W plate without carbon source (2 days incubation). A. *Sphingobium japonicum* UT series strains. B. *Sphingobium japonicum* UT-DAX series strains.

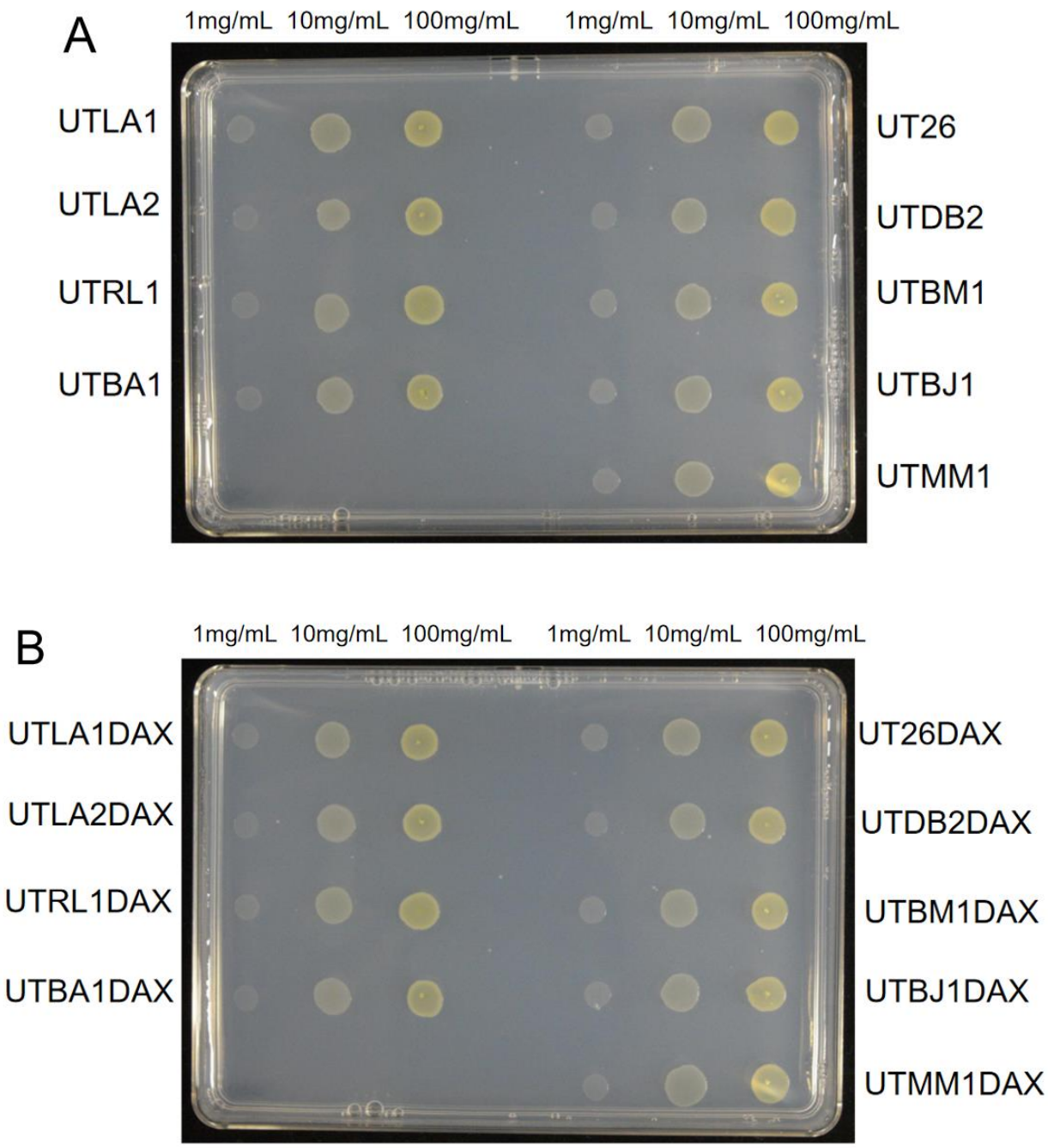

Fig.1-10 Spot assay of *Sphingobium japonicum linB* replacement strains on W plate with glucose (1 day incubation). A. *Sphingobium japonicum* UT series strains. B. *Sphingobium japonicum* UT-DAX series strains.

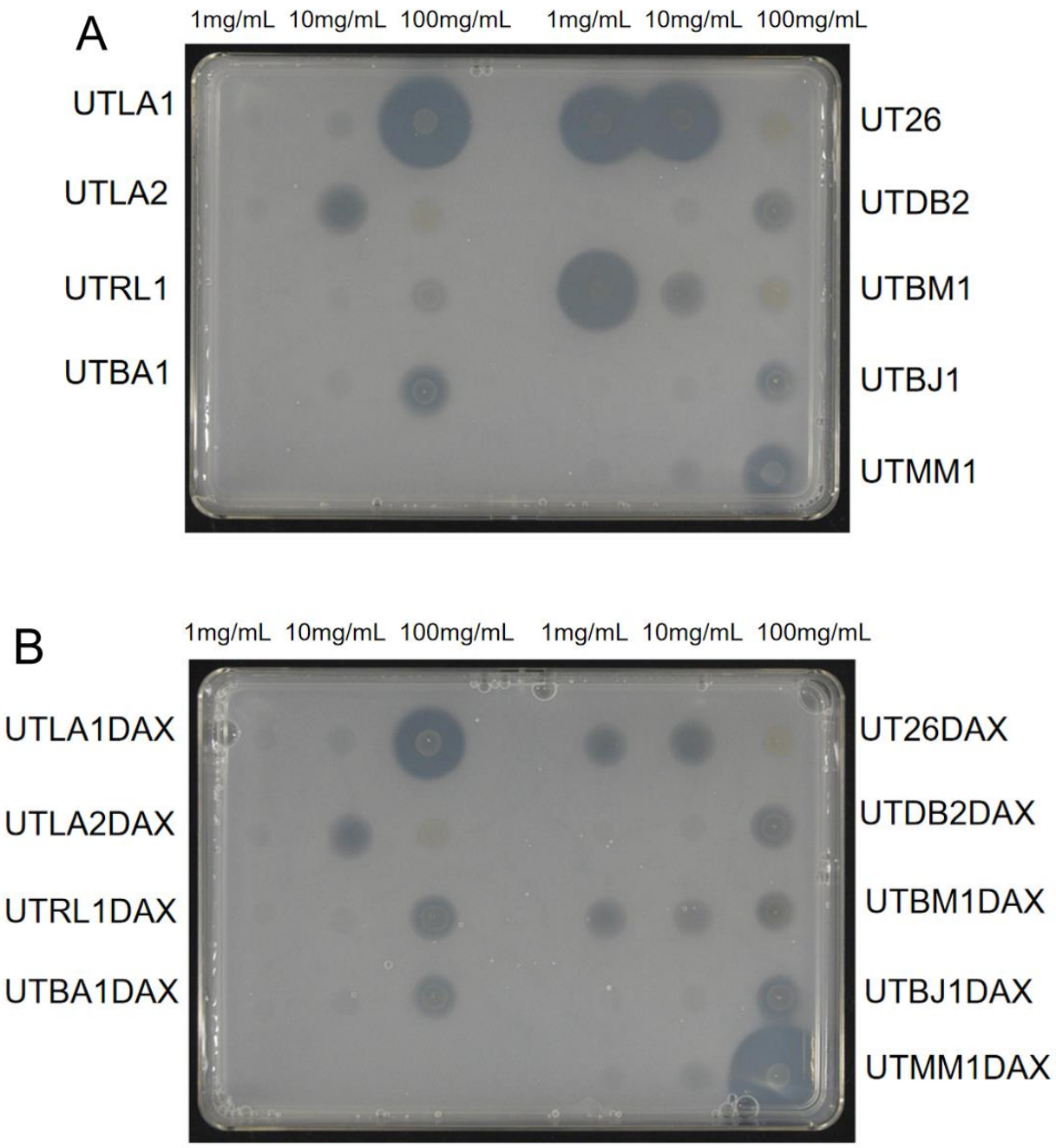

Fig.1-11 Spot assay of *Sphingobium japonicum linB* replacement strains on W-γ-HCH plate (14 days incubation). A. *Sphingobium japonicum* UT series strains. B. *Sphingobium japonicum* UT-DAX series strains.

1-4 Discussion

In this chapter, the *linB*-replacement strains of *S. japonicum* UT26 were constructed by using homologous recombination, in which the $linB_{UT}$ gene was replaced with $linB_{MI}$, *dbjA*, *dmmA*, *rluc*, *rluc_anc*, *rluc_ancM* and *linB_dmbA_anc*. GC assay for the γ-HCH degradation activity and spot assay for the γ-HCH utilization demonstrated that Rluc_anc, Rluc_ancM, and DmmA have weak LinB-like activity for the γ-HCH utilization. It was clearly demonstrated that some HLDs besides LinB can potentially be involved in the γ-HCH utilization. This result could be predicted on the basis of the facts that HLDs or its homologues are widely distributed among bacterial strains and that HLDs generally have a broad range of substrate specificities

(Koudelakova et al., 2011), but it was experimentally confirmed for the first time in this study. Especially, it is important that 'natural' HLD DmmA showed the LinB activity.

DmmA is a HLD from marine metagenome and belongs to HLD-II subfamily, but its biological source is unknown. DmmA possesses an unusually large active-site cavity comparing with other structurally characterized HLDs (Gehret et al., 2012), and shows unusual broad substrate specificity. DmmA showed activity toward all 29 substrates constituting a set of representative HLD substrates (Koudelakova et al., 2011). Additionally, DmmA is active toward all poorly degradable chlorinated environmental pollutants, *e.g.*, 1,2-dichloroethane, 1,2-dichloropropane, 1,2,3-trichloropropane, and chlorocyclohexane as well as toward newly identified substrates of this enzyme family (Daniel et al., 2015). The broad substrate specificity of DmmA may be linked to its large active site and readily accessible active site. Analysis of access tunnels using CAVER identified the widely open mouth without any sign of bottleneck, which is unique to DmmA and has never been observed with other family members (Gehret et al., 2012). This wide opening provides easy access of a large spectrum of diverse molecules to the enzyme active site. While complementary analysis of LinB revealed clear bottlenecks which separate the active site from the surrounding water solvent. All of these results suggested that DmmA possesses a combination of several unique properties attractive for practical applications.

On the other hand, it should be also noted that DbjA did not show the LinB activity, indicating that not all HLDs with broad substrate specificities show the LinB activity. DbjA from *Bradyrhizobium japonicum* USDA110 has been intensively analyzed because it shows unique substrate specificity such as a high catalytic activity for β-methylated haloalkanes and high enantioselectivity with β-brominated alkanes (Sato et al., 2005). Since this enzyme possessed unique catalytic activity, structural stability in a broad pH range, combined with high enantioselectivity with particular substrates, it still be used in the protein engineering analysis and further mutations on this enzyme will make it a very versatile biocatalyst. Determinants for the LinB activity will be revealed by comparing HLDs that show the LinB activity and those not.

Rluc_ancM seems to have higher LinB-like activity than Rluc_anc and DmmA, since (i) UTLA2 (UTLA2DAX) produced larger amount of 2,5-DCHQ and 2,5-DCP than UTLA1 (UTLA1DAX) and UTMM1 (UTMM1DAX) (Fig. 1-12 and 1-13), and (ii) UTLA2 (UTLA2DAX) grew well at the cell concentration of 10 mg cells/mL than UTLA1 (UTLA1DAX) and UTMM1 (UTMM1DAX) (Fig. 1-11). It is interesting because only one amino acid residue is different between Rluc_anc and Rluc_ancM. This result strongly suggest that (i) HLDs can change their LinB-like activity only by small number of amino acid residue substitution, and (ii) the assay system used in this study is sensitive enough to detect the difference.

Taken together, strains constructed in this study can be used as starting materials in the functional evolution and engineering studies. Especially, DAX-series strains are usefully for avoiding false positive clones that grow well on the solid minimal salt medium without adding any carbon sources in the screening process.

Chapter 2 Construction of *in vivo* and *in vitro* evolution systems of HLDs toward the γ-HCH utilization

2-1 Background

In Chapter 1, it was revealed that some HLDs besides LinB can potentially be involved in the γ-HCH utilization. Furthermore, it was suggested that (i) HLDs can change their LinB-like activity only by small number of amino acid residue substitution, and (ii) the assay system used in this study is sensitive enough to detect the difference.

In this chapter, to get some insights into HLDs evolution toward the optimized γ-HCH utilization, experimental evolution systems of HLDs were constructed. As *in vivo* evolution system, the engineered strains constructed in Chapter 1 were directly used for the screening. Considering the possibility that mutation rate is too low to obtain the evolved genes in the *in vivo* evolution system, (i) hypermutator strains were constructed for the *in vivo* evolution system by the introduction of the mutated *dnaQ* gene into the *linB* replacement strains, and (ii) *in vitro* evolution system was constructed, in which error-prone PCR was used for random mutagenesis. Strategies used in this study are summarized in Fig. 2-2.

2-2 Materials and methods

2-2-1 Strains, plasmids, medium composition and culture condition

The strains and plasmid used in this chapter were shown in Table 2-1. The medium and culture conditions were in accordance with Chapter 1. In addition, chloramphenicol (Cm) was used at the final concentration of 25 μg/mL.

2-2-2 DNA manipulations

The basic DNA manipulations were in accordance with Chapter 1. Primers used in this chapter were shown in Table 2-2. HIT Competent *E.coli* DH5α 619 cells (RBC Bioscience) showing higher efficient transformation rate than 618 cells were used for construction of mutant libraries of HLD or its related genes in *E. coli*.

Table 2-1 Bacterial strains and plasmids used in this chapter

Strains or plasmid	Relevant characteristics	Source or reference
Sphingomonads		
Sphingobium japonicum UT26DAX	γ-HCH degrader, Δ*adhX*	(Inaba et al., 2020)
Sphingobium japonicum UTDB2DAX	Δ*linB*, Δ*adhX*	(Inaba et al., 2020)
Sphingobium japonicum UTBM1DAX	*linB* -> $linB_{MI}$, Δ*adhX*	This study
Sphingobium japonicum UTBJ1DAX	*linB* -> *dbjA*, Δ*adhX*	This study
Sphingobium japonicum UTMM1DAX	*linB* -> *dmmA*, Δ*adhX*	This study
Sphingobium japonicum UTLA1DAX	*linB* -> *rluc_ancM*, Δ*adhX*	This study
Sphingobium japonicum UTLA2DAX	*linB* -> *rluc_anc*, Δ*adhX*	This study
Sphingobium japonicum UTRL1DAX	*linB* -> *rluc*, Δ*adhX*	This study
Sphingobium japonicum UTBA1DAX	*linB* ->*linB_dmbA_anc*, Δ*adhX*	This study
Sphingobium japonicum UT26DAX/pBDQ1	γ-HCH degrader, Δ*adhX*, pBDQ1	This study
Sphingobium japonicum UTDB2DAX/pBDQ1	Δ*linB*, Δ*adhX*, pBDQ1	This study
Sphingobium japonicum UTBM1DAX/pBDQ1	*linB* -> $linB_{MI}$, Δ*adhX*, pBDQ1	This study
Sphingobium japonicum UTBJ1DAX/pBDQ1	*linB* -> *dbjA*, Δ*adhX*, pBDQ1	This study
Sphingobium japonicum UTMM1DAX/pBDQ1	*linB* -> *dmmA*, Δ*adhX*, pBDQ1	This study
Sphingobium japonicum UTLA1DAX/pBDQ1	*linB* -> *rluc_ancM*, Δ*adhX*, pBDQ1	This study
Sphingobium japonicum UTLA2DAX/pBDQ1	*linB* -> *rluc_anc*, Δ*adhX*, pBDQ1	This study
Sphingobium japonicum UTRL1DAX/pBDQ1	*linB* -> *rluc*, Δ*adhX*, pBDQ1	This study
Sphingobium japonicum UTBA1DAX/pBDQ1	*linB* ->*linB_dmbA_anc*, Δ*adhX*, pBDQ1	This study
Sphingobium japonicum UTDB2DAX/pBLB1	Δ*linB*, Δ*adhX*, pBBR5TP::$linB_{UT}$	This study
Sphingobium japonicum UTDB2DAX/pBLB2	Δ*linB*, Δ*adhX*, pBBR5TP::$linB_{MI}$	This study
Sphingobium japonicum UTDB2DAX/pBBJ1	Δ*linB*, Δ*adhX*, pBBR5TP::*dbjA*	This study
Sphingobium japonicum UTDB2DAX/pBMM1	Δ*linB*, Δ*adhX*, pBBR5TP::*dmmA*	This study
Sphingobium japonicum UTDB2DAX/pBLA1	Δ*linB*, Δ*adhX*, pBBR5TP::*rluc_ancM*	This study
Sphingobium japonicum UTDB2DAX/pBLA2	Δ*linB*, Δ*adhX*, pBBR5TP::*rluc_anc*	This study
Sphingobium japonicum UTDB2DAX/pBRL1	Δ*linB*, Δ*adhX*, pBBR5TP::*rluc*	This study
Sphingobium japonicum UTDB2DAX/pBBA1	Δ*linB*, Δ*adhX*, pBBR5TP::*linB_dmbA_anc*	This study
E.coli		
DH5α	*recA1 endA1 gyrA96 thi-1 hsdR17 supE44 relA1 Δ(lacZYA-argF) Φ80lacZΔM15*	(Marietta et al., 1988)
Plasmid		
pBDQ1	pBBR MCS-1 (Cm) -UT26$dnaQ^{exo}$	(Inaba et al., 2020)
pBBR5T	pBBR1MCS-5_terminator	This study
pBBR5TP	pBBR1MCS-5 carrying T1	This study
pBLB1	pBBR5TP::$linB_{UT}$	This study
pBLB2	pBBR5TP::$linB_{MI}$	This study
pBBJ1	pBBR5TP::*dbjA*	This study
pBMM1	pBBR5TP::*dmmA*	This study
pBLA1	pBBR5TP::*rluc_ancM*	This study
pBLA2	pBBR5TP::*rluc_anc*	This study

pBRL1	pBBR5TP::*rluc*	This study
pBBA1	pBBR5TP::*linB_dmbA_anc*	This study

Table 2-2 Primers used in this chapter

Primer	Sequence(5'→3')	Amplification target
pBBR5TP_Hin_linB_up	gtgcttggatcaaggtccgaagcttAGACCAGAAAATCGCTCAAG	*hlds* genes
pBBR5TP_Cla_linB_down	gggccccccctcgaggtcgacggtatcgaTCGGATCTTAGAAAATGAGC	*hlds* genes
M4out	GCTGCAAGGCGATTAAG	Colony PCR and Sequence checking
RVout	GGCTCGTATGTTGTGTG	Colony PCR and Sequence checking

2-2-3 Construction of plasmids

The terminator sequence was introduced into the broad-host-range vector pBBR1-MCS-5, and the resultant plasmid was named pBBR5T. The promoter sequence Pu necessary for constitutive expression of *linA* gene in *S. japonicum* UT26 was introduced into pBBR5T, and the resultant plasmid was named pBBR5TP. The $linB_{UT}$, $linB_{MI}$, *dbjA*, *dmmA*, *rluc*, *rluc_anc*, *rluc_ancM*, and *linB_dmbA_anc* genes were introduced into pBBR5TP, and the resultant plasmids were named pBLB1, pBLB2, pBBJ1, pBMM1, pBRL1, pBLA1, pBLA2, and pBBA1, respectively (Fig. 2-1).

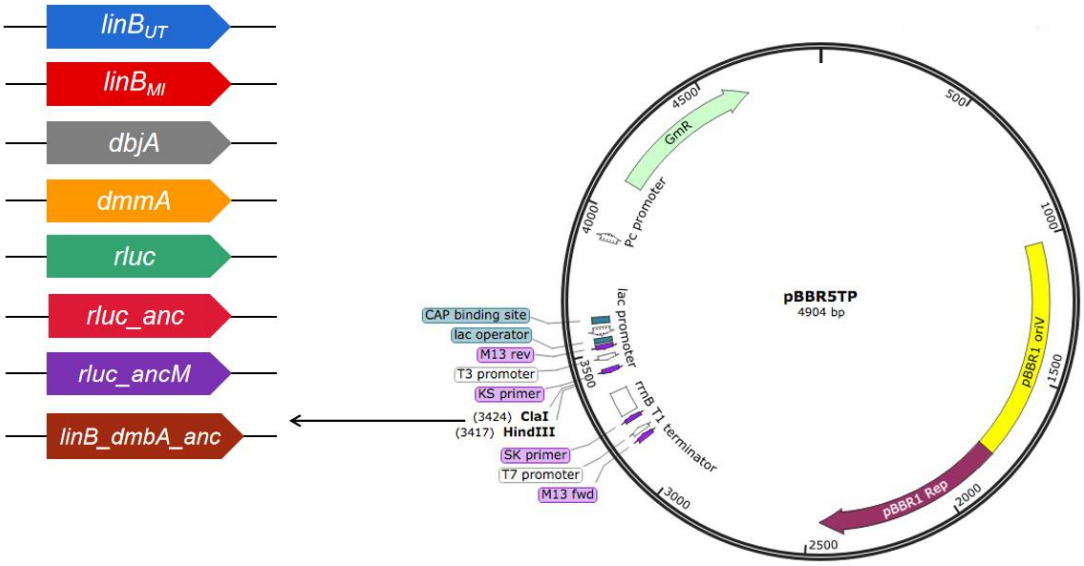

Fig. 2-1 Construction of plasmids for expression of HLD and its homologue genes in *Sphingobium* strains.

2-2-4 Construction of the hypermutator strains

Hypermutator strains were constructed by introduction of pBDQ1, which carries the mutated *dnaQ* gene of UT26 ($dnaQ^{exo}$) (Inaba et al., 2020), into the *linB*-replacement strains by using electroporation.

2-2-5 Screening for clones having the improved γ-HCH utilization ability

Cells (Table 2-3) cultured by appropriate medium were collected, washed, and suspended in PBS at the concentration of 10 mg/mL. 100 μL of cell suspension was spread on W-γ-HCH plate and incubated at 30℃ for two weeks. Colonies grew well with larger clear zone than others were selected for further analysis.

2-2-6 Error-prone PCR

Random mutagenesis of the HLD and its related genes was conducted by error-prone PCR. The composition of the reaction solution is shown in Table 2-4. The reaction condition consisted of a denaturation step for 1 min at 94℃, followed by 30 cycles of denaturation at 94℃ for 30 sec, annealing at 56℃ for 30 sec, and extension at 72℃ for 30 sec, with a final extension step at 72℃ for 10 min. Mutation rate was adjusted to 0.2~0.3% by concentration of Mn^{2+} and PCR cycles.

2-2-7 Construction of mutant libraries of HLD and its related genes

Mutated genes generated by error-prone PCR were cloned into pBBR5TP by using Gibson Assembly kit and transformed into *E. coli* DH5α, and the resultant transformants were used as mutant libraries in *E. coli*. Insertion rate of the PCR-amplified fragments and their mutation rate were estimated by using plasmids extracted from clones of the libraries that were randomly selected. The mixture of plasmids were extracted from the libraries in *E. coli*, and introduced by EP into *S. japonicum* UTDB2DAX (Δ*linB*, Δ*adhX*) to obtain the libraries in *Sphigobium*.

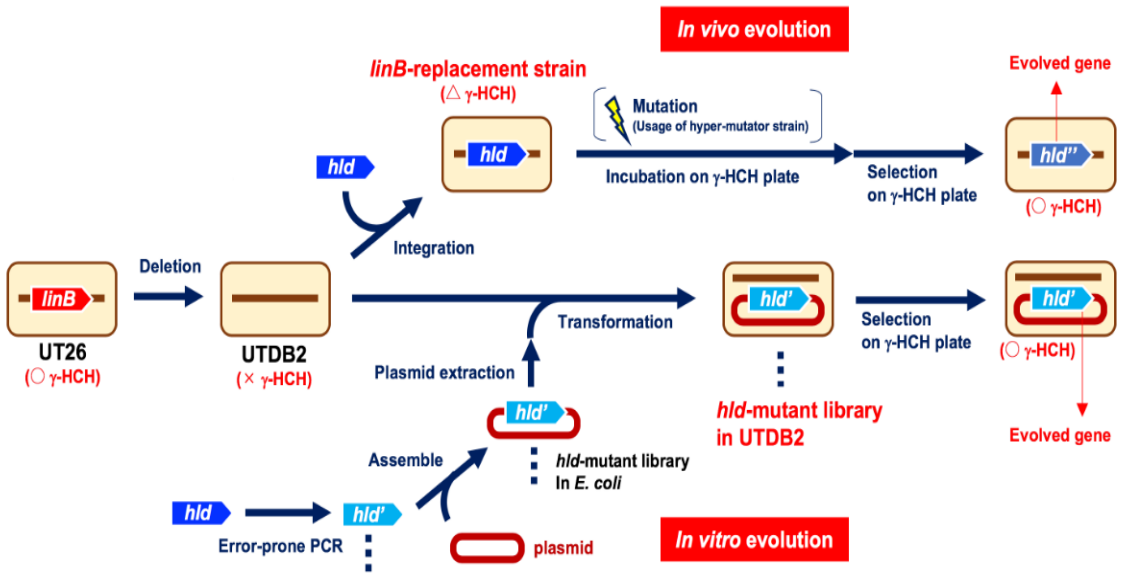

Fig. 2-2 Strategy used in this study

Table 2-3 Strains used in the *in vivo* evolution system

Strain	Relevant characteristics	Growth on HCH (low cell density)	Growth on HCH (high cell density)
Sphingobium japonicum UT26DAX	γ-HCH degrader	Yes	Yes (death)
Sphingobium japonicum UTBM1DAX	*linB* -> $linB_{MI}$, Δ*adhX*	Yes	Yes (death)
Sphingobium japonicum UTBJ1DAX	*linB* -> *dbjA*, Δ*adhX*	No	No
Sphingobium japonicum UTMM1DAX	*linB* -> *dmmA*, Δ*adhX*	No	Yes (weak)
Sphingobium japonicum UTLA1DAX	*linB* -> *rluc_ancM*, Δ*adhX*	No	Yes (weak)
Sphingobium japonicum UTLA2DAX	*linB* -> *rluc_anc*, Δ*adhX*	No	Yes(weak)
Sphingobium japonicum UTRL1DAX	*linB* -> *rluc*, Δ*adhX*	No	No
Sphingobium japonicum UTBA1DAX	*linB*->*linB_dmbA_anc*, Δ*adhX*	No	Yes
Sphingobium japonicum UT26DAX/pBDQ1	γ-HCH degrader	Yes	Yes (death)
Sphingobium japonicum UTBM1DAX/pBDQ1	*linB* -> $linB_{MI}$, Δ*adhX*	Yes	Yes (death)
Sphingobium japonicum UTBJ1DAX/pBDQ1	*linB* -> *dbjA*, Δ*adhX*	No	No
Sphingobium japonicum UTMM1DAX/pBDQ1	*linB* -> *dmmA*, Δ*adhX*	No	Yes (weak)
Sphingobium japonicum UTLA1DAX/pBDQ1	*linB* -> *rluc_ancM*, Δ*adhX*	No	Yes (weak)
Sphingobium japonicum UTLA2DAX/pBDQ1	*linB* -> *rluc_anc*, Δ*adhX*	No	Yes(weak)
Sphingobium japonicum UTRL1DAX/pBDQ1	*linB* -> *rluc*, Δ*adhX*	No	No
Sphingobium japonicum UTBA1DAX/pBDQ1	*linB*->*linB_dmbA_anc*, Δ*adhX*	No	Yes
Sphingobium japonicum UTDB2DAX/pBLB1	pBBR5TP::$linB_{UT}$	Yes	Yes (death)
Sphingobium japonicum UTDB2DAX/pBLB2	pBBR5TP::$linB_{MI}$	Yes	Yes (death)
Sphingobium japonicum UTDB2DAX/pBBJ1	pBBR5TP::*dbjA*	No	No
Sphingobium japonicum UTDB2DAX/pBMM1	pBBR5TP::*dmmA*	No	Yes (weak)
Sphingobium japonicum UTDB2DAX/pBLA1	pBBR5TP::*rluc_ancM*	No	Yes (weak)
Sphingobium japonicum UTDB2DAX/pBLA2	pBBR5TP::*rluc_anc*	No	Yes(weak)
Sphingobium japonicum UTDB2DAX/pBRL1	pBBR5TP::*rluc*	No	No
Sphingobium japonicum UTDB2DAX/pBBA1	pBBR5TP::*linB_dmbA_anc*	No	Yes

Table 2-4 Compositions of solution for error-prone PCR

Reagents	Volume
Template	0.5 μL (plasmid was diluted by TE buffer* to 100 fold)
pBBR5TP_Hin_linB_up (50pmol/μl)	0.5 μL
pBBR5TP_Cla_linB_down (50pmol/μl)	0.5 μL
rTaq (5U/μl)	0.5 μL
10×buffer (Mg^{2+} free)	5 μL
dNTP mixture	4 μL
DMSO	2.5 μL
$MgCl_2$ (25mM)	3 μL
$MnCl_2$ (10mM)	0.5 μL
Sterilized water	Up to 50 μL

*TE buffer:

1M Tris (pH 8.0) 2 mL

0.5M EDTA (pH 8.0) 400 μL

Sterilized water up to 200 mL

2-3 Results

2-3-1 *In vivo* evolution system

The *linB*-replacement UT26 (wild type)- and UT-DAX-series strains constructed in Chapter 1 were incubated on the W-γ-HCH plate, and clones that grew well with larger clear zone than others were selected. Considering the possibility that spontaneous mutation rate is too low to obtain the evolved genes in this system, hypermutator strains were also constructed by the introduction of the mutated *dnaQ* gene into the UT-DAX-series strains. The γ-HCH utilization ability of the resultant strains was assayed on the W-γ-HCH plate (Fig. 2-3). These strains showed the same tendency with UT-DAX-series strains (Fig. 1-11).

Some candidate clones were obtained by the screening for further analysis. HLD or its related genes of such candidates were amplified by PCR and sequenced. However, they carried the same gene as original or the *linB* gene. The former indicates that mutation(s) in the genome other than HLD or its related genes improved the γ-HCH utilization ability. The latter is probably due to the contamination with strains having the *linB* gene.

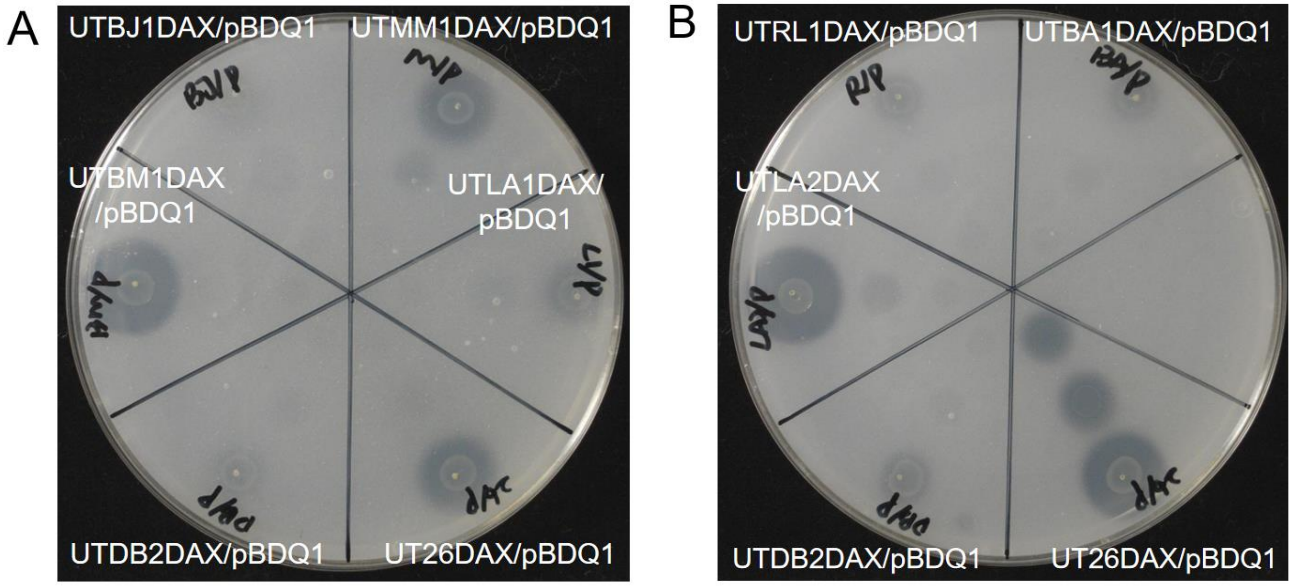

Fig. 2-3 Spot assay of UT-DAX(pBDQ1)-series strains (9 days incubation). Concentration of cells from outer to inner is 100 mg/mL, 10 mg/mL and 1 mg/mL.

2-3-2 Introduction of HLD or its related genes into UTDB2DAX by using a broad-host-range vector

The *linB*$_{UT}$, *linB*$_{MI}$, *dbjA*, *dmmA*, *rluc*, *rluc_anc*, *rluc_ancM*, and *linB_dmbA_anc* genes were cloned into a broad-host-range vector pBBR5TP, and the resultant plasmids were named pBLB1, pBLB2, pBBJ1, pBMM1, pBRL1, pBLA1, pBLA2, and pBBA1 (Fig. 2-1).These plasmids were introduced into UTDB2DAX (Δ*linB*, Δ*adhX*), and the γ-HCH utilization ability of the resultant strains was assayed on the W-γ-HCH plate (Fig. 2-4). The positive control strains, UTDB2DAX (pBLB1) and UTDB2DAX (pBLB2), showed obvious γ-HCH utilization activity, while the negative control strain UTDB2DAX showed no γ-HCH utilization activity (Fig. 2-4A). As expected from the results of Chapter 1, UTDB2DAX (pBBJ1) and UTDB2DAX (pBRL1) showed no γ-HCH utilization activity, and UTDB2DAX (pBMM1), UTDB2DAX (pBLA1), and UTDB2DAX (pBLA2) showed weak γ-HCH utilization activity (Fig. 2-4). Unexpectedly, UTDB2DAX (pBBA1) showed weak γ-HCH utilization activity (Fig. 2-4B), suggesting that LinB_dmbA_anc has faint LinB-like activity. The activity was detected only in UTDB2DAX (pBBA1), probably because LinB_dmbA_anc was expressed at higher level in UTDB2DAX (pBBA1) than in UTBA1.

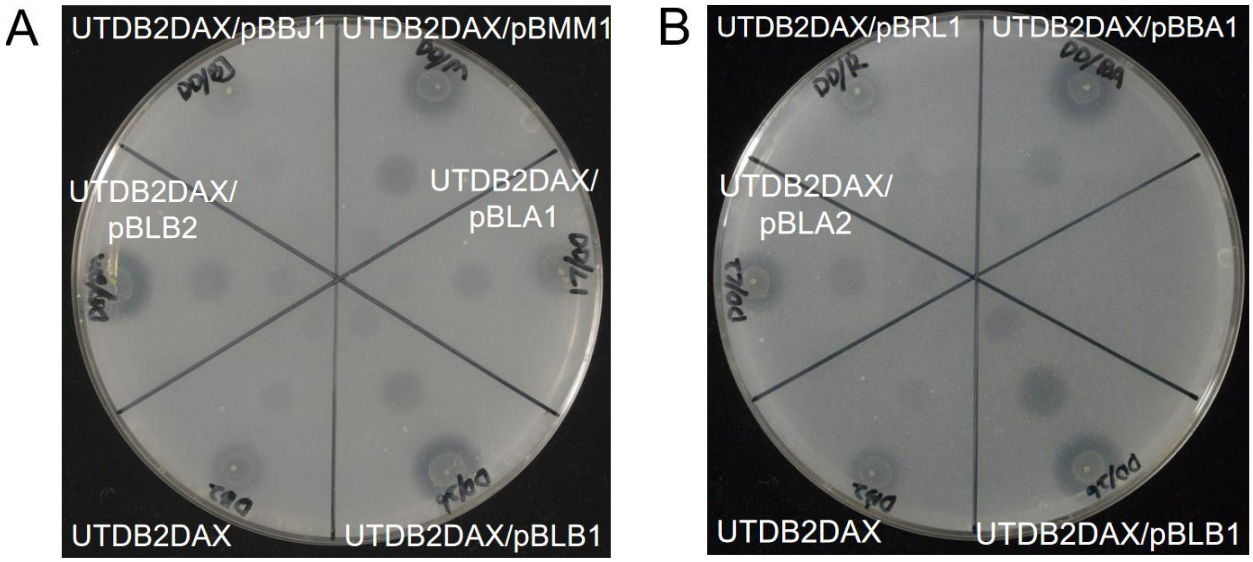

Fig. 2-4 Spot assay of *Sphingobium japonicum* UTDB2DAX/pBBR5TP::*linB* replacement genes strains (7 days incubation. Concentration of cells from outer to inner is 100 mg/mL, 10 mg/mL and 1 mg/mL.

2-3-3 *In vitro* evolution system

In Chapter 1, it was shown that DmmA, Rluc_anc, and Rluc_ancM have weak LinB-like activity. In addition, it was suggested that LinB_dmbA_anc has faint LinB-like activity in the previous section. Although the LinB-like activity of DbjA and Rluc has not been detected, they may change to enzymes showing LinB-like activity by small number of mutations. On the other hand, it was also expected that $LinB_{UT26}$ and $LinB_{MI}$ still have chance to improve their activity for the γ-HCH utilization. Thus, *in vitro* evolution system for these genes toward the γ-HCH utilization was constructed.

Random mutation was introduced into the *linB*$_{UT}$, *linB*$_{MI}$, *dbjA*, *dmmA*, *rluc*, *rluc_anc*, *rluc_ancM*, and *linB_dmbA_anc* genes by error-prone PCR, and their mutant libraries were constructed in *E. coli*. Each library consists of about 1,000 clones, and their insertion and mutation rates were estimated from clones randomly selected (Table 2-5).

The mixture of plasmids were extracted from the libraries in *E. coli*, and introduced into *S. japonicum* UTDB2DAX to obtain the libraries in *Sphigobium*. The resultant libraries in *Sphingobium* were screened on the W-γ-HCH plate, and clones that grew well with larger clear zone than others were selected. The selected clones were sub-cultured on another W-γ-HCH plate with control strains, and their improved growth on the plate was confirmed. Plasmids carrying the mutated genes were extracted from the candidate clones, re-introduced into UTDB2, and their positive effect on the growth on the W-γ-HCH plate was confirmed (Fig. 2-5). The final candidate evolved genes were sequenced and the results were summarized in Table 2-6.

Table 2-5 Mutant libraries of HLD and its related genes for the first round screening

Genes	Library size	Insertion rate (%)	Mutation rate (%)
linB$_{UT}$	923	62.5	0.23
linB$_{MI}$	905	75	0.27
dbjA	893	50	0.19
dmmA	925	75	0.30
rluc_ancM	934	50	0.42
rluc_anc	946	50	0.32
rluc	902	50	0.23
linB_dmbA_anc	881	62.5	0.33

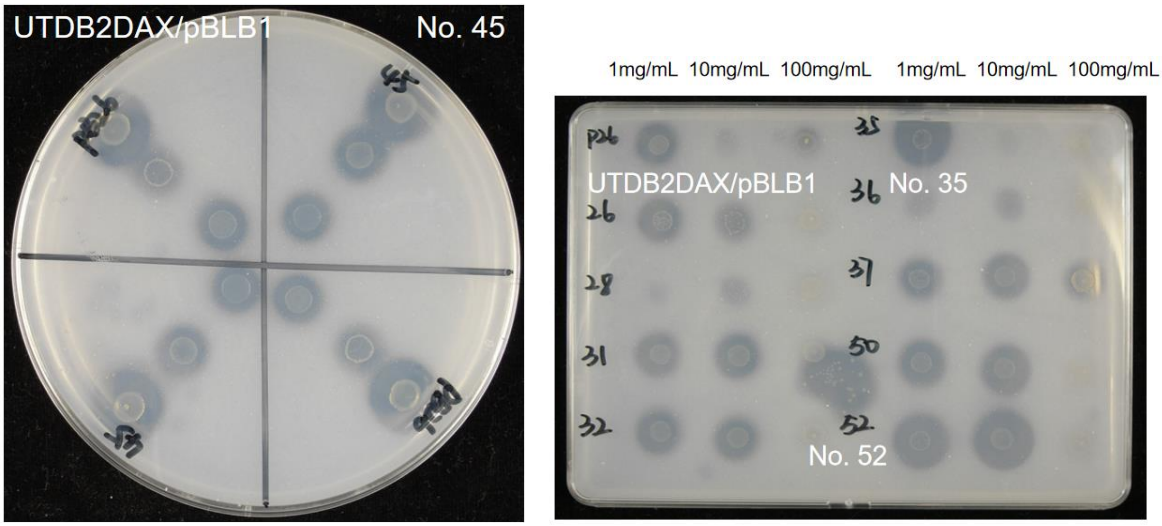

Fig. 2-5A 1st screening of *linB*$_{UT}$ and its mutant colonies (No. 45, No. 52 and No.35, 8 days incubation, on the circle plate, concentration of cells from outer to inner is 100mg/mL, 10mg/mL and 1mg/mL)

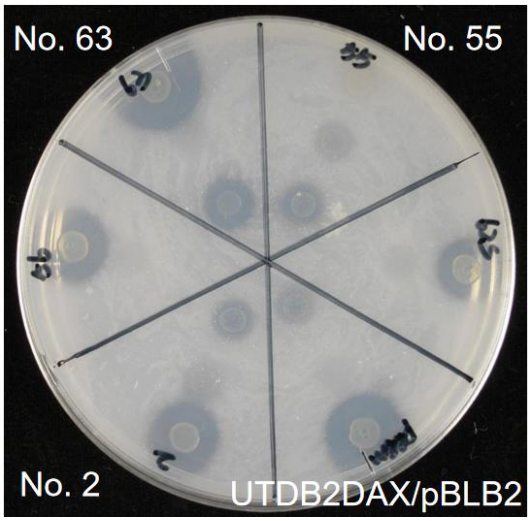

Fig. 2-5B 1st screening of *linB*$_{MI}$ and its mutant colonies (No.2, No.55 and No.63, 8 days incubation, on the circle plate, concentration of cells from outer to inner is 100mg/mL, 10mg/mL and 1mg/mL)

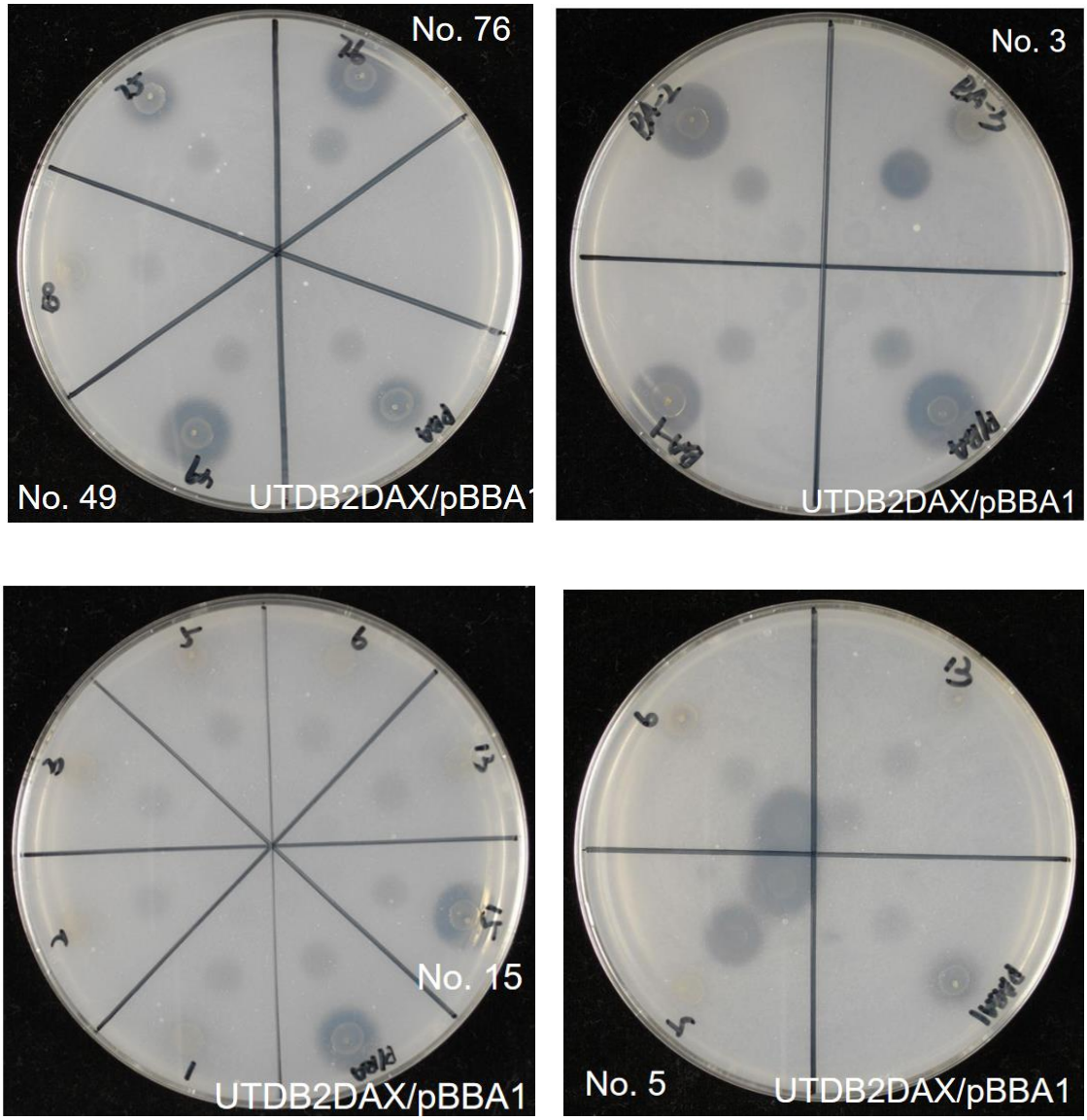

Fig. 2-5C 1st screening of *linB_dmbA_anc* and its mutant colonies (No.3, No.5, No.15, No.49 and No.76, 8 days incubation, on the circle plate, concentration of cells from outer to inner is 100mg/mL, 10mg/mL and 1mg/mL)

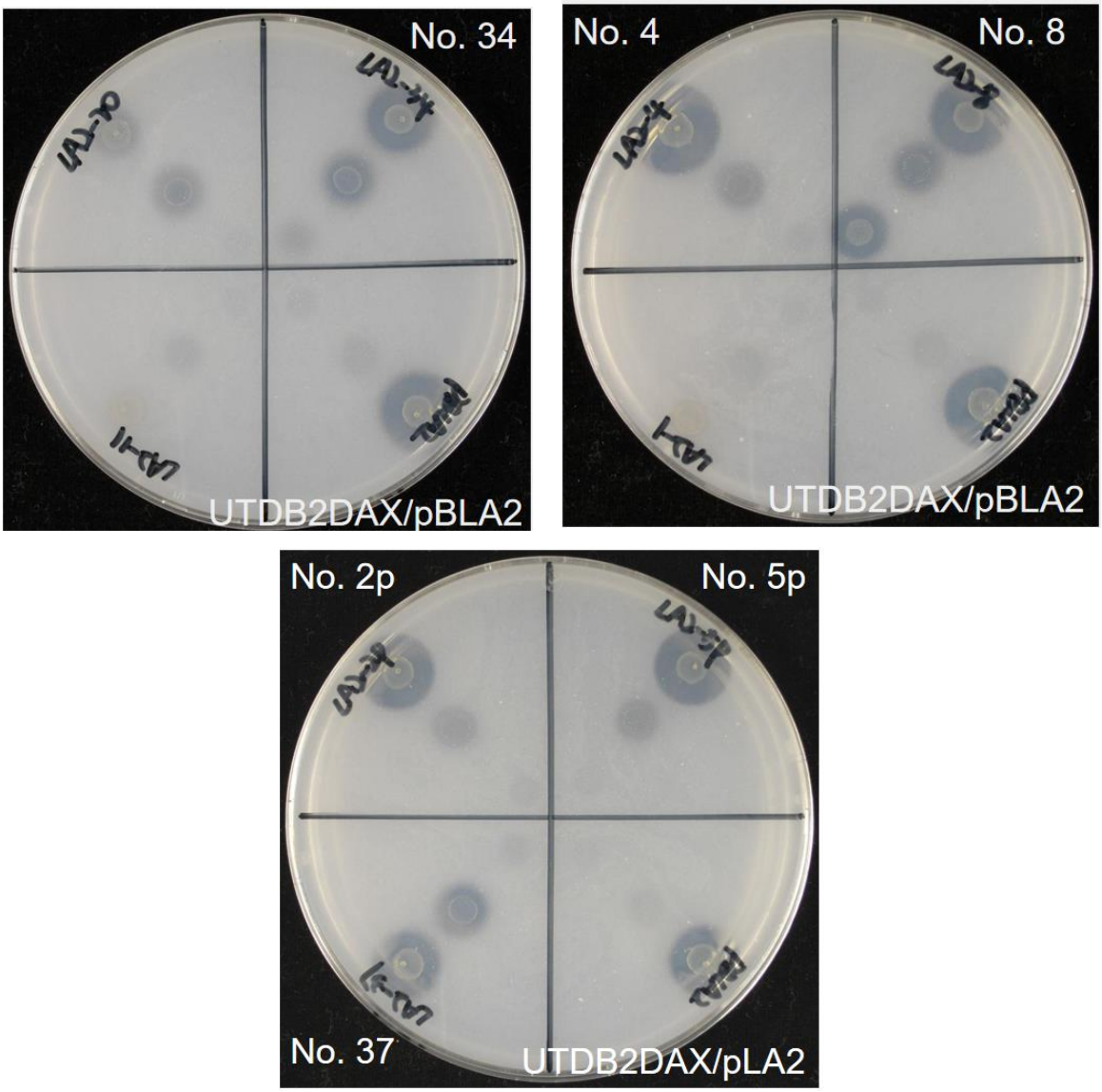

Fig. 2-5D 1st screening of *rluc_anc* and its mutant colonies (No.4, No.8, No.34, No.37, No.2p and No.5p, 8 days incubation, on the circle plate, concentration of cells from outer to inner is 100mg/mL, 10mg/mL and 1mg/mL)

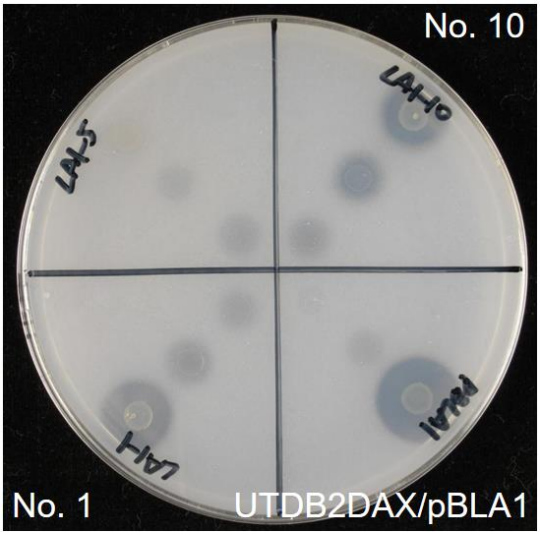

Fig. 2-5E 1st screening of *rluc_ancM* and its mutant colonies (No.1 and No.10, 8 days incubation, on the circle plate, concentration of cells from outer to inner is 100mg/mL, 10mg/mL and 1mg/mL)

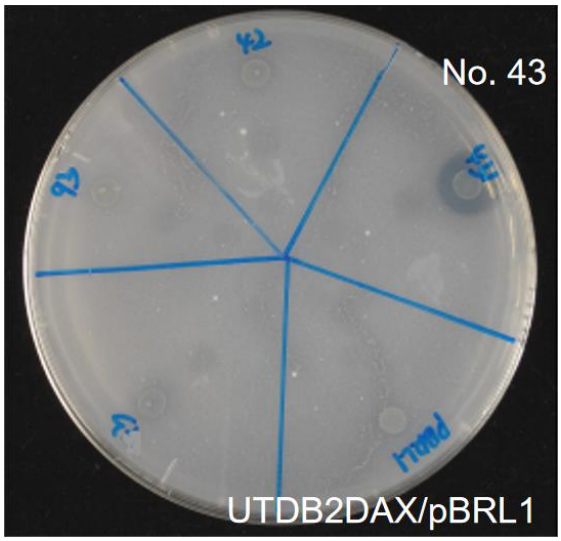

Fig. 2-5F 1st screening of *rluc* and its mutant colonies (No. 43, 8 days incubation, on the circle plate, concentration of cells from outer to inner is 100mg/mL, 10mg/mL and 1mg/mL)

Table 2-6 Summary of the candidate evolved genes obtained by the 1st round screening

HLD	No	Mutation site
$LinB_{UT}$	35	A141V(GCG→GTG)
	52	P203T(CCG→ACG)
$LinB_{MI}$	63	G4S(GGC→AGC), I128V(ATT→GTT), A269T(GCA→ACA)
	2	T81S(ACC→TCC), L239H(CTC→CAC)
	55	D90V(GAC→GTC), A95T(GCG→ACG), L195S(CTC→TCC)
	45	T81S (ACC→TCC), L239H (CTC→CAC)
LinB_dmbA_anc	15	P158L(CCG→CTA), L294V(CTG→GTG)
	3	R125C(CGT→TGT), E161V(GAA→GTA)
	5	A3T(GCA→ACA), E147V(GAA→GTA), V148A(GTT→GCT), L196P(CTG→CCT), V222A(GTT→GCT)
	19	No mutation
	35	E187K(CAG→AAG)
	47	R210C(CGT→TGT)
	49	T2A(ACC→GCC)
	76	L90P(CTG→CCG), S226N(AGC→AAC), G299D(GGT→GAT)
Rluc_anc	4	G122S (GGT→AGT), I298M (ATT→ATG)
	8	N87S(AAT→AGT), D104G(GAT→GGT), K136R(AAA→AGA), I161V(ATT→GTT), S187C(AGC→TGC), K247E(AAA→GAA)
	34	S32N(AGC→AAC), F261L(TTT→CTT),
	37	K237N(AAA→AAT), F261L(TTT→CTT)
	2p	S246C(AGC→TGC), V268M(GTG→ATG), L302Q(CTG→CAG)
	5p	N129S(AAT→AGT), V268E(GTG→GAG)
Rluc_ancM	1	P7R(CCT→CGT), S32N(AGC→AAC), F261L(TTT→CTT), E304V(GAA→GTA), L305P(CTG→CCG)
	10	P7R(CCT→CGT), K237N(AAA→AAT), F261L(TTT→CTT)
Rluc	43	E132D(GAG→GAC), E151G(GAA→GGA), E211G(GAA→GGA)

2-3-4 The 2nd round screening in the *in vitro* evolution system

Since the *in vitro* evolution system seemed to work, the second round screening was also conducted. Eight evolved genes, *linB*$_{MI}$-45, *linB*$_{UT}$-52, *linB*$_{MI}$-63, *rluc_anc*-4, *rluc_anc*-8, *linB_dmbA_anc*-3, *linB_dmbA_anc*-5, and *rluc*-43, whose positive effect on the γ-HCH utilization was obvious (Fig. 2-5), were selected for the second round screening.

Random mutation was introduced into the eight genes by error-prone PCR, and their mutant libraries were constructed in *E. coli*. Each library consists of about 1,000 clones, and their insertion and mutation rates were estimated from clones randomly selected (Table 2-7). The mixture of plasmids were extracted from the libraries in *E. coli*, and introduced into *S. japonicum* UTDB2DAX to obtain the libraries in *Sphigobium*. The resultant libraries in *Sphingobium* were screened on the W-γ-HCH plate, and clones that grew well with larger clear zone than others were selected.

The second round screening was more difficult than the first screening, since they relatively formed many colonies. However, the selected clones were sub-cultured on another W-γ-HCH plate with control (corresponding mutant strains selected from the 1st round of screening), and their improved growth on the plate was confirmed. Plasmids carrying the mutated genes were extracted from the candidate clones, re-introduced into the UTDB2, and their positive effect on the growth on the W-γ-HCH plate was confirmed (Fig. 2-6). The final candidate evolved genes were sequenced and the results were summarized in Table 2-8.

Table 2-7 Mutant libraries of HLD and its related genes for the first round screening

Genes	Library size	Insertion rate (%)	Mutation rate (%)
linB$_{MI}$-45	957	75	0.23
linB$_{UT}$-52	875	62.5	0.30
linB$_{MI}$-63	783	62.5	0.23
rluc_anc-4	898	75	0.30
rluc_anc-8	790	62.5	0.33
linB_dmbA_anc-3	843	50	0.32
linB_dmbA_anc-5	882	62.5	0.33
rluc-43	925	62.5	0.3

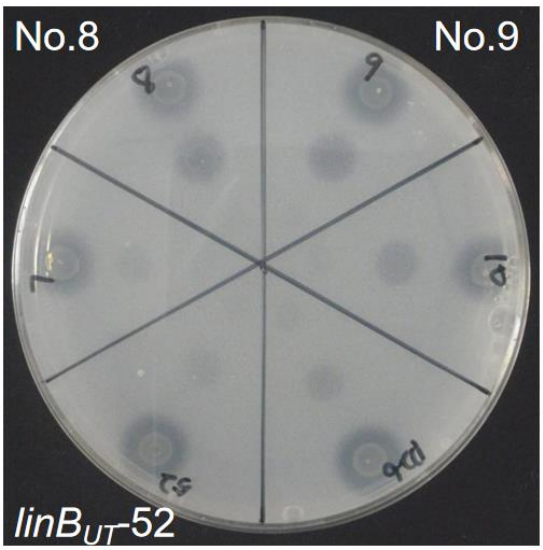

Fig. 2-6A 2nd screening of *linB*$_{UT}$-52 and its mutant colonies (No.8 and No.9, 7days incubation, on the circle plate, concentration of cells from outer to inner is 100mg/mL, 10mg/mL and 1mg/mL)

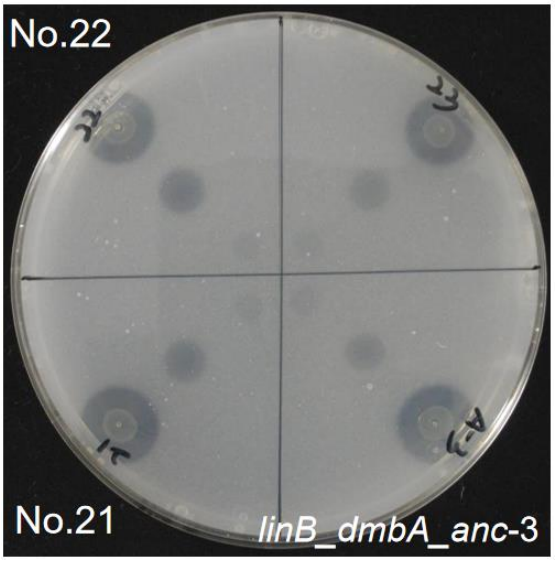

Fig. 2-6B 2nd screening of *linB_dmbA_anc*-3 and its mutant colonies (No.21 and No.22, 7days incubation, on the circle plate, concentration of cells from outer to inner is 100mg/mL, 10mg/mL and 1mg/mL)

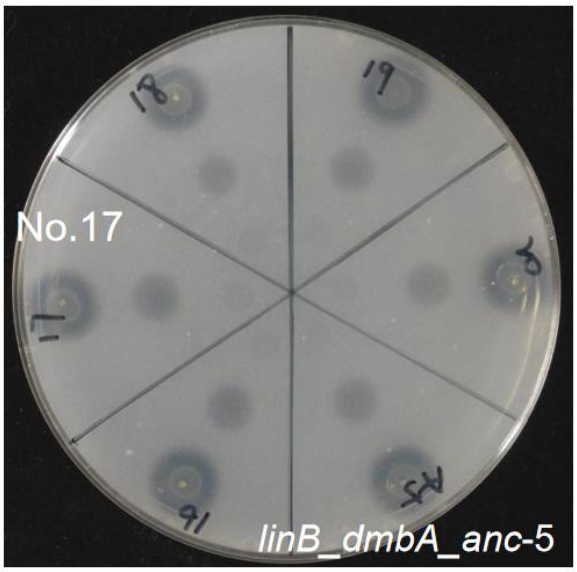

Fig. 2-6C 2nd screening of *linB_dmbA_anc*-5 and its mutant colonies (No.17, 7days incubation, on the circle plate, concentration of cells from outer to inner is 100mg/mL, 10mg/mL and 1mg/mL)

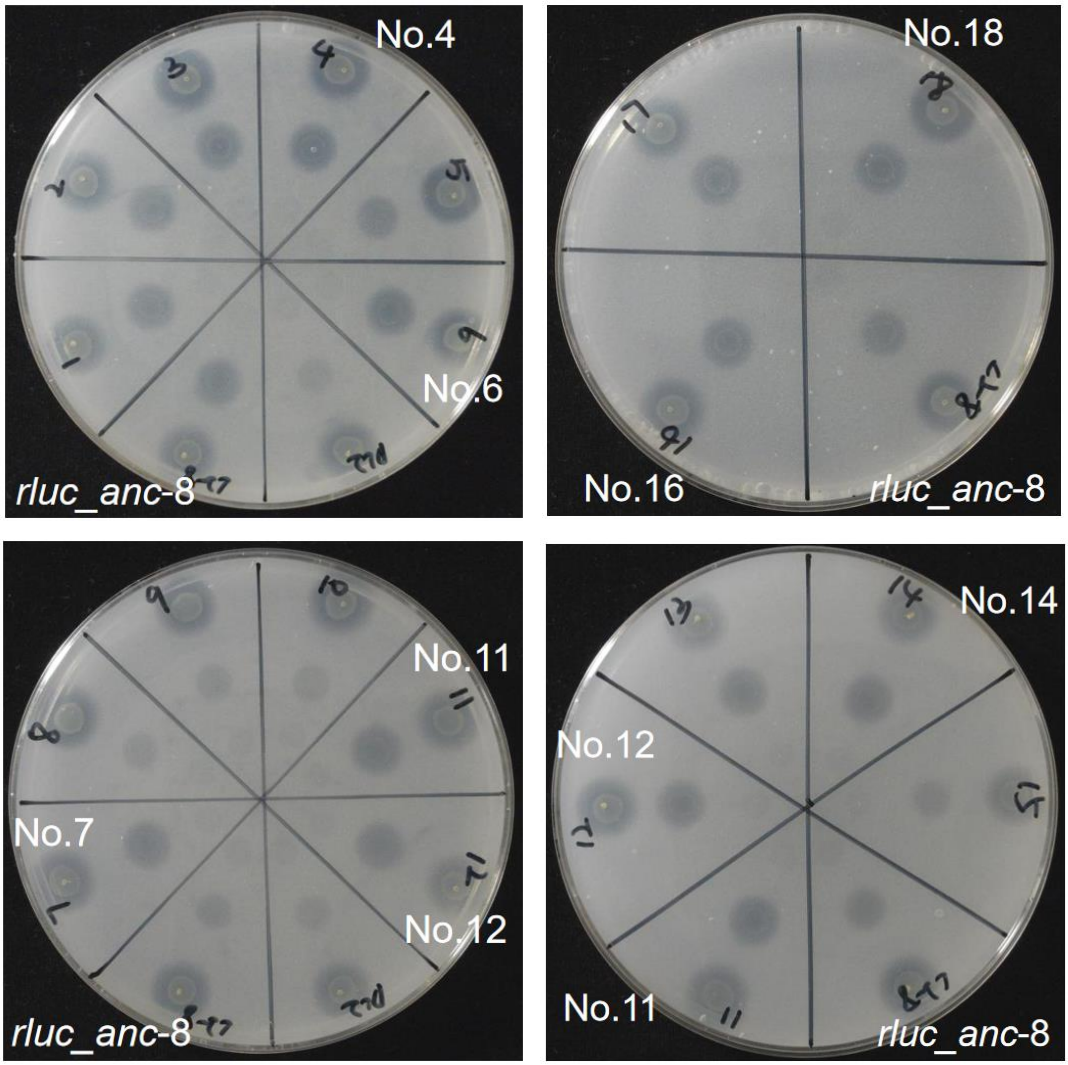

Fig. 2-6D 2nd screening of *rluc_anc*-8 and its mutant colonies (No.4, No.6, No.7, No.11, No. 12, No.14, No.16 and No.18, 7days incubation, concentration of cells from outer to inner is 100mg/mL, 10mg/mL and 1mg/mL)

Table 2-8 Sequence of candidates showed in Fig. 3-23 during the 2nd round screening

HLD	No.	Mutation site
Rluc_anc-8	18	E171A(GAA→GCA), C187S(TGC→AGC), S188N(AGC→AAC)
	16	S188N(AGC→AAC), L286P(CTG→CCG)
	14	S188N(AGC→AAC)
	4	S188Y(AGC→TAC), N255S(AAC→AGC), S238C(AGC→TGC)
	7	V65A(GTT→GCT), S188N(AGC→AAC), K241E(AAA→GAA)
	6	S188N(AGC→AAC), F261L(TTT→CTT), N271Y(AAT→TAT)
	12	Q6R(CAG→CGG), S188N(AGC→AAC), P204S(CCG→TCG), V268E(GTG→GAG)
	11	S188Y(AGC→TAC), R213C(CGT→TGT)
$LinB_{UT}$-52	9	I14V(ATT→GTT)
	8	Q165R(CAG→CGG)
LinB_dmbA_anc-3	22	E146G(GAA→GGA)
	21	S43G(AGC→GGC)
LinB_dmbA_anc-5	17	I25T(ATT→ACT)

2-4 Discussion

In this chapter, experimental evolution systems of HLD and its related genes toward the optimized γ-HCH utilization were constructed. The *in vivo* evolution system did not work well, mainly because candidate clones that grew well with larger clear zone on the W-γ-HCH plate than others had no mutation in the HLD or its related genes. Probably, mutation(s) in the genome other than HLD or its related genes improved the γ-HCH utilization ability of the host cells. Although it is very interesting what mutation(s) have occurred in such clones, I did not further analyze them in this study.

On the other hand, the *in vitro* evolution system using error-prone PCR worked well, and many candidate evolved genes were successfully obtained. Eight genes, whose positive effect on the γ-HCH utilization were obvious, were selected and used as templates for the second round screening. However, the second round screening was more difficult than the first screening, since the screening system seems to be difficult to detect small difference of genes that have evolved to some extent. This system is suitable for selection of the evolved gene from the original gene encoding enzyme having weak or no LinB-like activity.

To finally conclude that the *in vitro* evolution system worked, it is necessary to confirm that the candidate genes indeed encode proteins having the improved LinB-like activity. Enzymatic activities of proteins encoded by the selected eight candidate genes were analyzed in the next chapter.

Interestingly, *rluc*-43, whose original *rluc* gene encodes protein having no LinB-like activity, was obtained as the evolved gene that confers the γ-HCH utilization ability to the host cells. Although the further evolved gene of *rluc*-43 was not obtained by the second round screening in this study, further trail deserves to be conducted.

Chapter 3 Purification and characterization of the putative evolved HLDs

3-1 Background

One of the goals of protein design and protein engineering is to construct the enzymes with improved activity and modified specificity. The introduction of mutations into the genes, gene expression and protein purification take considerable effort and it is desirable to extensively characterize constructed mutants to detect even subtle changes in the specificity of the constructs. Kinetic experiments with a few selected substrates are often used for characterization of catalytic properties of the engineered enzymes.

In the previous chapter, the candidate evolved genes toward the γ-HCH utilization were successfully obtained by using the *in vitro* evolution system, suggesting that the *in vitro* evolution system worked. However, it is necessary for the final conclusion to confirm that the candidate genes indeed encode proteins having the improved LinB-like activity.

In this chapter, eight candidate evolved genes obtained by the first round screening were selected (Table 3-3), and their protein products were expressed in *E. coli* as His-tagged proteins, purified, and characterized for their HLD and LinB-like activities. In addition, protein products of the candidate evolved genes obtained by the second round screening were also analyzed.

3-2 Materials and methods

3-2-1 Strains, plasmids, medium composition and culture condition

The strains and plasmids used in this chapter were shown in Table 3-1.

The medium and culture conditions were in accordance with Chapter 1. In addition, ampicillin (Ap) was used at the final concentration of 100 μg/mL.

3-2-2 DNA manipulations

The basic DNA manipulations were in accordance with Chapter 1. Primers used in this chapter were shown in Table 3-2.

Table 3-1 Bacterial strains and plasmids used in this chapter

Strains or plasmid	Relevant characteristics	Source or reference
E.coli		
DH5α	*recA1 endA1 gyrA96 thi-1 hsdR17 supE44 relA1 Δ(lacZYA-argF) Φ80lacZΔM15*	(Marietta et al., 1988)
BL21 Star ^{TM}(DE3)	*F ompT hsdSB (rB-mB-) gal ompT, λ(DE3)*	(Studier & Moffatt, 1986)
Plasmid		
pETWD1	*pET22b(+)+TEE-Hisx6-TEV-NdeI-XhoI*	Mr. Deng Master thesis
pETWD1-*linB*$_{UT}$	pETWD1::*linB*$_{UT}$	This study
pETWD1-*linB*$_{MI}$-45	pETWD1::*linB*$_{MI}$-45	This study
pETWD1-*linB*$_{UT}$-52	pETWD1::*linB*$_{UT}$-52	This study
pETWD1-*linB*$_{MI}$	pETWD1::*linB*$_{MI}$	This study
pETWD1-*linB*$_{MI}$-63	pETWD1::*linB*$_{MI}$-63	This study
pETWD1-*rluc_ancM*	pETWD1::*rluc_ancM*	This study
pETWD1-*rluc_anc*	pETWD1::*rluc_anc*	This study
pETWD1-*rluc_anc*-4	pETWD1::*rluc_anc*-4	This study
pETWD1-*rluc_anc*-8	pETWD1::*rluc_anc*-8	This study
pETWD1-*rluc*	pETWD1::*rluc*	This study
pETWD1-*rluc*-43	pETWD1::*rluc*-43	This study
pETWD1-*linB_dmbA_anc*	pETWD1::*linB_dmbA_anc*	This study
pETWD1-*linB_dmbA_anc*-3	pETWD1::*linB_dmbA_anc*-3	This study
pETWD1-*linB_dmbA_anc*-5	pETWD1::*linB_dmbA_anc*-5	This study
pUC18	multiple cloning site internal to *lacZ* gene	Fermentas Inc.
pAQN	pMB9 replicon, *lacI*^{q} *aqn*	(Terada et al., 1990)
pUC18-*rluc*-43	pUC18::*rluc*-43	This study
pAQN-*rluc*-43	pAQN::*rluc*-43	This study

3-2-3 Construction of plasmids

The plasmids for expression of proteins with His-tag at N-terminus in *E. coli* were constructed by using pETWD1 (constructed by insert translation enhancing element (TEE), 6×His-tag at N terminal, also insert tobacco etch virus (TEV) protease recognition and cleavage site) for *linB*$_{UT}$, *linB*$_{MI}$-45, *linB*$_{UT}$-52, *linB*$_{MI}$, *linB*$_{MI}$-63, *rluc_anc*, *rluc_anc*-43, *rluc_ancM*, *rluc_anc*-4, *rluc_anc*-8, *linB_dmbA_anc*, *linB_dmbA_anc*-3, and *linB_dmbA_anc*-5 (Fig. 3-1). For the expression of *rluc_anc*-43, pUC18 and pAQN were also used.

Table 3-2 Primers used in this chapter

Primer	Sequence(5'→3')	purpose
pBBR5TP_Hin_linB_up	gtgcttggatcaaggtccgaagcttAGACCAGAAAATCGCTCAAG	Amplification of 1st evolved hlds genes
pBBR5TP_Cla_linB_down	gggccccccctcgaggtcgacggtatcgaTCGGATCTTAGAAAATGAGC	Amplification of 1st evolved hlds genes
pETWD1_LinB$_{MI}$_F	gaatctttattttcagggcaTGAGCCTCGGCGCAAAGC	Amplification of *linB*$_{MI}$
pETWD1_LinB$_{MI}$_R	agtggtggtggtggtggtgcTTATGCTGGGCGCAATCGC	Amplification of *linB*$_{MI}$
pETWD1_LinB$_{MI}$_F_M63	gaatctttattttcagggcaTGAGCCTCAGCGCAAAGC	Amplification of *linB*$_{MI}$*-63*
pETWD1_Rluc_anc_LA1_F	gaatctttattttcagggcaTGGTGAGCGCGAGCCAGC	Amplification of *rluc_ancM*
pETWD1_Rluc_anc_LA1_R	agtggtggtggtggtggtgc TCATTTGGTCAGTTCGTTCAGAAAATCGGC	Amplification of *rluc_ancM*
pETWD1_Rluc_anc_LA2_F	gaatctttattttcagggcaTGGTTAGCGCAAGCCAGC	Amplification of *rluc_anc*
pETWD1_Rluc_anc_LA2_R	agtggtggtggtggtggtgc TTATTTGGTCAGTTCGTTCAGAAAATCG	Amplification of *rluc_anc*
pETWD1_LinB_dmbA_anc_F	gaatctttattttcagggcaTGACCGCACTGGGTGCAG	Amplification of *linB_dmbA_anc*
pETWD1_LinB_dmbA_anc_R	agtggtggtggtggtggtgcTTAAACACCGGCTGCTGCAC	Amplification of *linB_dmbA_anc*
pETWD1_LinB_dmbA_anc_F_M5r	gaatctttattttcagggcaTGACCACACTGGGTGCAG	Amplification of *linB_dmbA_anc*-5
pETWD1_Rluc_F	gaatctttattttcagggcaTGACTTCGAAAGTTTATGATC	Amplification of *rluc*
pETWD1_Rluc_R	agtggtggtggtggtggtgcTTATTGTTCATTTTTGAGAACTC	Amplification of *rluc*
pET22b-F2	ggggttatgctagttattgctcag	Colony PCR and Sequence checking
pET22+b_seqR	gggaattgtgagcggataac	Colony PCR and Sequence checking
M4out	GCTGCAAGGCGATTAAG	Colony PCR and Sequence checking
RVout	GGCTCGTATGTTGTGTG	Colony PCR and Sequence checking

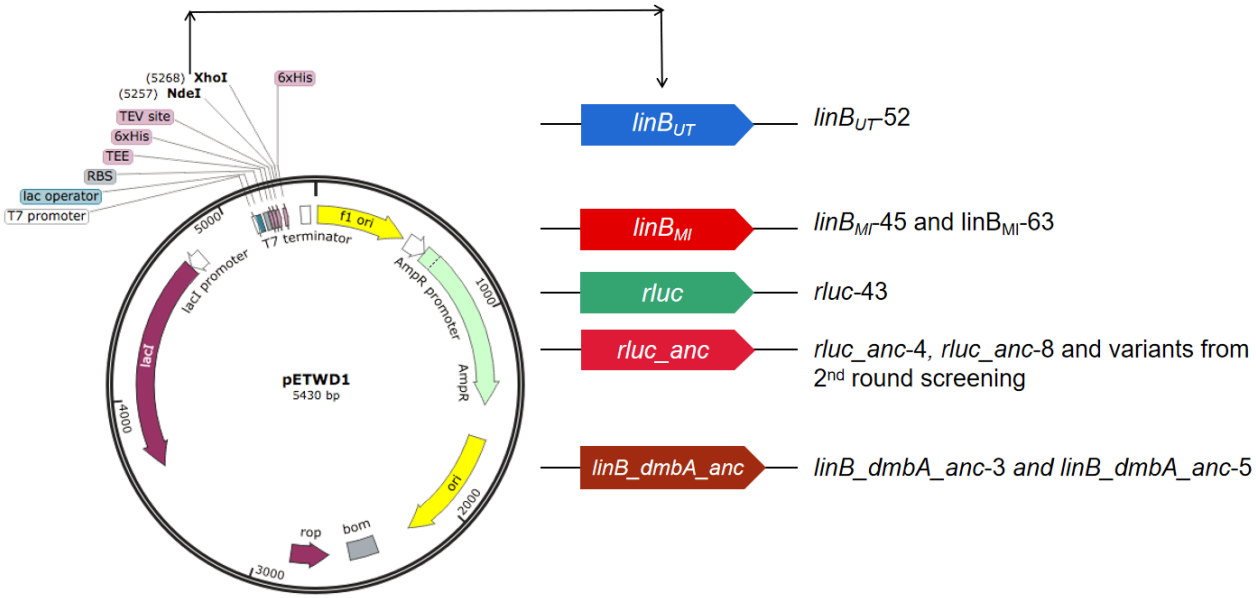

Fig. 3-1 Construction of plasmids for expression of HLD and its related proteins.

3-2-4 Expression of His-tagged proteins in *E. coli*

1. Plasmids for expression of His-tagged proteins were introduced into *E. coli* BL21 Star™ (DE3) by electroporation.
2. Cells were incubated until OD_{660} reached 0.6.
3. 0.5 mM IPTG was added, and incubated at 20℃ for 12h for expression of proteins.
4. Cells were collected and stocked at -80°C

3-2-5 Purification of His-tagged proteins

Reagents

・Wash buffer (pH 7.5, 0.5 M NaCl, 10 mM imidazole)

imidazole	0.68 g
NaCl	29.2 g
1 M K_2HPO_4	6.8 mL
1 M KH_2PO_4	3.2 mL
dH_2O	up to 1L

Wash buffer was used after autoclaving.

・Elution buffer (pH 7.5, 0.5 M NaCl, 0.5 M imidazole)

imidazole	34 g
NaCl	29.2 g
1 M K_2HPO_4	16.8 mL
1 M KH_2PO_4	3.2 mL
dH_2O	up to 1L

Elution buffer was used after autoclaving.

・Conservation buffer (pH7.5, 20 mM Tris-HCl, 5 mM $MgCl_2$, 100 mM NaCl, 0.1 mM EDTA)

・BD TALON Metal Affinity Resins (BD Bioscience)

Operations:

1. Cells were dissolved in conservation buffer (10-20 mL/g cells), and disrupted by ultrasonication (output 4, duty cycle 50%, 1 min x appropriate times with 5 min interval) until the solution become transparent.
2. Cells were centrifuged at 15,000 rpm for 20 min, supernatant was collected as crude extract.
3. BD TALON Metal Affinity Resins (0.2 g/100 μL) were washed with autoclaved dH_2O 3 times (1,000 rpm, 3-5 min), and washed with wash buffer 3 times (1,000 rpm, 3-5 min).
4. Crude extract was mixed with BD TALON Metal Affinity Resin and wash buffer (3 fold volume of crude enzyme), and rotated at 4℃ for 20 min.
5. The mixture was centrifuged at 1,000 rpm for 5 min, and supernatant was discarded
6. Resin was washed with wash buffer 3 times (1,000 rpm, 5 min).
7. Elution buffer was added and rotated at 4℃ for 10 min.
8. The mixture was centrifuged at 1,000 rpm for 5 min
9. Supernatant was collected and stocked as purified protein 1.
10. 7-8 was repeated, and supernatant was collected and stocked as purified protein 2.
11. Purified protein 1 and 2 were combined as purified protein.
12. Purified protein was divided into a small volume (10 μL) and stocked in PCR tubes at -80℃.

Table 3-3 Eight putative evolved HLDs selected from the 1st round screening

Original protein	No	Mutation sites
Rluc_anc	4	G122S (GGT→AGT), I298M (ATT→ATG)
	8	N87S (AAT→AGT), D104G (GAT→GGT), K136R (AAA→AGA), I161V (ATT→GTT), S187C (AGC→TGC), K247E (AAA→GAA)
$LinB_{MI}$	63	G4S (GGC→AGC), I128V (ATT→GTT), A269T (GCA→ACA)
	45	T81S (ACC→TCC), L239H (CTC→CAC)
$LinB_{UT}$	52	P203T (CCG→ACG)
Rluc	43	E132D (GAG→GAC), E151G (GAA→GGA), E211G (GAA→GGA)
LinB_dmbA_anc	3	R125C (CGT→TGT), E161V (GAA→GTA)
	5	A3T (GCA→ACA), E147V (GAA→GTA), V148A (GTT→GCT), L196P (CTG→CCT), V222A (GTT→GCT)

3-2-6 SDS-PAGE

Reagents:

Running buffer (1L)	3 g Tris
	14.4 g Glycine
	1 g SDS
Stain buffer	0.05% (w/v) Coomassie Brilliant Blue R-250
	50% methanol
	10% acetic acid
Destain buffer	25%methanol
	7% acetic acid

SDS-PAGE gel (12.5%):

Table 3-4 Composition of SDS-PAGE gel (12.5%)

	30% Acrylamide	buffer*	water	10% APS	TEMED
Separation gel	3.36 mL	2 mL	2.64 mL	24 μL	8 μL
Concentration gel	0.75 mL	1.25 mL	3 mL	15 μL	10 μL

* buffer

Separation gel: 1.5M Tris-HCl (pH 8.8), 0.4% SDS (Sodium Dodecyl Sulfate)

Concentration gel: 0.5M Tris-HCl (pH 6.8), 0.4% SDS (Sodium Dodecyl Sulfate)

Operations:

1. Protein samples were mixed with 2 × sample buffer (Bio-Rad) and heated at 95℃ for 10 min.
2. Samples were electrophoresed (running electric current 25mA) on SDS-PAGE gel with Marker (BIO-RAD).
3. Gel was stained for more than 40 min, and distain for overnight.

3-2-7 Concentration of purified protein

In order to stock protein for long time, purified protein was concentrated by using Vivaspin 2 (Sartorius).

Operations:

1. Vivaspin 2 tubes were washed with dH_2O 3 times (8,000 x*g*, 5 min).
2. Vivaspin 2 tubes were washed with concentration buffer 3 times (8,000 x*g*, 5 min)
3. Purified protein was concentrated to 200 μL.
4. Concentrated purified protein was divided into a small volume (10 μL) and stocked in PCR tubes at -80℃.

3-2-8 Assay for dehalogenase activity

HLD activity was assayed by using spectrophotometrical measurement of released halide ions according to the Iwasaki's method (Iwasaki et al., 1952) .

Reagents:

<u>50 mM glycine buffer (pH 8.6) (100 mL)</u>

0.2 M glycine 25 mL

0.2 M NaOH 2 mL

dH_2O 73 mL

<u>Hg solution (Sol I) (100 mL)</u>

$Hg(SCN_2)$ 0.3 g

100% ethanol 100 mL

<u>FAS solution (Sol II) (200 mL)</u>

$NH_4Fe(SO_4)_2 \cdot 12H_2O$ 12.32 g

70% HNO_3 72 mL

dH_2O 128 mL

<u>KBr（MW=119)</u>

- Prepare 476 mg/100 mL in DW (= 40000μmol/L) .
- Dilute to 0, 50, 100, 400, 1000, 4000μmol/L for calibration curve.

<u>KCl (MW=74.551)</u>

- Prepare 298.2 mg/100 ml DW (= 40,000μmol/L) .
- Dilute to 0, 50, 100, 400, 1000, 4000μmol/L for calibration curve.

Substrate: For LinA and HLD activity, γ-HCH (50 mg/mL in DMSO) and 1,3-dibromopropane were used, respectively.

One unit (U) was defined as enzymatic activity that requires for the release of 1 μmol halide ion per minute.

Operations:

1. 1 mL of glycine buffer was pre-incubated at 30℃ for 5 min.
2. 1μl of substrate was added and shaken for 30 sec.
3. 1μl of concentrated protein was added and shaken gently.
4. 200 μL of sample was collected at different time intervals: 0, 60 min, 180 min and 240 min.
5. 20 μL of Sol I was added into samples and shaken for 30 sec.
6. 40 μL of Sol II was added and shaken for 30 sec.
7. Samples were centrifuged at 15,000 rpm for 5 min.
8. Absorbance at 450 nm of the supernatant was measured by plate reader (Bio-Rad iMark Microplate Reader).
9. Calibration curve was prepared by using the standard samples.
10. Amount of released halide ions was calculated by using the calibration curve.

3-2-9 Assay for the LinB-like activity

γ-HCH is converted to 1,2,4-TCB, 2,5-DCP, and 2,5-DDOL by LinA and LinB (Fig. 3-2). Production of 2,5-DCP and 2,5-DDOL from γ-HCH under the condition with LinA was used as an indicator of LinB-like activity.

Operations:

1. 1 mL of glycine buffer was pre-incubated at 30℃ for 5 min.
2. 1 μL of substrate (50mg/ml γ-HCH dissolved in DMSO) was added and vortexed for 30 sec.
3. LinA* and sample protein were added and vortexed gently.
4. 200 μL of reaction solution was collected at different time intervals: 0, 10 min, 20 min and 30 min.
5. 200 μL of ethyl acetate containing 2 ppm dildrin as internal standard was added and mixed well.
6. The mixture was centrifuged at 15,000 rpm for 5 min.
7. Upper layer (ethyl acetate layer) was collected and used for GC(ECD) analysis (1-2-4).

* Amount of LinA was determined on the basis of the pilot analysis.

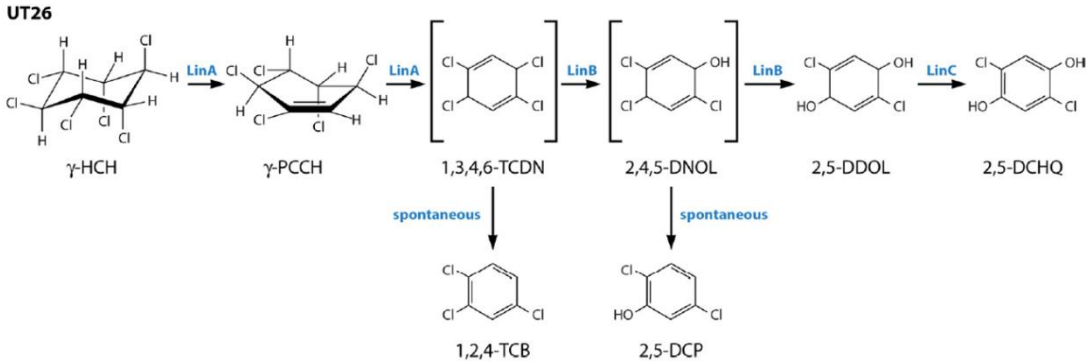

Fig. 3-2 Upstream degradation pathway of γ-HCH in UT26

3-3 Results

3-3-1 Expression and purification of the putative evolved HLDs

The 8 putative evolved HLDs, $LinB_{UT}$-52, $LinB_{MI}$-45, $LinB_{MI}$-63, Rluc-43, Rluc_anc-4, Rluc_anc-8, LinB_dmbA_anc-3, and LinB_dmbA_anc-5, their original proteins, and LinA were expressed in *E.coli* and purified (Fig. 3-3 to 3-5). All the proteins except $LinB_{UT}$-52 and Rluc-43 could be expressed well and purified successfully. Concentration of the finally purified proteins used for further analysis was shown in Table 3-5.

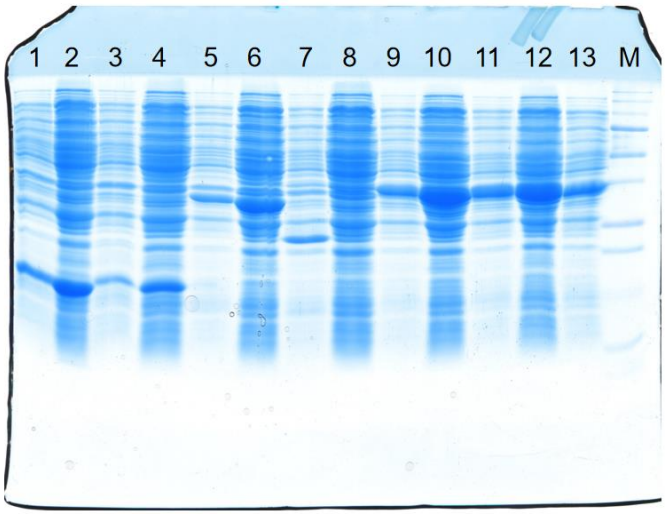

No.	Protein
1	LinA(Ap) Cell
2	LinA(Ap) CE
3	LinA(Km) Cell
4	LinA(Km) CE
5	$LinB_{UT}$ Cell
6	$LinB_{UT}$ CE
9	Rluc_anc Cell
10	Rluc_anc CE
11	Rluc_anc-4 Cell
12	Rluc_anc-4 CE
13	Rluc_anc-8 Cell

Fig. 3-3 SDS-PAGE of the whole cells and crude extracts

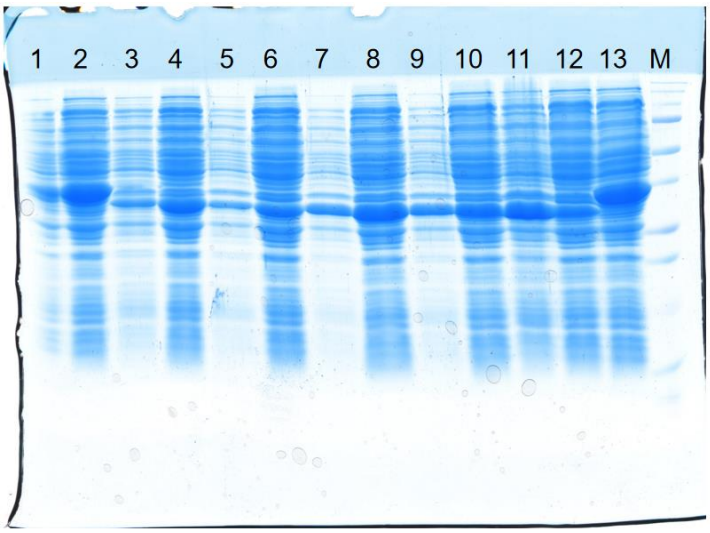

No.	Protein
1	LinB_dmbA_anc Cell
2	LinB_dmbA_anc CE
3	LinB_dmbA_anc-3 Cell
4	LinB_dmbA_anc-3 CE
5	LinB_dmbA_anc-5 Cell
6	LinB_dmbA_anc-5 CE
7	$LinB_{MI}$ Cell
8	$LinB_{MI}$ CE
9	$LinB_{MI}$-63 Cell
10	$LinB_{MI}$-63 CE
11	$LinB_{MI}$-45 Cell
12	$LinB_{MI}$-45 CE
13	Rluc_anc-8 CE

Fig. 3-4 SDS-PAGE of the whole cells and crude extracts

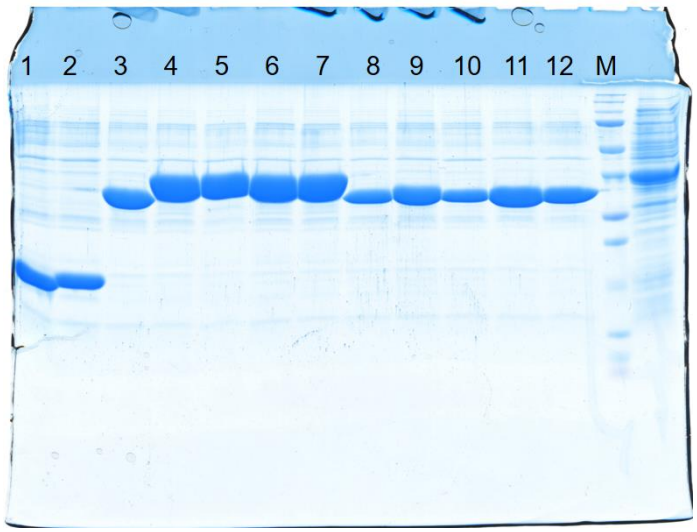

No.	Protein
1	LinA(Ap) Pu
2	LinA(Km) Pu
3	$LinB_{UT}$ Pu
4	Rluc_anc Pu
5	Rluc_anc-4 Pu
6	Rluc_anc-8 Pu
7	LinB_dmbA_anc Pu
8	LinB_dmbA_anc-3 Pu
9	LinB_dmbA_anc-5 Pu
10	$LinB_{MI}$-45 Pu
11	$LinB_{MI}$ Pu
12	$LinB_{MI}$-63 Pu

Fig. 3-5 SDS-PAGE of the purified proteins

Table 3-5 Concentration of evolved hlds

Protein name	Concentration of protein (mg/mL)
LinB	6.23
$LinB_{MI}$	7.98
$LinB_{MI}$-63	4.08
$LinB_{MI}$-45	3.76
LinB_dmbA_anc	2.17
LinB_dmbA_anc-3	2.47
LinB_dmbA_anc-5	1.86
Rluc_anc	5.1
Rluc_anc-4	1.54
Rluc_anc-8	2.92

3-3-2 HLD activity of the putative evolved HLDs

General HLD activity of the six putative evolved HLDs toward 1,3-dibromopropane, which is a general substrate of HLDs, was analyzed. Among them, $LinB_{MI}$-45 showed no significantly difference in HLD activity compare with $LinB_{MI}$ (Fig. 3-6). However, other five putative evolved HLDs showed higher HLD activity than their corresponding wild type proteins (Fig. 3-6 to 3-8). HLD activity of $LinB_{MI}$-63 was 1.97-fold higher than $LinB_{MI}$. Compared with LinB_dmbA_anc, LinB_dmbA_anc-3 and LinB_dmbA_anc-5 showed 2.87- and 2.65-fold higher activity, respectively. Rluc_anc-4 and Rluc_anc-8 showed 2.58- and 2.80-fold higher activity than Rluc_anc.

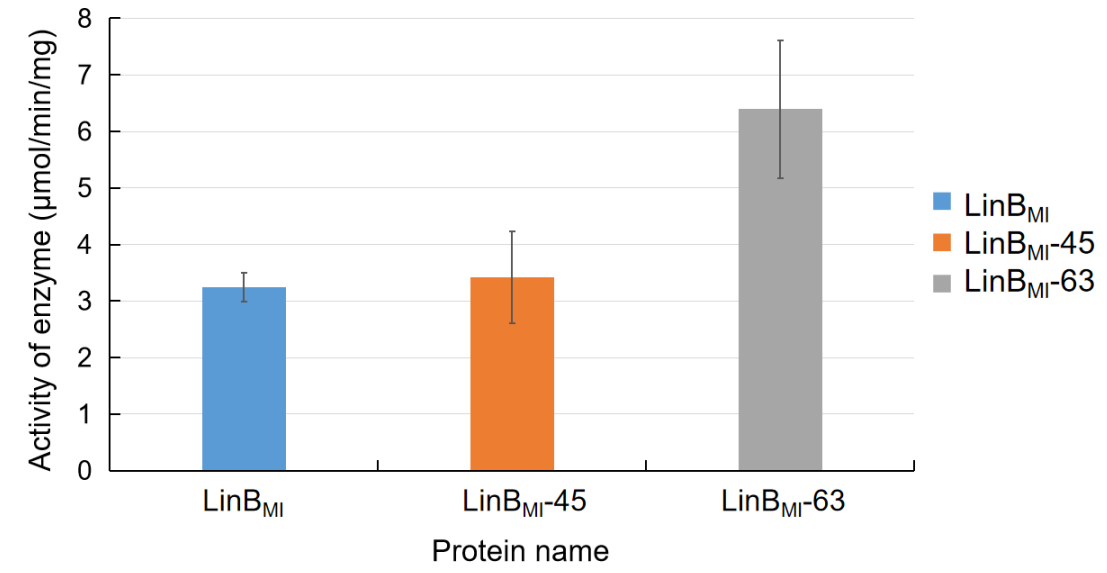

Fig. 3-6 HLD activity of $LinB_{MI}$ and its mutants, $LinB_{MI}$-45 and $LinB_{MI}$-63

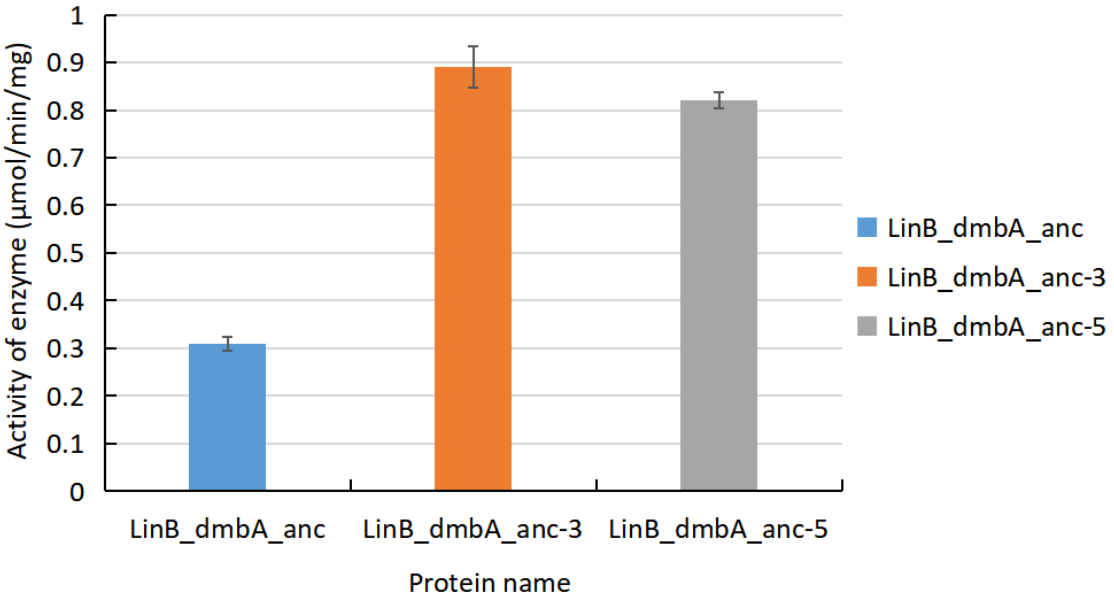

Fig. 3-7 HLD activity of LinB_dmbA_anc and its mutants, LinB_dmbA_anc-3 and LinB_dmbA_anc-5

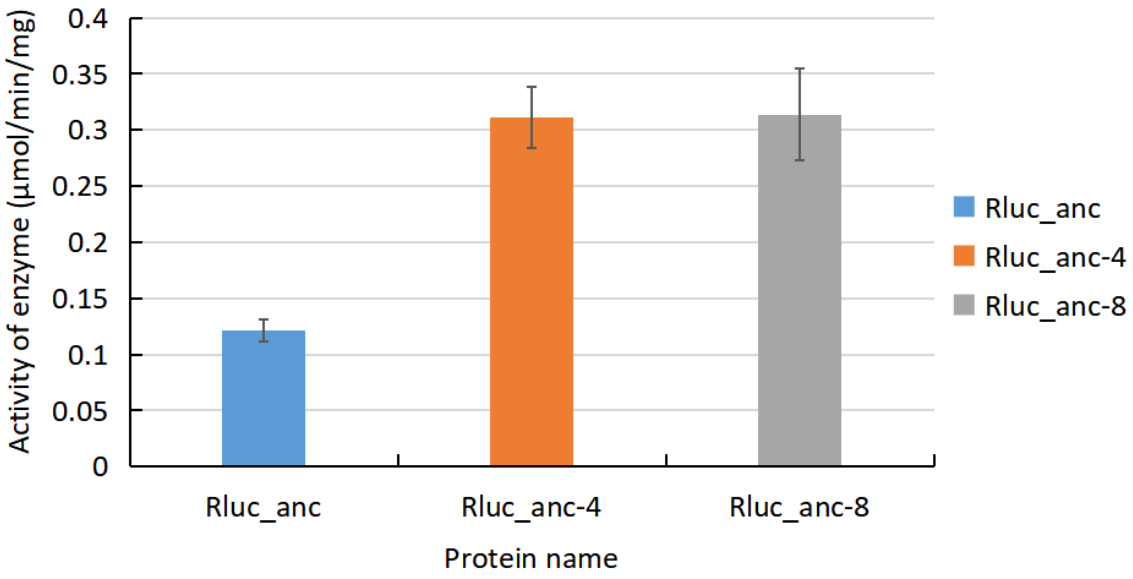

Fig. 3-8 HLD activity of Rluc_anc and its mutants, Rluc_anc-4 and Rluc_anc-8

3-3-3 LinB-like activity of the putative evolved HLDs

LinB-like activity of the five putative evolved HLDs was assessed by using γ-HCH as a starting substrate in the reaction solution containing LinA. Production of 2,5-DDOL, 1,2,4-TCB, and 2,5-DCP is shown in Fig. 3-9, Fig. 3-10 and Fig. 3-11.

The difference between $LinB_{MI}$ and $LinB_{MI}$-63 was faint, but larger amount of 2,5-DDOL seemed to be produced by $LinB_{MI}$-63 (Fig. 3-9A).

Rluc_anc-4 and Rluc_anc-8 obviously produced larger amount of 2,5-DDOL and 2,5-DCP and smaller amount of 1,2,4-TCB than Rluc_anc (Fig. 3-10), indicating that LinB-like activity these two proteins is higher than their original protein.

Similarly, LinB_dmbA_anc-3 and LinB_dmbA_anc-5 obviously produced larger amount of 2,5-DDOL and 2,5-DCP and smaller amount of 1,2,4-TCB than LinB_dmbA_anc (Fig. 3-11), indicating that LinB-like activity of these two proteins is higher than their original protein.

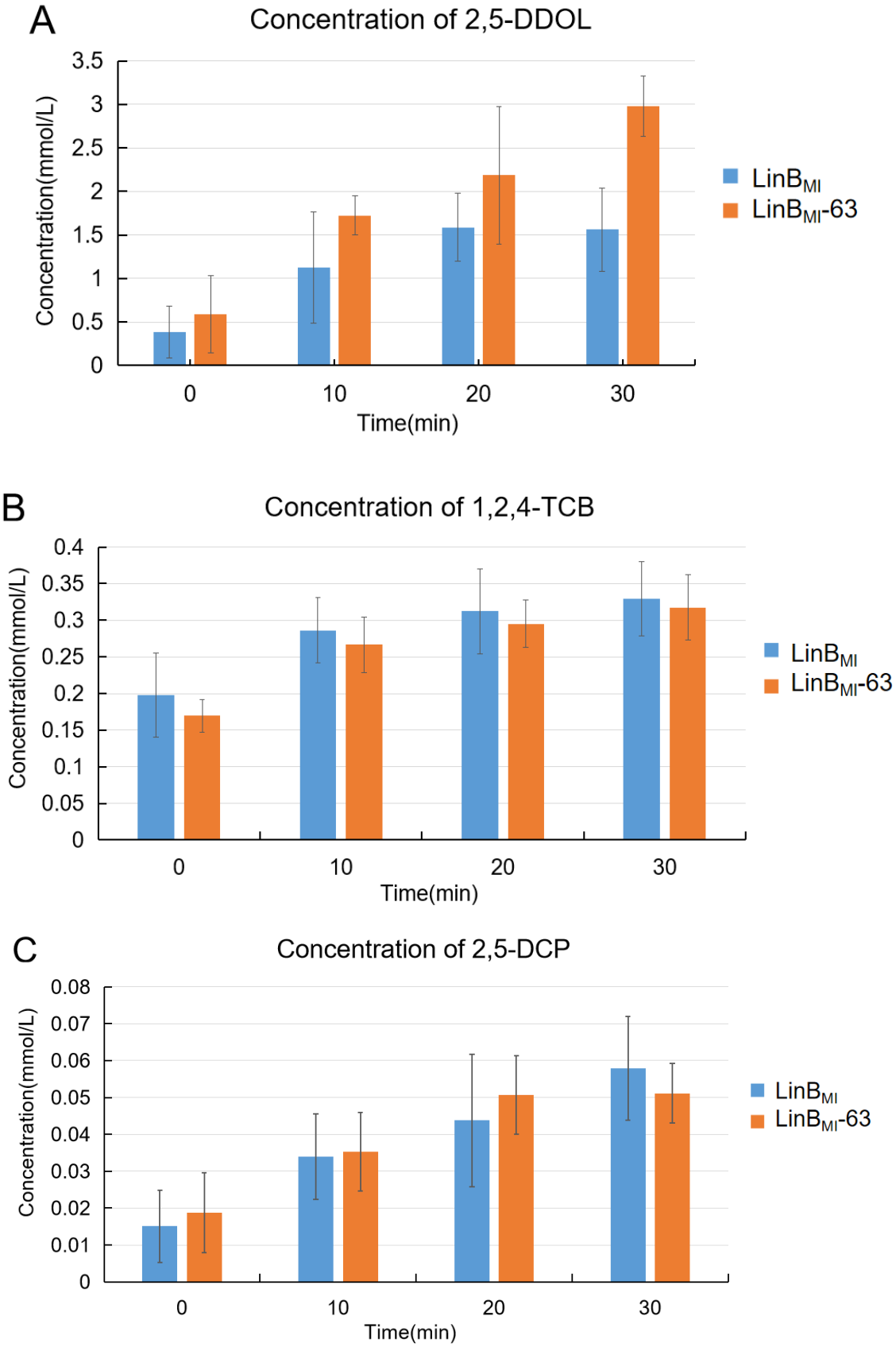

Fig. 3-9 Production of 2,5-DDOL, 1,2,4-TCB and 2,5-DCP by $LinB_{MI}$ and $LinB_{MI}$-63 (A: Concentration of 2,5-DDOL; B: Concentration of 1,2,4-TCB; C: Concentration of 2,5-DCP)

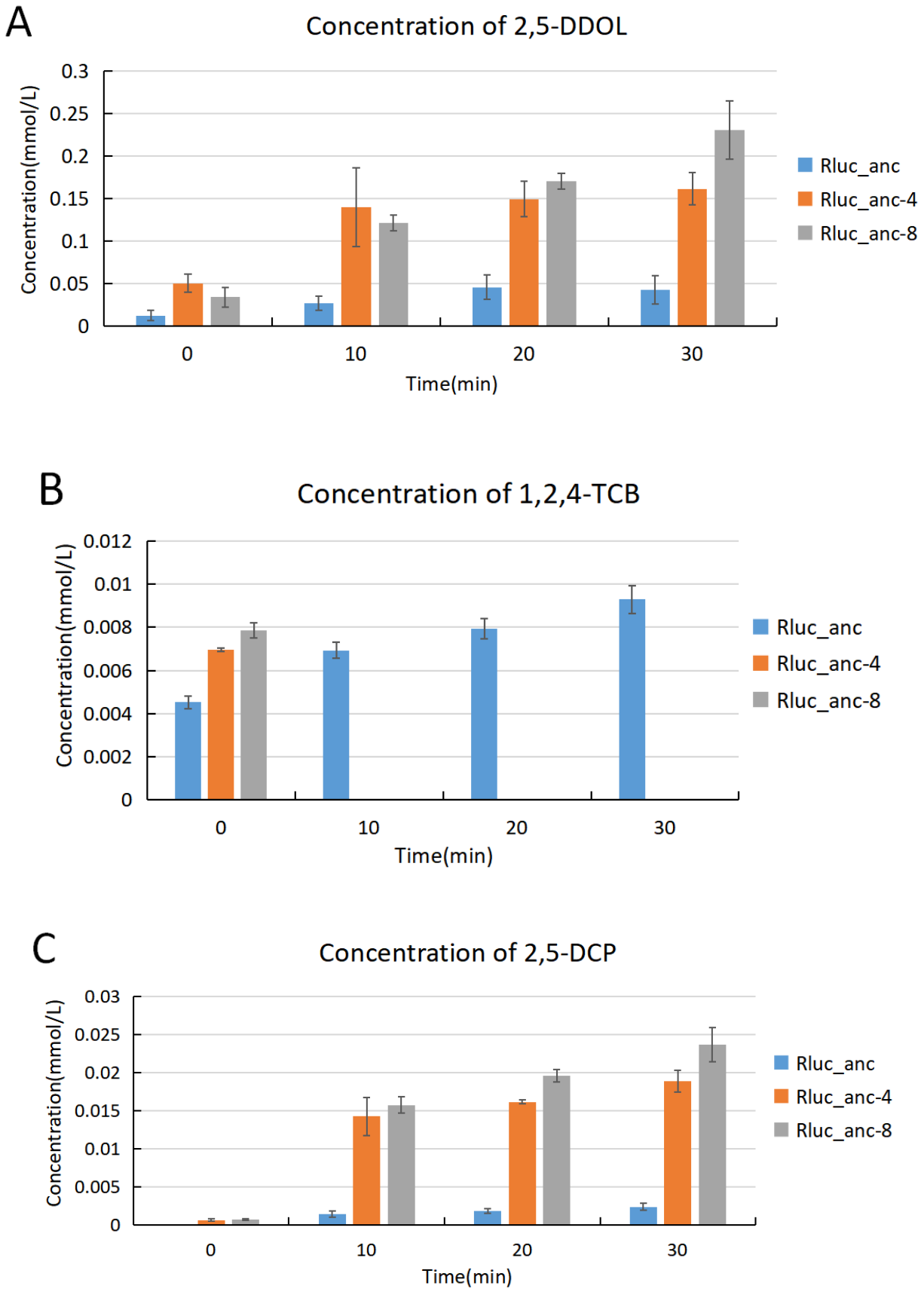

Fig. 3-10 Production of 2,5-DDOL, 1,2,4-TCB and 2,5-DCP by Rluc_anc, Rluc_anc-4 and Rluc_anc-8 (A: Concentration of 2,5-DDOL; B: Concentration of 1,2,4-TCB; C: Concentration of 2,5-DCP)

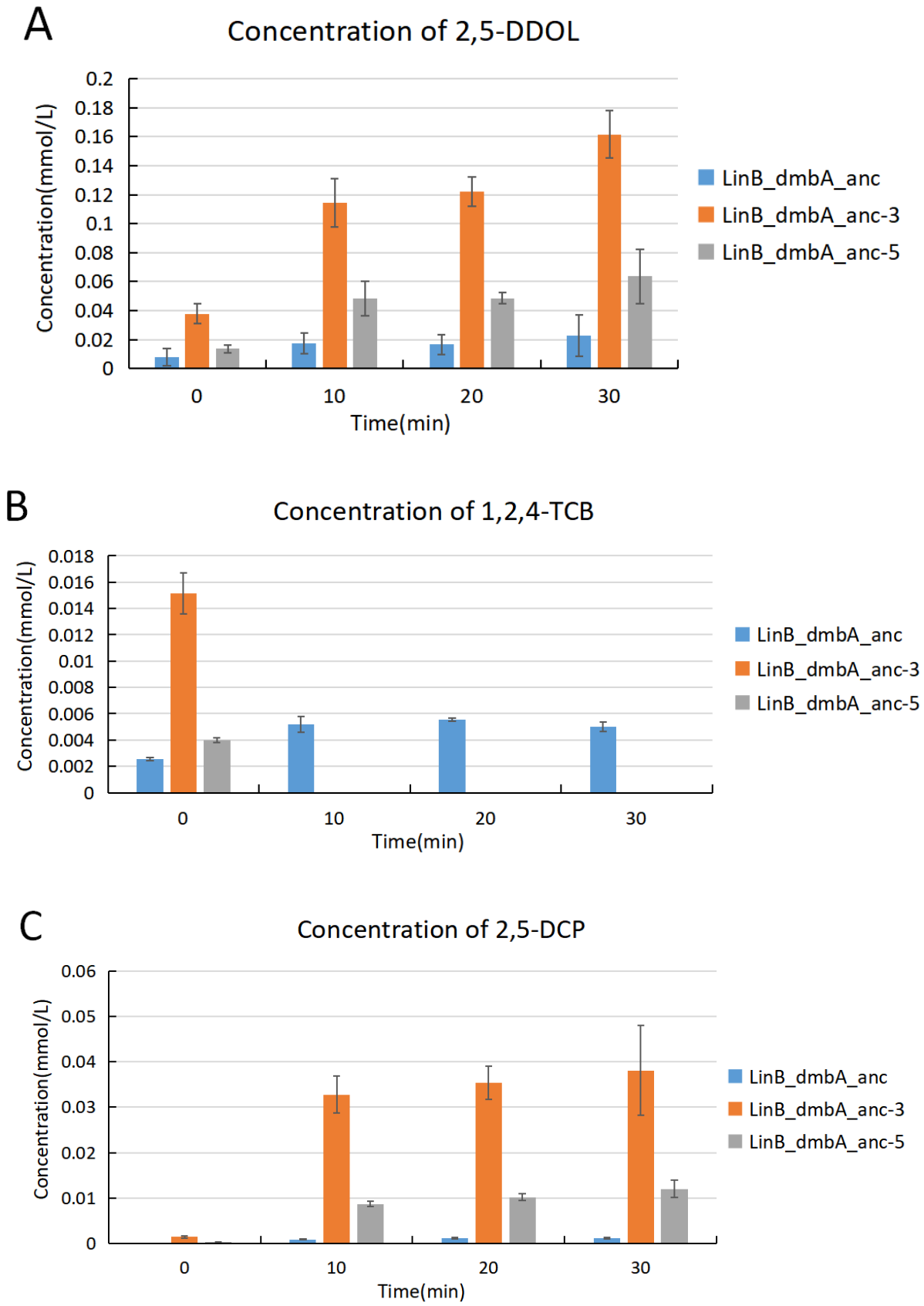

Fig. 3-11 Production of 2,5-DDOL, 1,2,4-TCB and 2,5-DCP by LinB_dmbA_anc, LinB_dmbA_anc-3 and LinB_dmbA_anc-5 (A: Concentration of 2,5-DDOL; B: Concentration of 1,2,4-TCB; C: Concentration of 2,5-DCP)

3-3-4 Expression, purification and characterization of Rluc and Rluc-43

Rluc could be expressed and purified well by using vector pETWD1 (Fig. 3-12), but Rluc-43 could not. So other expression vectors, pAQN and pUC18, were used for expression of Rluc-43. Rluc-43 was successfully expressed and purified by using pAQN vector (Fig. 3-13). Concentration of the finally purified proteins used for further analysis was shown in Table 3-6.

Significant HLD activity of Rluc and Rluc-43 was not detected (data not shown). On the other hand, when these enzymes were incubated with γ-HCH and LinA, only Rluc-43 produced very faint amount of 2,5-DDOL (Fig. 3-14), suggesting that Rluc-43 has faint LinB-like activity.

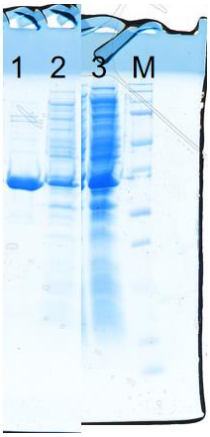

No.	Protein
1	Rluc Pu
2	Rluc Cell
3	Rluc Crude extract

Fig. 3-12 SDS-PAGE of Rluc

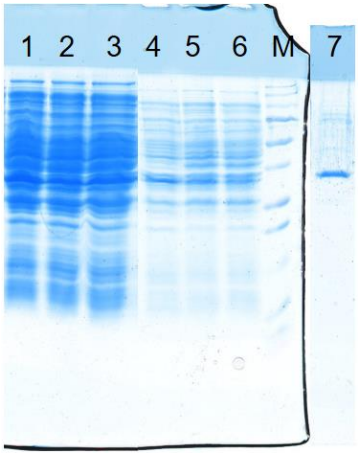

No.	Protein
1	pAQN/Rluc-43 Crude extract
2	pUC18/Rluc-43 Crude extract
3	pETWD1/Rluc-43 Crude extract
4	pAQN/Rluc-43 Cell
5	pUC18/Rluc-43 Cell
6	pETWD1/Rluc-43 Cell
7	pAQN/Rluc-43 Pure protein

Fig. 3-13 SDS-PAGE of Rluc-43

Table 3-6 Concentration of Rluc and Rluc-43

Protein name	Concentration(mg/ml)
Rluc	0.98
Rluc-43	1.05

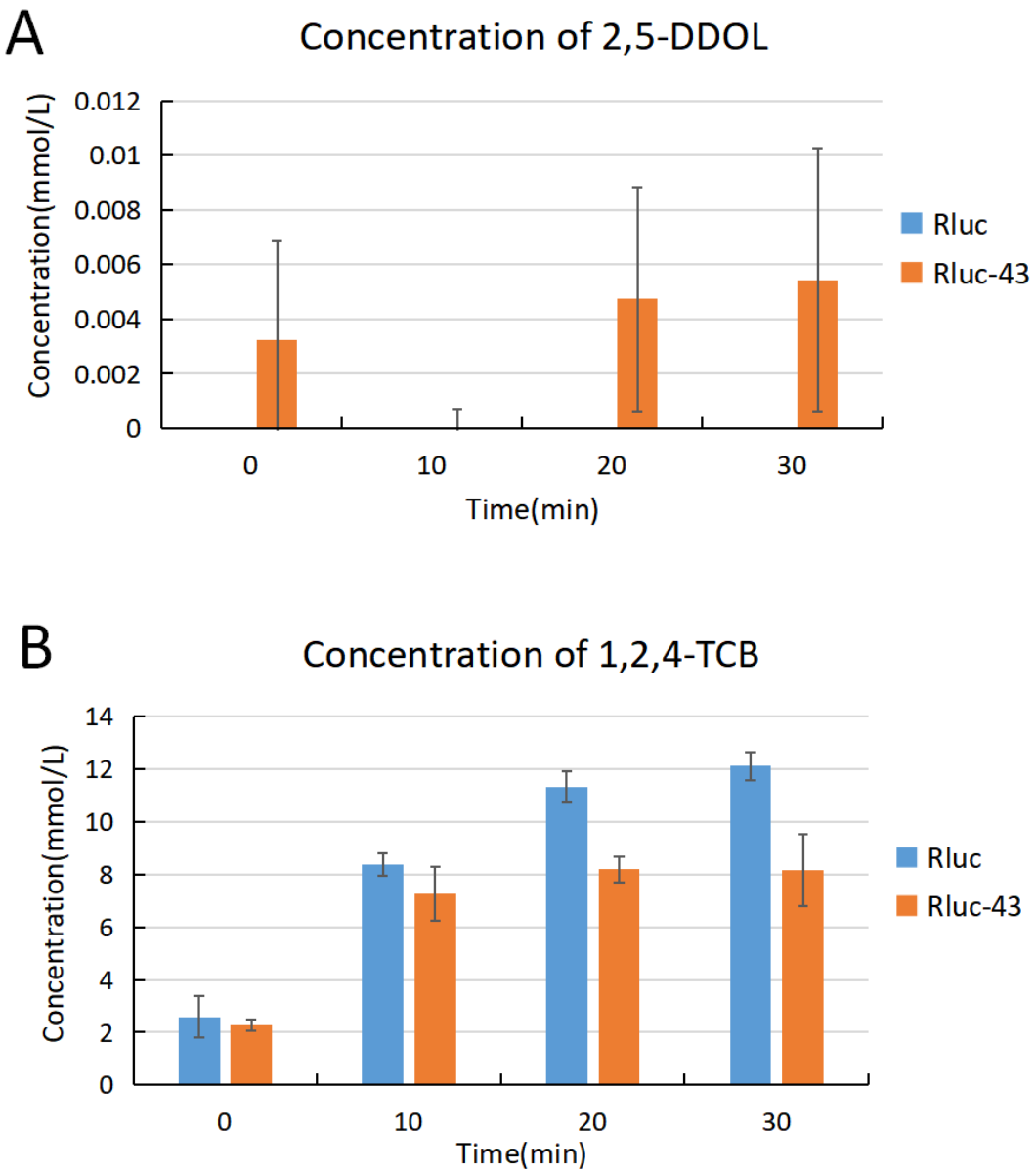

Fig. 3-14 Production of 2,5-DDOL and 1,2,4-TCB by Rluc and Rluc-43 (A: Concentration of 2,5-DDOL; B: Concentration of 1,2,4-TCB)

3-3-5 Expression, purification, and characterization of the putative evolved proteins obtained by the 2nd round screening

The second round screening was more difficult than the first screening, since the screening system seems to be difficult to detect small difference of genes that have evolved to some extent. This system is suitable for selection of the evolved gene from the original gene encoding enzyme having weak or no LinB-like activity. Thus, only the putative evolved proteins of Rluc_anc-8 were further analyzed. Eight proteins obtained from the 2nd screening and four proteins selected from the 1st screening were expressed and purified (Fig. 3-15, 3-16 and 3-17). Concentration of the finally purified proteins used for further analysis was shown in Table 3-7.

Among these candidates, only Rluc_anc-8-6 and Rluc_anc-8-37 showed high LinB-like activity than Rluc_anc-8, HLD activity of Rluc_anc-8-6 and Rluc_anc-8-37 was higher compared with Rluc_anc-8 (Fig. 3-18). LinB-like activity of the putative evolved proteins was assessed by using γ-HCH as a starting substrate

in the reaction solution containing LinA (Fig. 3-19). Since Rluc_anc-8-6 and Rluc_anc-8-37 produced lesser amount of 2,5-DCP and larger amount of 2,5-DDOL than Rluc_anc-8, more detailed analysis was conducted for these two proteins (Fig. 3-19). Rluc_anc-8-6 and Rluc_anc-8-37 also produced lesser amount of 2,5-DCP and larger amount of 2,5-DDOL than Rluc_anc-8 in this experiment, indicating that these two proteins have improved relative activity of the second LinB-catalyzed step to the first one.

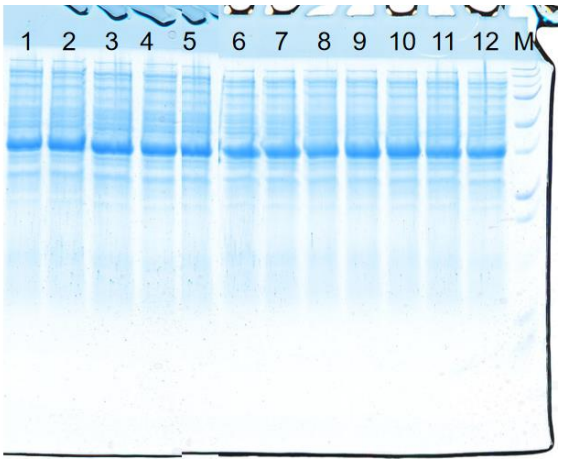

No.	Protein
1	Rluc_anc-2p Cell
2	Rluc_anc-5p Cell
3	Rluc_anc-34 Cell
4	Rluc_anc-37 Cell
5	Rluc_anc-8-6 Cell
6	Rluc_anc-8-11 Cell
7	Rluc_anc-8-14 Cell
8	Rluc_anc-8-16 Cell
9	Rluc_anc-8-18 Cell
10	Rluc_nc-8-12 Cell
11	Rluc_anc-8-4 Cell
12	Rluc_anc-8-7 Cell

Fig. 3-15 Whole cells of variants of Rluc_anc-8

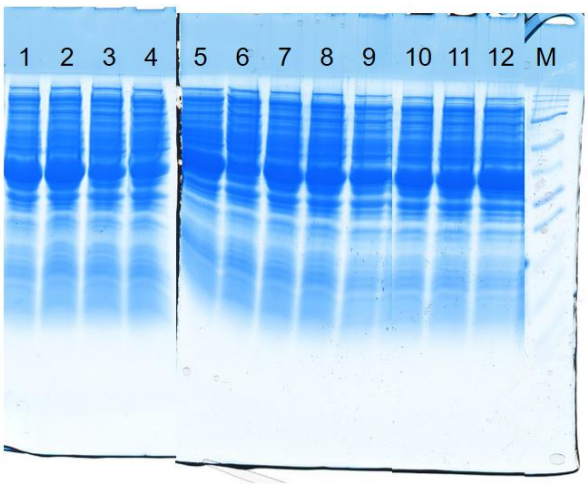

No.	Protein
1	Rluc_anc-2p Crude enzyme
2	Rluc_anc-5p Crude enzyme
3	Rluc_anc-34 Crude enzyme
4	Rluc_anc-37 Crude enzyme
5	Rluc_anc-8-6 Crude enzyme
6	Rluc_anc-8-11 Crude enzyme
7	Rluc_anc-8-14 Crude enzyme
8	Rluc_anc-8-16 Crude enzyme
9	Rluc_anc-8-18 Crude enzyme
10	Rluc_anc-8-12 Crude enzyme
11	Rluc_anc-8-4 Crude enzyme
12	Rluc_anc-8-7 Crude enzyme

Fig. 3-16 Crude enzyme of variants of Rluc_anc-8

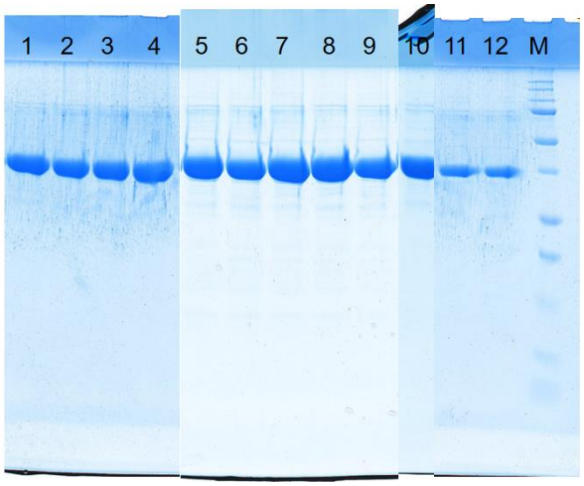

No.	Protein
1	Rluc_anc-2p Purified enzyme
2	Rluc_anc-5p Purified enzyme
3	Rluc_anc-34 Purified enzyme
4	Rluc_anc-37 Purified enzyme
5	Rluc_anc-8-6 Purified enzyme
6	Rluc_anc-8-11 Purified enzyme
7	Rluc_anc-8-14 Purified enzyme
8	Rluc_anc-8-16 Purified enzyme
9	Rluc_anc-8-18 Purified enzyme
10	Rluc_anc-8-12 Purified enzyme
11	Rluc_anc-8-4 Purified enzyme
12	Rluc_anc-8-7 Purified enzyme

Fig. 3-17 Purified protein of variants of Rluc_anc-8

Table 3-7 Concentration of purified protein of variants of Rluc_anc-8

Protein name	Concentration of protein (mg/mL)	Protein name	Concentration of protein (mg/mL)
Rluc_anc-2p	3.54	Rluc_anc-8-14	6.73
Rluc_anc-5p	4.08	Rluc_ancc-8-16	1.64
Rluc_anc-34	2.15	Rluc_anc-8-18	3.83
Rluc_anc-37	4.12	Rluc_anc-8-12	3.50
Rluc_anc-8-6	4.45	Rluc_anc-8-4	1.73
Rluc_anc-8-11	2.17	Rluc_anc-8-7	1.05

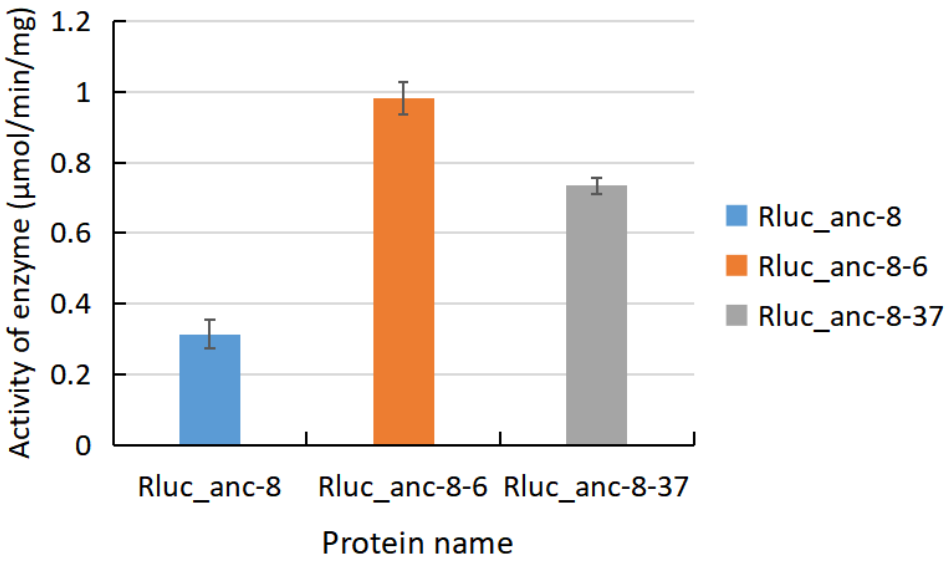

Fig. 3-18 HLD activity of Rluc_anc-8, Rluc_anc-8-6 and Rluc_anc-8-37 and it two improved variants

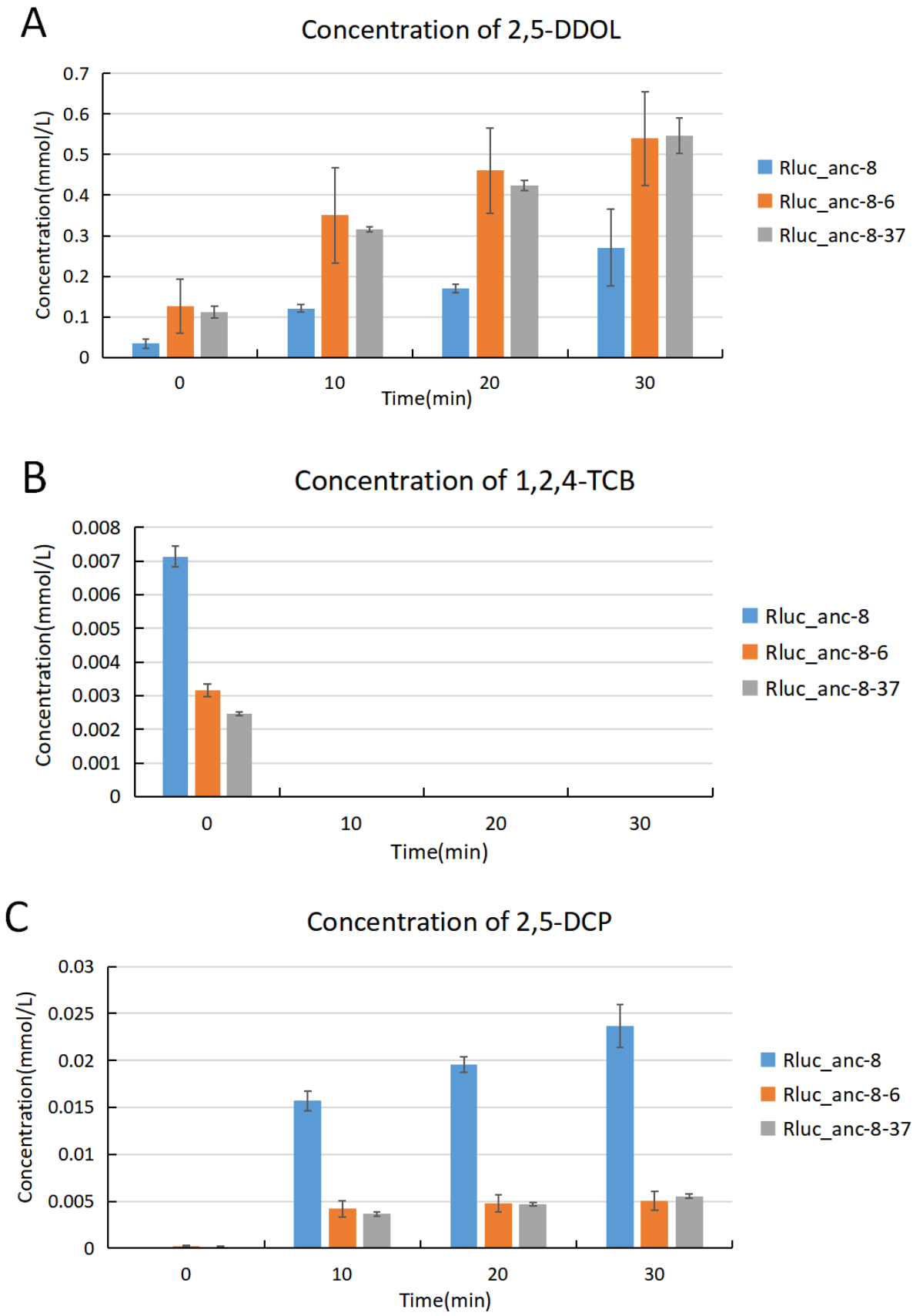

Fig. 3-19 Production of 2,5-DDOL, 1,2,4-TCB and 2,5-DCP by Rluc_anc-8, Rluc_anc-8-6 and Rluc_anc-8-37 variants (A: Concentration of 2,5-DDOL; B: Concentration of 1,2,4-TCB; C: Concentration of 2,5-DCP)

3-4 Discussion

In this chapter, protein products of the candidate evolved genes obtained by the *in vitro* evolution system were expressed in *E. coli* as His-tagged proteins, purified, and characterized. Most of the putative evolved proteins showed improved HLD activity toward 1,3-dibromopropane, which is a general substrate of HLDs, and LinB-like activity than their corresponding original enzymes. These results clearly demonstrated that the *in vitro* evolution system constructed in this study successfully worked.

LinB-like activity was assessed by the production of 2,5-DCP and 2,5-DDOL from γ-HCH in the reaction solution containing LinA, since substrates of LinB in the γ-HCH degradation pathway are unstable and the direct assay is impossible. To quantify the LinB-like activity more critically, the assay system should be improved.

$LinB_{MI}$-63 showed the higher LinB-like activity than $LinB_{MI}$, indicating that $LinB_{MI}$ can be more improved for the LinB activity in the γ-HCH utilization. This result strongly suggest that γ-HCH degraders can be optimized more for the γ-HCH utilization at the steps catalyzed by LinB. The dead-end product 2,5-DCP is toxic for cells, thus the second LinB-catalyzed step should be improved more than the first LinB-catalyzed step. Theoretical design of such delicate feature seems to be difficult, and thus the *in vitro* system constructed in this study will be useful for the purpose. Indeed, the putative evolved proteins, Rluc_anc-8-6 and Rluc_anc-8-37, obtained by the second round screening improved relative activity of the second LinB-catalyzed step to the first one.

LinB_dmbA_anc-3 and LinB_dmbA_anc-5, and Rluc_anc-4 and Rluc_anc-8 showed improved LinB-like activity than their original proteins, LinB_dmbA_anc and Rluc_anc, respectively. Although more analysis is necessary, the candidate evolved proteins were also obtained by the 2^{nd} round screening by using HLDs showing very week or no LinB-like activity. The evolution process of HLDs toward the γ-HCH utilization may be traced by using this system and such HLDs.

Discussions

Haloalkane dehalogenases (HLDs) (EC 3.8.1.5) that belong to the α/β-hydrolase superfamily convert halogenated compounds to corresponding alcohols by simple hydrolytic mechanism (Nagata et al., 2015). HLDs were originally identified from bacterial strains that utilize halogenated environmental pollutants as enzymes catalyzing dehalogenation step(s) of such halogenated compounds and were thought to be specific enzymes for the degradation of artificial compounds. However, it has been revealed that many bacterial strains including those that have not been reported as degraders of halogenated compounds also possess HLD homologues. Now it is obvious that many HLD-like genes can be identified in the genomes of various bacteria by database searches. If such HLD homologues are biochemically confirmed to be 'real' HLDs, they are expected to be valuable materials for protein-engineering studies attempting to develop efficient catalysts for biotechnological applications, since HLDs generally (i) have a broad range of substrate specificities, (ii) are promiscuous, and (iii) are ready to change their activities towards various substrates.

LinB is one of prototypical HLDs and was originally identified as an enzyme necessary for utilization of a man-made chlorinated pesticide γ-hexachlorocyclohexane (γ-HCH) in *Sphingobium japonicum* UT26. To date, many γ-HCH-degrading bacterial strains including UT26 have been isolated from various sites contaminated with HCH isomers around the world. Interestingly, all the γ-HCH-degrading bacterial strains whose genes and enzymes for the γ-HCH degradation have been identified use LinB for the corresponding steps. In other words, no γ-HCH degrader has been identified that uses other HLDs besides LinB for the γ-HCH utilization. Considering the facts that HLDs or its homologues are widely distributed among bacterial strains and that HLDs generally have a broad range of substrate specificities, HLDs other than LinB might be involved in the γ-HCH degradation.

The main purpose of this study is to understand the process and mechanisms of functional evolution of HLDs for the degradation of persistent organic pollutants. For the purpose, *in vivo* and *in vitro* evolution systems of HLDs toward the γ-HCH utilization were constructed.

In Chapter 1, firstly, the *linB*-deletion strain UTDB2 was constructed, in which just open reading frame of the *linB* gene was deleted. Then, the *linB*-replacement strains were constructed using UTDB2, into which $linB_{MI}$, *dbjA*, *dmmA*, *rluc*, *rluc_anc*, *rluc_ancM* and *linB_dmbA_anc* had been introduced at the *linB* site. GC assay for the γ-HCH degradation activity and spot assay for the γ-HCH utilization demonstrated that Rluc_anc, Rluc_ancM, and DmmA have weak LinB-like activity for the γ-HCH utilization. It was clearly demonstrated that some HLDs besides LinB can potentially be involved in the γ-HCH utilization. This result could be predicted on the basis of the facts that HLDs or its homologues are widely distributed among bacterial strains and that HLDs generally have a broad range of substrate specificities (Koudelakova et al., 2011), but it was experimentally confirmed for the first time in this study. Especially, it is important that 'natural' HLD DmmA showed the LinB activity.

On the other hand, strains constructed in this chapter can be used as starting materials in the functional evolution and engineering studies. Especially, DAX-series strains are usefully for avoiding false positive clones that grow well on the solid minimal salt medium without adding any carbon sources in the screening process.

In Chapter 2, experimental evolution systems of HLD and its related genes toward the optimized γ-HCH utilization were constructed. However, the *in vivo* evolution system did not work well, mainly because

candidate clones that grew well with larger clear zone on the W-γ-HCH plate than others had no mutation in the HLD or its related genes. Probably, mutation(s) in the genome other than HLD or its related genes improved the γ-HCH utilization ability of the host cells. Although it is very interesting what mutation(s) have occurred in such clones, I did not further analyze them in this study.

On the other hand, the *in vitro* evolution system using error-prone PCR worked well. There was no research reported about evolution of HLDs by using error-prone PCR. This research proved that error-prone PCR could be used to trace evolution process of HLDs for the first time. In this process, many candidate evolved genes were successfully obtained. Interestingly, *rluc*-43, whose original *rluc* gene encodes protein having no LinB-like activity, was obtained as the evolved gene that confers the γ-HCH utilization ability to the host cells. In the *in vitro* evolution system, it was also revealed that LinB_dmbA_anc has faint LinB-like activity, which was not detected by the *in vivo* evolution system, probably because its expression level is higher in the *in vitro* system than the *in vivo* one. This result suggests that *in vitro* system is more sensitive than the *in vivo* system for detection of the weak LinB-like activity.

Eight genes, whose positive effect on the γ-HCH utilization were obvious, were selected and used as templates for the second round screening. However, the second round screening was more difficult than the first screening, since the screening system seems to be difficult to detect small difference of genes that have evolved to some extent. This system is suitable for selection of the evolved gene from the original gene encoding enzyme having weak or no LinB-like activity.

In Chapter 3, protein products of the candidate evolved genes obtained by the *in vitro* evolution system were expressed in *E. coli* as His-tagged proteins, purified, and characterized. Most of the putative evolved proteins obtained by the first round screening showed improved HLD activity toward 1,3-dibromopropane, which is a general substrate of HLDs, and LinB-like activity than their corresponding original enzymes. These results clearly demonstrated that the *in vitro* evolution system constructed in this study successfully worked.

LinB-like activity was assessed by the production of 2,5-DCP and 2,5-DDOL from γ-HCH in the reaction solution containing LinA, since substrates of LinB in the γ-HCH degradation pathway are unstable and the direct assay is impossible. However, the assay system should be more improved to quantify the LinB-like activity critically.

$LinB_{MI}$-63 showed the higher LinB-like activity than $LinB_{MI}$, indicating that $LinB_{MI}$ can be more improved for the LinB activity in the γ-HCH utilization. This result strongly suggest that γ-HCH degraders can be optimized more for the γ-HCH utilization at the steps catalyzed by LinB. The dead-end product 2,5-DCP is toxic for cells, thus the second LinB-catalyzed step should be improved more than the first LinB-catalyzed step. Theoretical design of such delicate feature seems to be difficult, and thus the *in vitro* system constructed in this study will be useful for the purpose.

LinB_dmbA_anc-3 and LinB_dmbA_anc-5, and Rluc_anc-4 and Rluc_anc-8 showed improved LinB-like activity than their original proteins, LinB_dmbA_anc and Rluc_anc, respectively. Although more analysis is necessary, the candidate evolved proteins (Rluc_anc-8-6 and Rluc_anc-8-37) were also obtained by the 2^{nd} round screening by using HLDs showing very week or no LinB-like activity. These two variants could not only produce more 2,5-DDOL than Rluc_anc-8, but also decreased amount of 2,5-DCP, which was a dead-end product produced by LinB in the γ-HCH degradation pathway. 2,5-DCP was toxic to cells and degradation of this dead end product was benefit to γ-HCH degradation (Endo et al., 2006). The evolution process of HLDs toward the γ-HCH utilization may be traced by using this system and such HLDs.

Error-prone PCR was often used to improve enzyme activity or catalytic efficiency in many researches (Lin et al., 2016) (Cheng et al., 2016) (Baek et al., 2017) (Crum et al., 2016). Two mutants E135V and E135R of an

alkaline xylanase Xyn11A-LC from *Bacillus* sp. SN5 were obtained by directed evolution (error-prone PCR) and site saturation mutagenesis. These two variants were found possess better alkalophilicity than wild type enzyme. Structural analysis showed that the residue at position 135, located in the eight-residue loop on the protein surface, might improve the alkalophilicity and catalytic activity by the elimination of the negative charge and the formation of salt-bridge (Bai et al., 2016). An engineered variant of isopentenyl diphosphate isomerase (IDI, E.C. 5.3.3.2) from *Saccharomyces cerevisiae* with improved catalytic activity by combining random (three runs of error-prone PCR) and site directed mutagenesis. The best mutant produced by this approach enhanced catalytic activity while also displaying improved stability in pH, enhanced thermostability and longer half-life (Chen et al., 2018). One of the identified mutants of *Klebsiella pneumonia* PDOR generated by error-prone PCR, which includes a single mutation A199S. This variant improved activity with 4.9 times that of the wild type enzyme (Jiang et al., 2015). Two glycoside hydrolase variants, LXYL-P1-2-EP1 (EP1, S91D) and LXYL-P1-2-EP2 (EP2, T368E), from *Lentinula edodes*, were obtained from the library generated by error-prone PCR and exhibited 17% and 47% increases in their catalytic efficiencies on 7-β-xylosyl-10-eacetyltaxol (Chen et al., 2017). The *baxA* gene encoding *Bacillus amyloliquefaciens* xylanase A was mutated by error-prone PCR. The mutant, pCbaxA50, which has a single mutation site S138T, was obtained from the mutant library by using the 96-well plate high-throughput screening method. The specific activity of the purified variant enzyme was 9.38 U/mg, which was 3.5 times higher than that of its parent (Xu et al., 2016). Error-prone PCR was also used to increase activity of organophosphorus enzyme. Five mutants, which were obtained after one round of error-prone PCR, were shown more ability than the native strains to degrade of diazinon, with more than 25% raising ratio (Rezaie et al., 2018).

As conclusions, the following two points are the most important in this study.

(1) The *linB*-replacement strains were constructed, into which genes encoding HLD or its homologues including putative ancestral proteins had been introduced at the *linB* site, and by using these strains it was demonstrated that some HLDs besides LinB can potentially be involved in the γ-HCH utilization.

(2) The *in vivo* and *in vitro* evolution systems of HLDs toward the optimized γ-HCH utilization were constructed, and some evolved enzymes were successfully obtained by using the *in vitro* evolution system, indicating that the system can be used for tracing the evolutionary process of HLDs toward the optimized γ-HCH utilization.

Acknowledgement

I am very appreciate it that I can study and do research in this lab. Firstly, I want to express my sincerely thanks to Yuji Nagata professor. He is a very kindly and professional professor. He teaches me many things in experiments and also help me generate interests in this research gradually. I respect him very much and obtain many ideas and good suggestions from him. From him, I know research is very interesting and preciseness. We should deal with it with chariness and responsibility. On the other hand, Mr. Nagata often provide many delicious food for us, which could make our stressed life relaxing. With the help of Mr. Nagata, I attend three times of conference in Japan, which offer me many things. In the future, I will sustain this interests and passion to research and continue my research life. I hope I can do well in it. I am very honor to be a student of him and instructed by him.

I also want to thankful to Mr. Ohtsubo, he gives me many good suggestions in my study. He treats me very kindly. Mr. Tsuda, Mr. Kato, Mr. Yano and Ms. Yukari are also extremely kindly teachers, they help me in research more or less. Mr. Tsuda is very serious in research. His earnest attitude toward research impressed me deeply. Mr. Kato is very patiently and teaches me experiment very carefully. Mr. Yano and Ms. Yukari often provide some useful suggestions to my research. I am very happy to study with all teachers and I am very appreciate to join in this big family.

Secondly, I want to thank for all students in our lab. They help me much and we get along with each other. I feel very happy together with them. Thanks for Kafayat and Idola, they give me many suggestions about my research and life. My life become more colorful with the accompany of them. I wish all of them have a brightly future and happy life.

Thirdly, thanks for Annapoorni and Daya professer from India. I do some researches with them together. I learn many things from them. They are very kindly and friendly. I like them very much.

Lastly, I want to thank for my parents. They support me much in mental and money. I am very grateful they are always positive of me. Thanks for their help.

References

Abhilash, P. C., Jamil, S., Singh, V., Singh, A., Singh, N., & Srivastava, S. C. (2008). Occurrence and distribution of hexachlorocyclohexane isomers in vegetation samples from a contaminated area. *Chemosphere*, *72*(1), 79-86. https://doi.org/10.1016/j.chemosphere.2008.01.056

Ang, T. F., Maiangwa, J., Salleh, A. B., Normi, Y. M., & Leow, T. C. (2018). Dehalogenases: From improved performance to potential microbial dehalogenation applications. *Molecules*, *23*(5), 1-40. https://doi.org/10.3390/molecules23051100

Babkova, P., Sebestova, E., Brezovsky, J., Chaloupkova, R., & Damborsky, J. (2017). Ancestral Haloalkane Dehalogenases Show Robustness and Unique Substrate Specificity. *ChemBioChem*, *18*(14), 1448-1456. https://doi.org/10.1002/cbic.201700197

Baek, S. C., Ho, T. H., Lee, H. W., Jung, W. K., Gang, H. S., Kang, L. W., & Kim, H. (2017). Improvement of enzyme activity of β-1,3-1,4-glucanase from Paenibacillus sp. X4 by error-prone PCR and structural insights of mutated residues. *Applied Microbiology and Biotechnology*, *101*(10), 4073-4083. https://doi.org/10.1007/s00253-017-8145-4

Bai, W., Cao, Y., Liu, J., Wang, Q., & Jia, Z. (2016). Improvement of alkalophilicity of an alkaline xylanase Xyn11A-LC from Bacillus sp. SN5 by random mutation and Glu135 saturation mutagenesis. *BMC Biotechnology*, *16*(1), 1-9. https://doi.org/10.1186/s12896-016-0310-9

Ballschmiter, K. (2003). Pattern and sources of naturally produced organohalogens in the marine environment: Biogenic formation of organohalogens. *Chemosphere*, *52*(2), 313-324. https://doi.org/10.1016/S0045-6535(03)00211-X

Barber, J. L., Sweetman, A. J., Van Wijk, D., & Jones, K. C. (2005). Hexachlorobenzene in the global environment: Emissions, levels, distribution, trends and processes. *Science of the Total Environment*, *349*(1-3), 1-44. https://doi.org/10.1016/j.scitotenv.2005.03.014

Bloom, J. D., & Arnold, F. H. (2009). In the light of directed evolution: Pathways of adaptive protein evolution. *In the Light of Evolution*, *3*, 149-163. https://doi.org/10.17226/12692

Böltner, D., Moreno-morillas, S., & Ramos, J. (2005). *<51 Boltner2005.Pdf>*. *7*, 1329-1338. https://doi.org/10.1111/j.1462-2920.2005.00820.x

Bosma, T., Damborský, J., Stucki, G., & Janssen, D. B. (2002). Biodegradation of 1,2,3-trichloropropane through directed evolution and heterologous expression of a haloalkane dehalogenase gene. *Applied and Environmental Microbiology*, *68*(7), 3582-3587. https://doi.org/10.1128/AEM.68.7.3582-3587.2002

Buryska, T., Babkova, P., Vavra, O., Damborsky, J., & Prokop, Z. (2018). A haloalkane dehalogenase from a marine microbial consortium possessing exceptionally broad substrate specificity. *Applied and Environmental Microbiology*. *84*(2), e01684-17. https://doi.org/10.1128/AEM.01684-17

Cérémonie, H., Boubakri, H., Mavingui, P., Simonet, P., & Vogel, T. M. (2006). Plasmid-encoded γ-hexachlorocyclohexane degradation genes and insertion sequences in Sphingobium francense (ex-Sphingomonas paucimobilis Sp+). *FEMS Microbiology Letters*, *257*(2), 243-252. https://doi.org/10.1111/j.1574-6968.2006.00188.x

Chaloupkova, R., Liskova, V., Toul, M., Markova, K., Sebestova, E., Hernychova, L., Marek, M., Pinto, G. P., Pluskal, D., Waterman, J., Prokop, Z., & Damborsky, J. (2019). Light-Emitting Dehalogenases: Reconstruction of Multifunctional Biocatalysts. *ACS Catalysis*. *9*, 4810−4823. https://doi.org/10.1021/acscatal.9b01031

Chaloupkova, R., Prokop, Z., Sato, Y., Nagata, Y., & Damborsky, J. (2011). Stereoselectivity and conformational stability of haloalkane dehalogenase DbjA from Bradyrhizobium japonicum USDA110: The effect of pH and temperature. *FEBS Journal*, *278*(15), 2728-2738. https://doi.org/10.1111/j.1742-4658.2011.08203.x

Chaloupkova, R., Prudnikova, T., Rezacova, P., Prokop, Z., Koudelakova, T., Daniel, L., Brezovsky, J., Ikeda-Ohtsubo, W., Sato, Y., Kuty, M., Nagata, Y., Smatanova, I. K., & Damborsky, J. (2014). Structural and functional analysis of a novel haloalkane dehalogenase with two halide-binding sites. *Acta Crystallographica Section D: Biological Crystallography*, *70*(7), 1884-1897. https://doi.org/10.1107/S1399004714009018

Chaloupková, R., Sýkorová, J., Prokop, Z., Jesenská, A., Monincová, M., Pavlová, M., Tsuda, M., Nagata, Y., & Damborský, J. (2003). Modification of Activity and Specificity of Haloalkane Dehalogenase from Sphingomonas paucimobilis UT26 by Engineering of Its Entrance Tunnel. *Journal of Biological Chemistry*, *278*(52), 52622-52628. https://doi.org/10.1074/jbc.M306762200

Chan, W. Y., Wong, M., Guthrie, J., Savchenko, A. V., Yakunin, A. F., Pai, E. F., & Edwards, E. A. (2010). Sequence- and activity-based screening of microbial genomes for novel dehalogenases. *Microbial Biotechnology*, *3*(1), 107-120. https://doi.org/10.1111/j.1751-7915.2009.00155.x

Chang, Z., Sitachitta, N., Rossi, J. V., Roberts, M. A., Flatt, P. M., Jia, J., Sherman, D. H., & Gerwick, W. H. (2004). Biosynthetic pathway and gene cluster analysis of curacin A, an antitubulin natural product from the tropical marine cyanobacterium Lyngbya majuscula. *Journal of Natural Products*, *67*(8), 1356-1367. https://doi.org/10.1021/np0499261

Chen, H., Li, M., Liu, C., Zhang, H., Xian, M., & Liu, H. (2018). Enhancement of the catalytic activity of Isopentenyl diphosphate isomerase (IDI) from Saccharomyces cerevisiae through random and site-directed mutagenesis. *Microbial Cell Factories*, *17*(1), 1-14. https://doi.org/10.1186/s12934-018-0913-z

Chen, J. J., Liang, X., Li, H. X., Chen, T. J., & Zhu, P. (2017). Improving the catalytic property of the glycoside hydrolase LXYL-P1–2 by directed evolution. *Molecules*. *22*(12), 2133-2146. https://doi.org/10.3390/molecules22122133

Cheng, Q., Gao, H., & Hu, N. (2016). A trehalase from Zunongwangia sp.: Characterization and improving catalytic efficiency by directed evolution. *BMC Biotechnology*, *16*(1), 6-13. https://doi.org/10.1186/s12896-016-0239-z

Chovancová, E., Kosinski, J., Bujnicki, J. M., & Damborský, J. (2007). Phylogenetic analysis of haloalkane dehalogenases. *Proteins: Structure, Function and Genetics*. *67*(2):305-316. https://doi.org/10.1002/prot.21313

Contag, C. H., Spilman, S. D., Contag, P. R., Oshiro, M., Eames, B., Dennery, P., Stevenson, D. K., & Benaron, D. A. (1997). Visualizing Gene Expression in Living Mammals Using a Bioluminescent Reporter. *Photochemistry and Photobiology*, *66*(4), 523-531. https://doi.org/10.1111/j.1751-1097.1997.tb03184.x

Crum, M. A., Trevor Sewell, B., & Benedik, M. J. (2016). Bacillus pumilus cyanide dihydratase mutants with higher catalytic activity. *Frontiers in Microbiology*, *7*(AUG), 1-10. https://doi.org/10.3389/fmicb.2016.01264

Daniel, L., Buryska, T., Prokop, Z., Damborsky, J., & Brezovsky, J. (2015). Mechanism-based discovery of novel substrates of haloalkane dehalogenases using in silico screening. *Journal of Chemical Information and Modeling*, *55*(1), 54-62. https://doi.org/10.1021/ci500486y

De Jong, R. M., & Dijkstra, B. W. (2003). Structure and mechanism of bacterial dehalogenases: Different ways to cleave a carbon-halogen bond. In *Current Opinion in Structural Biology*. *13*(6), 722 -730. https://doi.org/10.1016/j.sbi.2003.10.009

Dean, A. M., & Thornton, J. W. (2007). Mechanistic approach to study evolution. *Nature Reviews Genetics*, *8*(9), 675-688.

Dogra, C., Raina, V., Pal, R., Suar, M., Lal, S., Gartemann, K., Holliger, C., & Meer, J. R. Van Der. (2004). Organization of lin Genes and IS6100 among Different Strains of Evidence for Horizontal Gene Transfer. *Journal of Bacteriology*, *186*(8), 2225-2235. https://doi.org/10.1128/JB.186.8.2225

Endo, R., Ohtsubo, Y., Tsuda, M., & Nagata, Y. (2006). Growth inhibition by metabolites of γ-hexachlorocyclohexane in Sphingobium japonicum UT26. *Bioscience, Biotechnology and Biochemistry*, *70*(4), 1029-1032. https://doi.org/10.1271/bbb.70.1029

Engene, N., Rottacker, E. C., Kaštovský, J., Byrum, T., Choi, H., Ellisman, M. H., Komárek, J., & Gerwick, W. H. (2012). Moorea producens gen. nov., sp. nov. and Moorea bouillonii comb. nov., tropical marine cyanobacteria rich in bioactive secondary metabolites. *International Journal of Systematic and Evolutionary Microbiology*, *62*(5), 1171-1178. https://doi.org/10.1099/ijs.0.033761-0

Forloni, M., Liu, A. Y., & Wajapeyee, N. (2018). Random mutagenesis using error-prone DNA polymerases. *Cold Spring Harbor Protocols*. *2018*(3). https://doi.org/10.1101/pdb.prot097741

Gehret, J. J., Gu, L., Geders, T. W., Brown, W. C., Gerwick, L., Gerwick, W. H., Sherman, D. H., & Smith, J. L. (2012). Structure and activity of DmmA, a marine haloalkane dehalogenase. *Protein Science*, *21*(2), 239-248. https://doi.org/10.1002/pro.2009

Gonzalez, D., Hiblot, J., Darbinian, N., Miller, J. C., Gotthard, G., Amini, S., Chabriere, E., & Elias, M. (2014). Ancestral mutations as a tool for solubilizing proteins: The case of a hydrophobic phosphate-binding protein. *FEBS Open Bio*, *4*, 121-127. https://doi.org/10.1016/j.fob.2013.12.006

Harms, M. J., & Thornton, J. W. (2010). Analyzing protein structure and function using ancestral gene reconstruction. In *Current Opinion in Structural Biology*. *20*(3), 360-366. https://doi.org/10.1016/j.sbi.2010.03.005

Inaba, S., Sakai, H., Kato, H., Horiuchi, T., Yano, H., Ohtsubo, Y., Tsuda, M., & Nagata, Y. (2020). Expression of an alcohol dehydrogenase gene in a heterotrophic bacterium induces carbon dioxide-dependent high-yield growth under oligotrophic conditions. *Microbiology*, 166, 531-545. https://doi.org/10.1099/mic.0.000908

Ito, M., Prokop, Z., Klvaňa, M., Otsubo, Y., Tsuda, M., Damborský, J., & Nagata, Y. (2007). Degradation of β-hexachlorocyclohexane by haloalkane dehalogenase LinB from γ-hexachlorocyclohexane-utilizing bacterium Sphingobium sp. MI1205. *Archives of Microbiology*, *188*(4), 313-325. https://doi.org/10.1007/s00203-007-0251-8

Iwasaki, I., Utsumi, S., & Ozawa, T. (1952). New Colorimetric Determination of Chloride using Mercuric Thiocyanate and Ferric Ion. *225*(3), 226. *Bulletin of the Chemical Society of Japan*. https://doi.org/10.1246/bcsj.25.226

Janssen, D. B. B. T.-A. in A. M. (2007). Biocatalysis by Dehalogenating Enzymes. *Academic Press*. *61*, 233-252. https://doi.org/https://doi.org/10.1016/S0065-2164(06)61006-X

Jesenská, A., Pavlová, M., Strouhal, M., Chaloupková, R., Těšínská, I., Monincová, M., Prokop, Z., Bartoš, M., Pavlík, I., Rychl k, I., M öbius, P., Nagata, Y., & Damborsk ý, J. (2005). Cloning, biochemical properties, and distribution of mycobacterial haloalkane dehalogenases. *Applied and Environmental Microbiology*, *71*(11), 6736-6745. https://doi.org/10.1128/AEM.71.11.6736-6745.2005

Jiang, W., Zhuang, Y., Wang, S., & Fang, B. (2015). Directed evolution and resolution mechanism of 1, 3-propanediol oxidoreductase from Klebsiella pneumoniae toward higher activity by error-prone PCR and bioinformatics. *PLoS ONE*, *10*(11), 1-10. https://doi.org/10.1371/journal.pone.0141837

Kaczmarczyk, A., Vorholt, J. A., & Francez-Charlot, A. (2012). Markerless gene deletion system for sphingomonads. *Applied and Environmental Microbiology*, *78*(10), 3774-3777. https://doi.org/10.1128/AEM.07347-11

Kahm, M., Hasenbrink, G., Lichtenberg-Frat é, H., Ludwig, J., & Kschischo, M. (2010). Grofit: Fitting biological growth curves with R. *Journal of Statistical Software*. *33*(7), 1-21. https://doi.org/10.18637/jss.v033.i07

Koudelakova, T., Bidmanova, S., Dvorak, P., Pavelka, A., Chaloupkova, R., Prokop, Z., & Damborsky, J. (2013). Haloalkane dehalogenases: Biotechnological applications. In *Biotechnology Journal*. *8*(1), 32-45. https://doi.org/10.1002/biot.201100486

Koudelakova, T., Chovancova, E., Brezovsky, J., Monincova, M., Fortova, A., Jarkovsky, J., & Damborsky, J. (2011). Substrate specificity of haloalkane dehalogenases. Biochemical Journal. 435(2), 345-354. https://doi.org/10.1042/BJ20101405

Kumari, R., Subudhi, S., Suar, M., Dhingra, G., Raina, V., Dogra, C., Lal, S., Van der Meer, J. R., Holliger, C., & Lal, R. (2002). Cloning and characterization of lin genes responsible for the degradation of hexachlorocyclohexane isomers by Sphingomonas paucimobilis strain B90. *Applied and Environmental Microbiology*, *68*(12), 6021-6028.

https://doi.org/10.1128/AEM.68.12.6021-6028.2002

Lal, R., Dogra, C., Malhotra, S., Sharma, P., & Pal, R. (2006). Diversity, distribution and divergence of lin genes in hexachlorocyclohexane-degrading sphingomonads. *Trends in Biotechnology*, *24*(3), 121-130. https://doi.org/10.1016/j.tibtech.2006.01.005

Lal, R., Pandey, G., Sharma, P., Kumari, K., Malhotra, S., Pandey, R., Raina, V., Kohler, H.-P. E., Holliger, C., Jackson, C., & Oakeshott, J. G. (2010). Biochemistry of Microbial Degradation of Hexachlorocyclohexane and Prospects for Bioremediation. *Microbiology and Molecular Biology Reviews*, *74*(1), 58-80. https://doi.org/10.1128/mmbr.00029-09

Li, Y. F., Scholtz, M. T., & Van Heyst, B. J. (2003). Global gridded emission inventories of β-hexachlorocyclohexane. *Environmental Science and Technology*, *37*(16), 3493-3498. https://doi.org/10.1021/es034157d

Lin, L., Fu, C., & Huang, W. (2016). Improving the activity of the endoglucanase, Cel8M from Escherichia coli by error-prone PCR. *Enzyme and Microbial Technology*, *86*, 52-58. https://doi.org/10.1016/j.enzmictec.2016.01.011

Loening, A. M., Fenn, T. D., Wu, A. M., & Gambhir, S. S. (2006). Consensus guided mutagenesis of Renilla luciferase yields enhanced stability and light output. *Protein Engineering, Design and Selection*, *19*(9), 391-400. https://doi.org/10.1093/protein/gzl023

Lorenz, W. W., McCann, R. O., Longiaru, M., & Cormier, M. J. (1991). Isolation and expression of a cDNA encoding Renilla reniformis luciferase. *Proceedings of the National Academy of Sciences of the United States of America*, *88*(10), 4438-4442. https://doi.org/10.1073/pnas.88.10.4438

Los, G. V., Encell, L. P., McDougall, M. G., Hartzell, D. D., Karassina, N., Zimprich, C., Wood, M. G., Learish, R., Ohana, R. F., Urh, M., Simpson, D., Mendez, J., Zimmerman, K., Otto, P., Vidugiris, G., Zhu, J., Darzins, A., Klaubert, D. H., Bulleit, R. F., & Wood, K. V. (2008). HaloTag: A novel protein labeling technology for cell imaging and protein analysis. *ACS Chemical Biology*, *3*(6), 373-382. https://doi.org/10.1021/cb800025k

Macdonald, R. W., Barrie, L. A., Bidleman, T. F., Diamond, M. L., Gregor, D. J., Semkin, R. G., Strachan, W. M. J., Li, Y. F., Wania, F., Alaee, M., Alexeeva, L. B., Backus, S. M., Bailey, R., Bewers, J. M., Gobeil, C., Halsall, C. J., Harner, T., Hoff, J. T., Jantunen, L. M. M., … Yunker, M. B. (2000). Contaminants in the Canadian Arctic: 5 years of progress in understanding sources, occurrence and pathways. In *Science of the Total Environment*. 254(2-3), 93-234. https://doi.org/10.1016/S0048-9697(00)00434-4

Marek, J., Vevodova, J., Smatanova, I. K., Nagata, Y., Svensson, L. A., Newman, J., Takagi, M., & Damborsky, J. (2000). Crystal structure of the haloalkane dehalogenase from Sphingomonas paucimobilis UT26. *Biochemistry*, *39*(46), 14082-14086. https://doi.org/10.1021/bi001539c

Marietta, M. A., Yoon, P. S., Iyengar, R., Leaf, C. D., & Wishnok, J. S. (1988). Molecular Cloning. A Laboratory Manual, Cold Spring Harbor Laboratory, Cold Spring Harbor. *Proc. Natl. Acad. Sci. U.S.A.*

Marvanová, S., Nagata, Y., Wimmerová, M., Sýkorová, J., Hynková, K., & Damborský, J. (2001). Biochemical characterization of broad-specificity enzymes using multivariate experimental design and a colorimetric microplate assay: Characterization of the haloalkane dehalogenase mutants. *Journal of Microbiological Methods*, *44*(2), 149-157. https://doi.org/10.1016/S0167-7012(00)00250-5

Moriuchi, R., Tanaka, H., Nikawadori, Y., Ishitsuka, M., Ito, M., Ohtsubo, Y., Tsuda, M., Damborsky, J., Prokop, Z., & Nagata, Y. (2014). Stepwise enhancement of catalytic performance of haloalkane dehalogenase LinB towards β-hexachlorocyclohexane. *AMB Express*, *4*(1), 1-10. https://doi.org/10.1186/s13568-014-0072-5

Nagata, Y., Nariya, T., Ohtomo, R., Fukuda, M., Yano, K., & Takagi, M. (1993). Cloning and sequencing of a dehalogenase gene encoding an enzyme with hydrolase activity involved in the degradation of γ-hexachlorocyclohexane in Pseudomonas paucimobilis. *Journal of Bacteriology*, *175*(20), 6403-6410. https://doi.org/10.1128/jb.175.20.6403-6410.1993

Nagata, Y, Endo, R., Ito, M., Ohtsubo, Y., & Tsuda, M. (2007). Aerobic degradation of lindane

(γ-hexachlorocyclohexane) in bacteria and its biochemical and molecular basis. In *Applied Microbiology and Biotechnology*. *76*, 741-752. https://doi.org/10.1007/s00253-007-1066-x

Nagata, Y, Kamakura, M., Endo, R., Miyazaki, R., Ohtsubo, Y., & Tsuda, M. (2006). Distribution of γ-hexachlorocyclohexane-degrading genes on three replicons in Sphingobium japonicum UT26. *FEMS Microbiology Letters*, *256*(1), 112-118. https://doi.org/10.1111/j.1574-6968.2005.00096.x

Nagata, Y, Mori, K., Takagi, M., Murzin, A. G., & Damborsk, J. (2001). Identification of protein fold and catalytic residues of γhexachlorocyclohexane dehydrochlorinase LinA. *Proteins: Structure, Function and Genetics*. *45*(4), 471-477. https://doi.org/10.1002/prot.10007

Nagata, Y, Natsui, S., Endo, R., Ohtsubo, Y., Ichikawa, N., Ankai, A., Oguchi, A., Fukui, S., Fujita, N., & Tsuda, M. (2011). Genomic organization and genomic structural rearrangements of Sphingobium japonicum UT26, an archetypal γ-hexachlorocyclohexane-degrading bacterium. *Enzyme and Microbial Technology*. *49*(6-7), 499-508. https://doi.org/10.1016/j.enzmictec.2011.10.005

Nagata, Y, Ohtsubo, Y., & Tsuda, M. (2015). Properties and biotechnological applications of natural and engineered haloalkane dehalogenases. *Applied Microbiology and Biotechnology*, *99*(23), 9865-9881. https://doi.org/10.1007/s00253-015-6954-x

Nagata, Y, Prokop, Z., Sato, Y., Jerabek, P., Kumar, A., Ohtsubo, Y., Tsuda, M., & Damborsk ý, J. (2005). Degradation of β-hexachlorocyclohexane by haloalkane dehalogenase LinB from Sphingomonas paucimobilis UT26. *Applied and Environmental Microbiology*, *71*(4), 2183-2185. https://doi.org/10.1128/AEM.71.4.2183-2185.2005

Naqvi, T., Warden, A. C., French, N., Sugrue, E., Carr, P. D., Jackson, C. J., & Scott, C. (2014). A 5000-fold increase in the specificity of a bacterial phosphotriesterase for malathion through combinatorial active site mutagenesis. *PLoS ONE*, *9*(4). e94177. https://doi.org/10.1371/journal.pone.0094177

Newman, J., Peat, T. S., Richard, R., Kan, L., Swanson, P. E., Affholter, J. A., Holmes, I. H., Schindler, J. F., Unkefer, C. J., & Terwilliger, T. C. (1999). Haloalkane dehalogenases: Structure of a Rhodococcus enzyme. *Biochemistry*, *38*(49), 16105-16114. https://doi.org/10.1021/bi9913855

Oakley, A. J., Klvaňa, M., Otyepka, M., Nagata, Y., Wilce, M. C. J., & Damborský, J. (2004). Crystal Structure of Haloalkane Dehalogenase LinB from Sphingomonas paucimobilis UT26 at 0.95 Å Resolution: Dynamics of Catalytic Residues. *Biochemistry*. *43*(4), 870-878. https://doi.org/10.1021/bi034748g

Okai, M., Kubota, K., Fukuda, M., Nagata, Y., Nagata, K., & Tanokura, M. (2010). Crystal Structure of Γ-Hexachlorocyclohexane Dehydrochlorinase LinA from Sphingobium japonicum UT26. *Journal of Molecular Biology*. *403*(2), 260-269. https://doi.org/10.1016/j.jmb.2010.08.043

Okai, M., Ohtsuka, J., Imai, L. F., Mase, T., Moriuchi, R., Tsuda, M., Nagata, K., Nagata, Y., & Tanokura, M. (2013). Crystal structure and site-directed mutagenesis analyses of haloalkane dehalogenase *linB* from sphingobium sp. Strain MI1205. *Journal of Bacteriology*, *195*(11), 2642-2651. https://doi.org/10.1128/JB.02020-12

Ortlund, E., Bridgham, J. T., Redinbo, M. R., & Thornton, J. W. (2007). Crystal Structure of an Ancienct Protein. *Science*, *317*(5844), 1544-1548. https://doi.org/10.1126/science.1142819.Crystal

Peisajovich, S. G., Rockah, L., & Tawfik, D. S. (2006). Evolution of new protein topologies through multistep gene rearrangements. *Nature Genetics*. *38*(2), 168-174. https://doi.org/10.1038/ng1717

Pritchard, L., Corne, D., Kell, D., Rowland, J., & Winson, M. (2005). A general model of error-prone PCR. *Journal of Theoretical Biology*, *234*(4), 497-509. https://doi.org/10.1016/j.jtbi.2004.12.005

Prokop, Zbyněk, Damborský, J., Janssen, D. B., & Nagata, Y. (2009). Method of production of optically active halohydrocarbons and alcohols using hydrolytic dehalogenation catalysed by haloalkane dehalogenases. *US Patent 7632666*. http://www.patentstorm.us/patents/7632666/description.html

Prokop, Zbyněk, Opluštil, F., DeFrank, J., & Damborský, J. (2006). Enzymes fight chemical weapons. *Biotechnology Journal*, *1*(12), 1370-1380. https://doi.org/10.1002/biot.200600166

Prokop, Zbynek, Sato, Y., Brezovsky, J., Mozga, T., Chaloupkova, R., Koudelakova, T., Jerabek, P., Stepankova, V., Natsume, R., Van Leeuwen, J. G. E., Janssen, D. B., Florian, J., Nagata, Y., Senda, T., & Damborsky, J. (2010). Enantioselectivity of haloalkane dehalogenases and its modulation by surface loop engineering. *Angewandte Chemie - International Edition*, *49*(35), 6111-6115. https://doi.org/10.1002/anie.201001753

Rezaie, E., Latifi, A. M., & Mirzaei, M. (2018). Activity improvement of organophosphorus hydrolase enzyme by error prone PCR method. *Journal of Applied Biotechnology Reports*, *5*(3), 100-104. https://doi.org/10.29252/JABR.05.03.03

Sato, Y., Monincová, M., Chaloupková, R., Prokop, Z., Ohtsubo, Y., Minamisawa, K., Tsuda, M., Damborsky, J., & Nagata, Y. (2005). Two rizobial srains, Mesorhizobium loti MAFF303099 and Bradyrhizobium japonicum USDA110, encode haloalkane dehalogenases with novel structures and substrate specificities. *Applied and Environmental Microbiology*, *71*(8), 4372-4379. https://doi.org/10.1128/AEM.71.8.4372-4379.2005

Sato, Y., Natsume, R., Tsuda, M., Damborsky, J., Nagata, Y., & Senda, T. (2007). Crystallization and preliminary crystallographic analysis of a haloalkane dehalogenase, DbjA, from Bradyrhizobium japonicum USDA110. *Acta Crystallographica Section F: Structural Biology and Crystallization Communications*, *63*(4), 294-296. https://doi.org/10.1107/S1744309107008652

Schäfer, A., Tauch, A., Jsger, W., Kalinowski, J., Thierbachb, G., & Piihler, A. (1994). pK18mobsacB. *Gene*.

Schweizer, H. P. (1992). Alielic exchange in Pseudomonas aeruginosa using novel ColE1-type vectors and a family of cassettes containing a portable oriT and the counter-selectable Bacillus subtilis sacB marker. *Molecular Microbiology*. *6*(9), 1195-1204. https://doi.org/10.1111/j.1365-2958.1992.tb01558.x

Smith, S. D., Wang, S., & Rausher, M. D. (2013). Functional evolution of an anthocyanin pathway enzyme during a flower color transition. *Molecular Biology and Evolution*, *30*(3), 602-612. https://doi.org/10.1093/molbev/mss255

Studier, F. W., & Moffatt, B. A. (1986). Use of bacteriophage T7 RNA polymerase to direct selective high-level expression of cloned genes. *Journal of Molecular Biology*. 189, 113-130. https://doi.org/10.1016/0022-2836(86)90385-2

Tabata, M., Ohhata, S., Nikawadori, Y., Kishida, K., Sato, T., Kawasumi, T., Kato, H., Ohtsubo, Y., Tsuda, M., & Nagata, Y. (2016). Comparison of the complete genome sequences of four c-hexachlorocyclohexane-degrading bacterial strains: insights into the evolution of bacteria able to degrade a recalcitrant man-made pesticide. *DNA Research*, *23*(6), 581-599. https://doi.org/10.1093/dnares/dsw041

Takenaka, Y., Noda-Ogura, A., Imanishi, T., Yamaguchi, A., Gojobori, T., & Shigeri, Y. (2013). Computational analysis and functional expression of ancestral copepod luciferase. *Gene*, *528*(2), 201-205. https://doi.org/10.1016/j.gene.2013.07.011

Terada, I., Kwon, S. T., Miyata, Y., Matsuzawa, H., & Ohta, T. (1990). Unique precursor structure of an extracellular protease, aqualysin I, with NH2- and COOH-terminal pro-sequences and its processing in Escherichia coli. *Journal of Biological Chemistry*. *265*(12), 6576-6581.

Trantírek, L., Hynková, K., Nagata, Y., Murzin, A., Ansorgová, A., Sklenář, V., & Damborský, J. (2001). Reaction Mechanism and Stereochemistry of γ-Hexachlorocyclohexane Dehydrochlorinase LinA. *Journal of Biological Chemistry*, *276*(11), 7734-7740. https://doi.org/10.1074/jbc.M007452200

Tratsiak, K., Degtjarik, O., Drienovska, I., Chrast, L., Rezacova, P., Kuty, M., Chaloupkova, R., Damborsky, J., & Kuta Smatanova, I. (2013). Crystallographic analysis of new psychrophilic haloalkane dehalogenases: DpcA from Psychrobacter cryohalolentis K5 and DmxA from Marinobacter sp. ELB17. *Acta Crystallographica Section F: Structural Biology and Crystallization Communications*, *69*(6), 683-688. https://doi.org/10.1107/S1744309113012979

Ugalde, J. A., Chang, B. S. W., & Matz, M. V. (2004). Evolution of coral pigments recreated. *Science*, *305*(5689), 1433. https://doi.org/10.1126/science.1099597

Varriale, S., Cerullo, G., Antonopoulou, I., Christakopoulos, P., Rova, U., Tron, T., Fauré, R., Jütten, P., Piechot, A., Brás, J. L. A., Fontes, C. M. G. A., & Faraco, V. (2018). Evolution of the feruloyl esterase MtFae1a from Myceliophthora thermophila towards improved catalysts for antioxidants synthesis. *Applied Microbiology and Biotechnology*, *102*(12), 5185-5196. https://doi.org/10.1007/s00253-018-8995-4

Vijgen, J., Abhilash, P. C., Li, Y. F., Lal, R., Forter, M., Torres, J., Singh, N., Yunus, M., Tian, C., Schäffer, A., & Weber, R. (2011). Hexachlorocyclohexane (HCH) as new Stockholm Convention POPs-a global perspective on the management of Lindane and its waste isomers. *Environmental Science and Pollution Research*, *18*(2), 152-162. https://doi.org/10.1007/s11356-010-0417-9

Wijma, H. J., Floor, R. J., & Janssen, D. B. (2013). Structure- and sequence-analysis inspired engineering of proteins for enhanced thermostability. *Current Opinion in Structural Biology*, *23*(4), 588-594. https://doi.org/10.1016/j.sbi.2013.04.008

Xu, X., Liu, M. Q., Huo, W. K., & Dai, X. J. (2016). Obtaining a mutant of Bacillus amyloliquefaciens xylanase A with improved catalytic activity by directed evolution. *Enzyme and Microbial Technology*, *86*, 59-66. https://doi.org/10.1016/j.enzmictec.2016.02.001

Yang, K. K., Wu, Z., & Arnold, F. H. (2019). Machine-learning-guided directed evolution for protein engineering. *Nature Methods*, *16*(8), 687-694. https://doi.org/10.1038/s41592-019-0496-6

Yokoyama, S. (2002). Molecular evolution of color vision in vertebrates. *Gene*, *300*(1–2), 69-78. https://doi.org/10.1016/S0378-1119(02)00845-4

Yokoyama, S., Tada, T., Zhang, H., & Britt, L. (2008). Elucidation of phenotypic adaptations: Molecular analyses of dim-light vision proteins in vertebrates. *Proceedings of the National Academy of Sciences of the United States of America*, *105*(36), 13480-13485. https://doi.org/10.1073/pnas.0802426105

Zulkifly, A. H., Roslan, D. D., Hamid, A. A. A., Hamdan, S., & Huyop, F. (2010). Biodegradation of low concentration of monochloroacetic acid-degrading Bacillus sp. TW1 isolated from terengganu water treatment and distribution plant. *Journal of Applied Sciences*, *10*(22), 2940-2944. https://doi.org/10.3923/jas.2010.2940.2944